

## Common borders. Common solutions.



**INNOVATIVE TECHNOLOGIES IN THE ASSESSMENT  
OF SOIL EROSION AND SEDIMENTS IN MOLDOVA**

**TEHNOLOGII INOVATOARE ÎN EVALUAREA EROZIUNILOR  
SOLULUI ȘI SEDIMENTELOR ÎN MOLDOVA**





Project funded by  
EUROPEAN UNION



**INNOVATIVE TECHNOLOGIES IN THE ASSESSMENT  
ON THE SOIL EROSION AND SEDIMENTS IN MOLDOVA:  
*The Baltata River Basin***

\*\*\*

**TEHNOLOGII INOVATOARE ÎN EVALUAREA EROZIUNILOR  
SOLULUI ȘI SEDIMENTELOR ÎN MOLDOVA:  
*Bazinul râului Bălțata***

**Eco-TIRAS  
Chisinau 2023**

CZU 504.453:631.459(478)(082)

I-54

Innovative technologies in the assessment on the soil erosion and sediments in Moldova: the Baltata River Basin. Tehnologii inovatoare în evaluarea eroziunilor solului și sedimentelor în Moldova: bazinul râului Bălțata. Chișinău: Eco-Tiras (SRL Arconteh), 2023. 92 pag.

DESCRIEREA CIP A CAMEREI NAȚIONALE A CĂRȚII DIN REPUBLICA MOLDOVA

**Innovative technologies in the assessment on the soil erosion and sediments in Moldova: *The Baltata River Basin*** = Tehnologii inovatoare în evaluarea eroziunilor solului și sedimentelor în Moldova: *Bazinul râului Bălțata* / International Association of River Keepers “Eco-Tiras”, Proiect funded by European Union. - Chișinău : Eco-TIRAS, 2023 (Arconteh). - 90 p. : fig., tab.

Rez.: lb. rom. - Referințe bibliogr.: p.: 77-83. - [300] ex.

ISBN 978-9975-3602-1-0.

© International Association of River Keepers “Eco-Tiras”, 2023.

Tipar: SRL Arconteh, str. Milescu Spătarul 9/1

## TABLE OF CONTENTS

<b>Introduction</b>	<b>3</b>
<i>Ilya Trombitsky</i>	
<b>1 Setting the scene.....</b>	<b>4</b>
<i>Roman Corobov, Gennadi Sirodov</i>	
1.1 Project relevance. ....	4
1.2 Work Packages and Groups of Activities.....	6
1.2.1 Work Package Nr 1.....	6
1.2.2 Work Package Nr 2.....	7
1.3 Study area.....	8
1.3.1 Short general description.....	8
1.3.2 Land use and soils.....	9
1.3.3 Current climate of the pilot area. ....	10
1.3.4 The Baltata River flow.....	12
<b>Hydrological modeling of the rivers streamflow</b>	
<b>2 and sedimentation.....</b>	<b>14</b>
<i>Gennadi Sirodov, Roman Corobov</i>	
2.1 Hydrological modeling as a concept.....	14
2.2 SWAT modeling of the Baltata River runoff under different climates.....	15
2.2.1 SWAT model: history, validation and calibration.....	15
2.2.2 SWAT model run.....	18
2.2.2 The Baltata River runoff under current climate.....	21
2.2.3 The Baltata River runoff under likely future climate....	22
2.3 WEPP modeling of soil erosion and sediment deposition	27
2.3.1 Soil erosion as a global challenge.....	27
2.3.2 GeoWEPP as a new modeling tool.....	29
2.3.3 Preparing the GeoWEPP impute information.....	34
2.3.4 GeoWEPP simulations and results.....	
<b>3 Using the remote sensing techniques to identify and map the erosion-prone areas in the small river watersheds</b>	<b>38</b>
<i>Igor Sirodov</i>	
3.1 Introduction.....	38

3.2	Implementation of Vegetation Indexes to map areas the most vulnerable to soil erosion.....	39
3.2.1	<i>Using the normalized difference indexes to determine erosion-prone areas.....</i>	39
3.2.2	<i>Initial data and methods.....</i>	40
3.2.3	<i>Spatial distribution of erosion-prone areas.....</i>	43
3.3	Satellite images in the assessment of trends in stream bank erosion.....	46
3.3.1	<i>Introduction.....</i>	46
3.3.2	<i>Data and method.....</i>	47
3.3.3	<i>Results and discussion.....</i>	51
4	<b>Drone mapping of erosion hotspots.....</b>	54
	<i>Vitalie Boico, Gennadi Sirodoev, Roman Corobov</i>	
4.1	Introduction.....	54
4.2	Methodic of the drone survey and mapping.....	55
4.2.1	<i>Drone description and testing.....</i>	56
4.2.2	<i>Drone survey planning and organization.....</i>	57
4.2.3	<i>Drone erosion mapping.....</i>	57
4.3	Drone erosion survey, data processing and results.....	58
4.3.1	<i>Drone survey report.....</i>	58
4.3.2	<i>Drone survey results.....</i>	60
5	<b>Fingerprinting method for identifying the suspended sediment sources.....</b>	65
	<i>Oleg Bogdevich</i>	
5.1	Introduction.....	65
5.2	Fingerprinting methods overview.....	66
5.3	Sampling methods.....	69
5.4	Results and discussion.....	71
6	<b>Litter trap.....</b>	76
		77
	References.....	77
	Rezumat.....	85

## Introduction






This brochure presents the project “*Protecting streams for a clean Black Sea by reducing sediment and litter pollution with joint innovative monitoring and control tools and nature-based practices*” (Acronym: *Protect-Streams-4-Sea*).

The project is realized under the “*Joint Operational Programme Black Sea Basin 2014-2020*”, which is one of the four maritime programmes, established in the framework of the *European Neighborhood Instrument (ENI) 2014-2020* – the Programming document for EU support of ENI Cross-Border Cooperation (CBC). The project focuses on the environmental monitoring of nonpoint source pollutants and litter, which get into the Black Sea. This activity corresponds to the Black Sea Programme’s main priority and is essential because the polluted enclosed sea is very difficult to depollute. The cleaning efforts should be focused both on the sea itself and along coastal areas where many pollutants and litter are provided by the watersheds.

The idea of the *Protect-Streams-4-Sea* project is to stop the nonpoint source pollutants and litter from their reaching the streams and rivers and consequently – the Black Sea. This goal should be achieved mainly by using different innovative methods, some of which, for example, fingerprinting, were applied in Moldova practically for the first time. In common, both traditional (erosion pins, runoff plots) and innovative (remote sensing, drones, hydrological modeling) methods promoted the pollutant estimations and pollution simulation at a river watershed scale. A Multi-Criteria Decision Analysis and a Decision Support System were developed to find “hot spots” and to recommend best management practices in each pilot area of the project.

The location of pilot areas in five Black Sea countries has allowed testing the used tools and methods in this region’s different representative environments, thus helping their further adoption by other countries and leading to a joint monitoring program for inland nonpoint source pollutants and litter. And finally, numerous and diverse communication activities helps to reach the project results to all target groups and stakeholders.

The project partners:

-  **Lead partner:** the International Hellenic University (IHU), legal successor to Technologiko Ekpedeftiko Idryma Anatolikis Makedonias kai Thrakis, GREEK;
-  **Partner 2:** Buzau-Ialomita Water Administration, ROMÂNIA;
-  **Partner 3:** “Young Foresters Union” non-governmental organization, ARMENIA;
-  **Partner 4:** Eco-TIRAS International Association of River Keepers; MOLDOVA;
-  **Partner 5:** Artvin Coruh University, *Türkiye*.

Such cooperation on the EU external borders is a key priority in the European Neighborhood Policy (*ENP*) and contributes to the ENI overall objective of the progress towards shared prosperity and good neighborliness between EU Member States and their neighbors.

The project *overall objective* is the environmental protection and reduction of pollutants and litter in Black Sea.

The project *specific objectives* are:

- ❖ Development of new tools for joint monitoring;
- ❖ Identification of the major sources of pollutants and litter, and their contributions to total pollution;
- ❖ Development and suggestion of the best management practices;

The project duration is 36 months: from 20.07.2020 to 19.07.2023.

The main purpose of this brochure is to inform the general public about the project, its activities in Moldova, and the results obtained.

## 1. Setting the scene

### 1.1 Project relevance

The coordination of marine water protection and joint reduction of its pollution is one of the major world challenges. Sediments and litter are seen as an emerging polluting material on a global level, especially in the marine environment. In turn, on a national level, governments have to assess quantities and types of water pollutants in their countries as part of the European Marine Strategy Framework Directive (MSFD)<sup>1</sup> implementation.

There are a number of scientific studies that have been conducted by researchers in Europe and outside showing that most marine pollution comes from land based sources. It is also anticipated that in the absence of mitigation measures, any region with large rivers can be considered as a substantial contributor to marine pollution. However, the scale of such contribution and the size of these pollutants distribution remain to be systematically quantified. Such quantification will aid in mapping both sources and amounts of pollutants in river systems and in providing an additional knowledge base

---

<sup>1</sup> Available at: [https://ec.europa.eu/environment/marine/eu-coast-and-marine-policy/marine-strategy-framework-directive/index\\_en.htm](https://ec.europa.eu/environment/marine/eu-coast-and-marine-policy/marine-strategy-framework-directive/index_en.htm)



for the MSFD implementation in terms of their emissions into the marine environment on the whole.

The most efficient and sustainable way to address this task is a joint environmental monitoring that allows identifying the major pollutant sources. At the same time, numerous literature reviews has revealed the lack of long-term, systematic programs on pollutant monitoring in the riverine or marine environment. Namely this evidence was the main idea behind the presented project. It is expected that project realization contributes to the development of tools based on new technologies, which will allow better monitoring and identifying the major sources of non-point source pollutants and littering flowing in the Black Sea, thus contributing to their effective and sustainable redaction. Improving the environmental conditions will be beneficial for the flora and fauna along for the people living within the basin of this enclosed and inland sea, almost fully isolated from the World Oceans. Because of the Black Sea limited water exchange with other seas, much of its inflowing waters remain in his basin unable to drain out or mix with other water bodies. This means that it is very difficult to clean its pollution by natural process and very expensive – by anthropogenic actions. Namely these difficulties have driven a reason to put out a project trying to implement methods to reduce the pollutant and litter before they have reached the Black Sea, through focusing on its contributing watersheds.

Moreover, the available researches are also stating the Black Sea is already under serious environmental threats, and measures based on scientifically sound data need to be taken in order to preserve, conserve and enhance this extremely important natural ecosystem. The current situation in the Black Sea is a consequence of the fact that its basin countries during the second part of the last century have begun to apply intensive usage of agricultural fertilizers leading to excessive amounts of pollutants entering the rivers and then inevitably falling into the sea. This causes its eutrophication, over-fertilization and increased phytoplankton, which in turn causes the shading of light and decreasing of water transparency with following dying of algae living in the larger depths. The decomposing organic matter and related bacteria use up more and more oxygen, leading to its deficiency or hypoxia, that brings to mass death of zoobenthos and demersal fish in large areas. The size and number of marine dead zones grow extensively in the past half-century, practically in all marine ecosystems, especially enclosed and inland.

At the same time, the rivers are a source of litter from the riparian cities and towns, causing serious environmental problems and becoming a major environmental priority for the region on the whole, and non-point source pollution and litter are main challenges the entire territory faces. Any proactive measures to mitigate these problems would benefit the ecosystems and the people that depend on and live in the Black Sea Basin. Moreover, in many cases the measures that stop the pollutants and litter before they reach the sea are the most sustainable and cost-effective. The basin rivers contribution to the marine environment should be estimated based on the data gathered during this project.

## **1.2 Work Packages and Groups of Activities**

By its structure, the project includes three main Groups of Activities (GA): Project management, Project implementation and Communication. However, based on the main purpose of this brochure – *to inform the general public about the project activities in Moldova and the results obtained* – its subsequent content is mainly devoted to the presentation of results.

### **1.2.1 Work Package Nr 1: *Identifying Hot Spots and Quantifying Erosion, Litter and Pollutant Sources***

This package's activities will identify and quantify the major sources of erosion, litter and pollutants that contribute to streams but eventually end in the Black Sea. Although these sources are major contributors to its degradation, they are not always quantified and identified accurately. In particular, this concerns the surface and stream bank erosions. Their measurement took place at different scales, specifically, at watershed and plot ones, and under different land-use/vegetation covers, while using different methodical approaches.

To determine the potential pollutants sources at the watershed scale there were used SWAT and WEPP calibrated hydrologic models. Furthermore, these models were run to evaluate the levels of future pollutant contributions based on the latest regional climate change projections. For identification of nonpoint pollutant sources, the *vegetation indices*, received via satellite images, were applied; based on the satellite survey results the most vulnerable to erosion areas were recognized in a GIS environment. *Drone mapping* was applied to investigate the sites with a smaller scale of different

land use/vegetation cover and, potentially, with a high surface erosion risk and litter gathering.

Because in many cases a stream bank erosion can contribute up to 90% of the nonpoint sources pollutant, for their estimation there were used both traditional (erosion pins, cross-section surveys) and innovative (e.g., the GIS Stream Bank Erosion Index, based on satellite images) methods. Drone mapping was tested to capture locations of litter accumulation, sediment and erosion deposition. On the whole, at different scales the above mentioned methods provide the potential contribution from stream bank erosion.

If possible, in the framework of this package the impact of different land-use/vegetation covers of riparian areas on stream bank erosion was also investigated.

### **1.2.2 Work Package Nr 2: *Monitoring and Mitigating Stream Pollutants and Litter***

The activities of this WP aimed to recognize the sources of major pollutants, focusing on the in-stream scale. To do this the water and sediment samples were collected at different locations along the study area and under different stream flow conditions, thus allowing seeing if a problem exists and by what kind of pollutants. To determine the pollutants sources, for the first time in Moldova and practically for Europe, the fingerprinting method was also used. The collected soil samples from different sources were afterwards analyzed for numerous parameters.

The final activity concerns the implementation of the best management practices through a multi-criteria decision analysis and online decision support system, with the subsequent development of these practices recommendation. In turn, the multi-criteria decision analysis determines what and where these practices, mainly via nature-based solutions, should be located to have the greatest effects. The online decision support system will propose their use based on specific parameters that are able online entering.

As an innovative ways to reduce litter entering the watercourse, this package includes implementation and testing of one special litter trap.

## 1.3 Study area

### 1.3.1 Short general description

For addressing the Project's tasks and correct understanding the nature and consequences of small rivers pollution for the Black Sea general pollution, the Baltata River was selected as the study area of Project Partner 4 (PP4) activities. This river – fairly typical small river of Moldova – is a right tributary of the Dniester River, which flows into the Black Sea, and where all surface pollution and litter that enter its main stream are directly transported to. This factor has based choosing the Baltata basin as a study area; moreover, it presents the current situation in other analogous small river basins of the country.

The study area has 153.9 km<sup>2</sup>, its length from northwest to southeast is 27.47 km, the width – 7.74 km; it includes 13 rural settlements and a very small part of the capital of Moldova, the city of Chisinau (Fig. 1.1). Most of the Baltata River basin is located within the steppe zone; a smaller north-western part – in the forest-steppe zone. The basin relief is predominantly flat; in the lower reaches it is low, in the upper – an elevated plain. The absolute heights vary from 16 m to 219 m, averaging 120 m. The slopes vary from sub-horizontal to steep (about 17°), on average being 40°28'; the slopes between 2° to 5° are the most common.

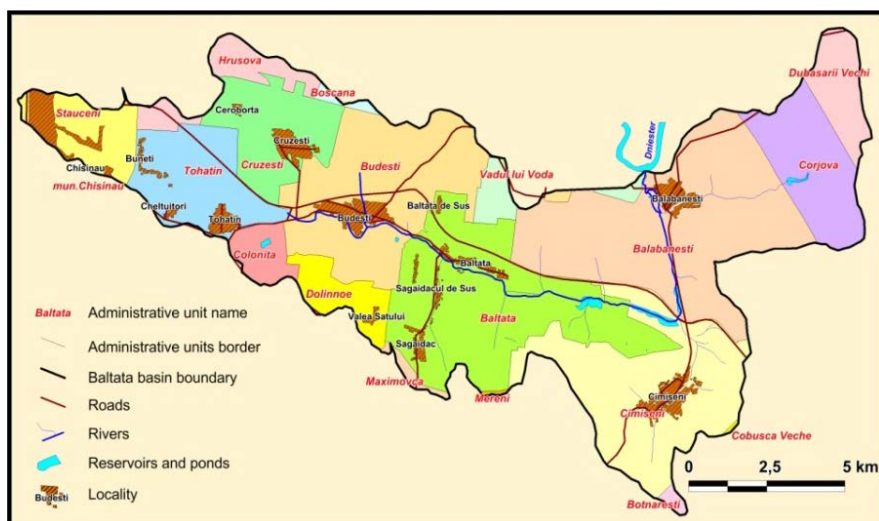


**Fig. 1.1** The Baltata River basin and its administrative division

### 1.3.2 Land use and soils

The principal land uses in the Baltata basin are agriculture, forests, pastures, meadows, perennial and built-up plots; 46.2% of the area is occupied by agricultural crops. Perennials and pastures occupy 13.8% and 11.4%, respectively; only 17.4% of the area is covered by forests (Fig. 1.2). As a result of intensive farming and its low culture, the Baltata basin's soils are degraded above 29%.

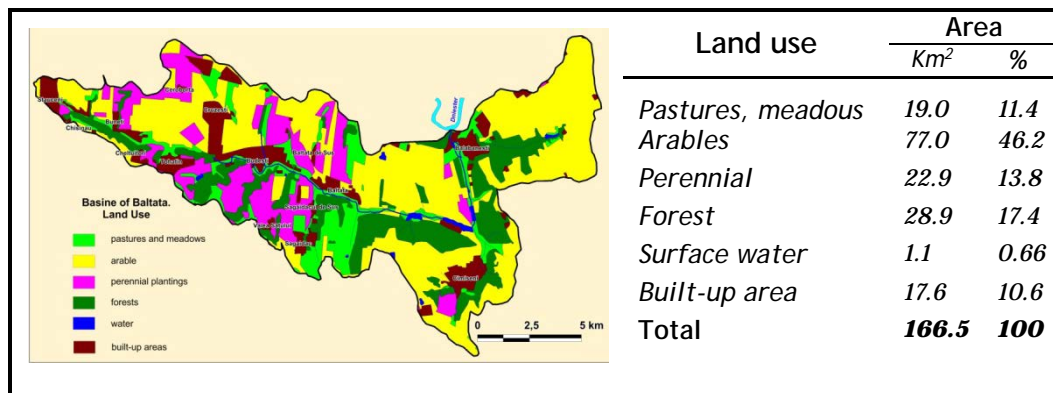


**Fig. 1.2** Land use and its distribution in the Baltata River basin

The Baltata soils belong to the region of leached chernozems of the eastern and southern spurs of the Codru forest-steppe. In terms of this project, the most important feature of the study area soils is their diversity. For example, only around Tohatin village there are more than 40 soils types. A second important feature of soils is the large percentage (about 70%) of chernozem that has different subtypes: typical, ordinary, podzolic, carbonate, leached, etc. (Fig. 1.3). Typical chernozem contains more than 6% of humus up to 1.20 m depth with a maximum soil bonitet (quality) score (100).

However, the soil cover here is presented not only by all subtypes of chernozems, but also by forest and alluvial soils in the river floodplains. Catchments and floodplains account for a third of the territory, with many ravines where light clays and heavy loams predominate, and erosion and land slide processes are especially manifested. The intensity of the soil erosion manifestation is also largely determined by the relief of an area, the main indicators of which are degree of surface dissection, depth of local erosion bases, length and shape of slopes (Leah and Kuharuk, 2017). In Moldova, depending on the relief morphometric characteristics, the degree of soil erosion manifestation is estimated by five degrees (Table 1.1).

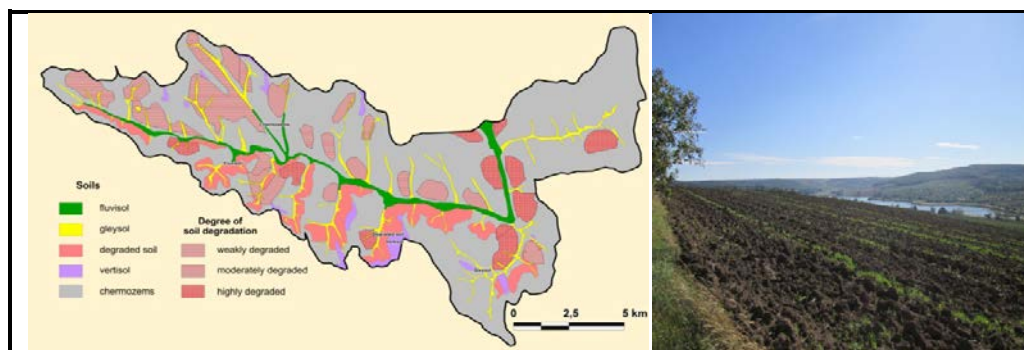


Fig. 1.3 Soil map of the Baltata basin and example of its ordinary chernozem

Table 1.1 Dependence of the soil erosion intensity on relief morphometric characteristics in Moldova (Source: Ursu, 2000)

Degree of erosion	Hydrographic network	Average slope length, m	Erosion base depth, m	Part of area (%) of slopes different steepness (degree)	
				More 20°	More 60°
Insignificant	0,3	<300	>50	20	5
Weak	0,3-0,5	300-500	50-70	20-40	5-10
Medium	0,5-0,6	500-700	100-100	40-50	10-20
Strong	0,6-0,7	700-1,000	100-150	50-70	20-25
Very strong	>0,7	>1,000	<150	>70	>25

The study area soils are strongly affected by erosion processes. About 60% of its carbonate and ordinary chernozems are subject to various types of erosion, and require anti-erosion measures. Without such measures the slightly eroded soils pass usually into the category of moderately eroded ones. The situation

Table 1.2 The eroded lands in the Baltata basin

Locality	Area of eroded lands, ha			Total
	Weak	Medium	Strong	
Mălăești	55	149	122	326
Balabanești	350	73	14	437
Bălțata	541	119	77	737
Budești	452	296	86	834
Cruzești	225	53	17	295
Tohatin	138	92	39	269
Stauceni	648	194	143	985
<b>Total</b>	<b>2410</b>	<b>976</b>	<b>498</b>	<b>3880</b>
<b>Percent</b>	<b>18.2</b>	<b>7.4</b>	<b>3.8</b>	<b>29.3</b>

with assessed here eroded lands, according to Moldavian classification, is shown in Table 1.2. Due to predominantly hilly landscapes, the landslides are very characteristic for Moldova's landscapes, provoking erosion. This is also linked with the deforestation processes and intensive pasturing, especially of goats and sheep.

### 1.3.3 Current climate of the pilot area

The key parameters of current climate in the study area are based on observation data at the Baltata weather station, located practically in their centre. The selected time interval (1981-2020) reflects the World Meteorological Organization (WMO) last climatic period (Hulme, 2020). Special attention is paid to maximum and minimum temperatures because an increase in frequency and amplitudes of extreme events is considered not only as a main climate change danger, but also as a driver of different extremes in exogenous processes. Mean values of corresponding meteorological parameters are shown in Table 1.3. The annual course of monthly mean air temperature, with its maximum in July and minimum in January, as well as precipitation sum, with maximum in June and minimum in February, are shown in Fig. 1.4.

**Table 1.3** Mean (*Tmean*), maximum (*Tmax*) and minimum (*Tmin*) air temperatures, precipitation (*P*) and wet days at the Baltata weather station in 1991-2020

Climatic parameter	Month											
	1	2	3	4	5	6	7	8	9	10	11	12
<i>Tmean</i> , °C	-1.8	-0.2	4.4	10.8	16.4	20.3	22.3	21.8	16.3	10.1	4.8	-0.1
<i>Tmax</i> , °C	1.6	3.9	9.9	17.2	23.1	26.8	29.1	29.0	23.0	16.1	8.7	3.2
<i>Tmin</i> , °C	-5.1	-3.9	-0.5	4.5	9.6	13.7	15.6	14.6	10.0	5.0	1.3	-3.3
<i>P</i> , mm	29	24	30	33	50	68	63	48	45	40	37	34
<i>Wet days</i>	3.5	3.4	4.3	5.5	6.4	7.4	6.3	5.3	4.4	4.2	4.2	4.4

Note: *Wet days* - a day with precipitation more 0.1 mm

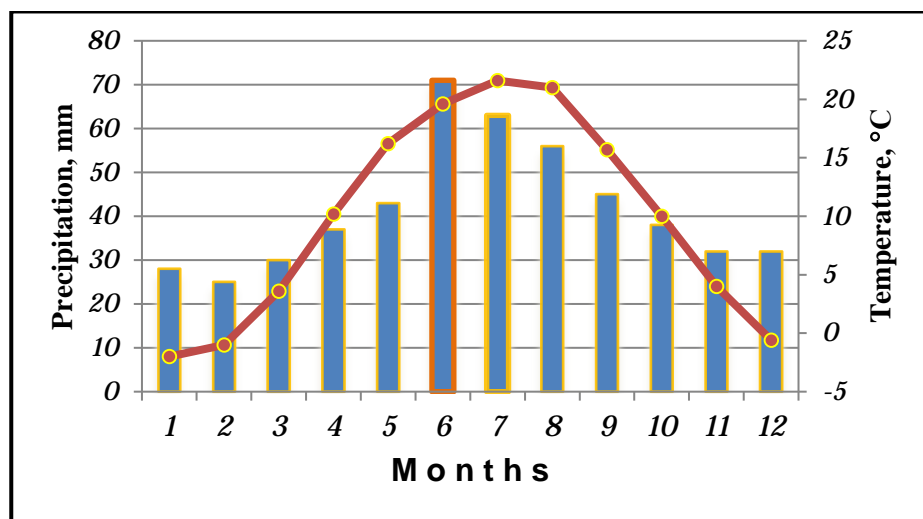


**Fig. 1.4.** Mean monthly precipitation (*columns*) and mean monthly air temperatures (red) at the Baltata weather station in 1981-2010



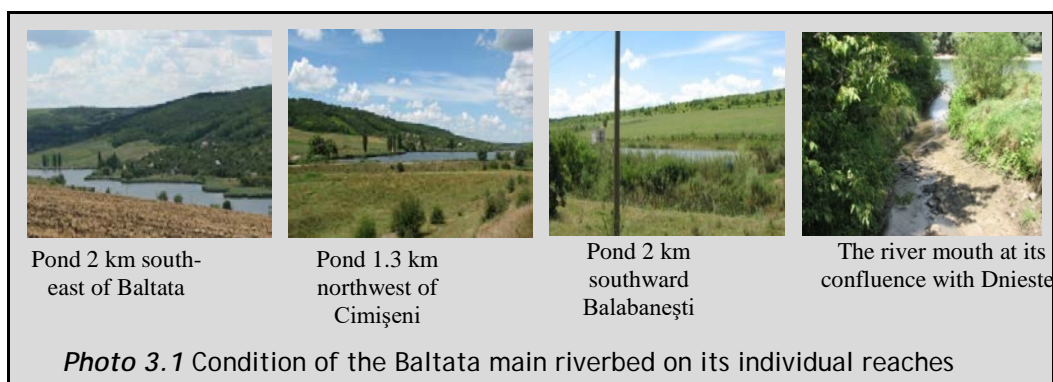
However, climate is described not only by mean values, but also by their variability. Air temperature in the pilot area is most variable in winter, reaching about 25-30% for maximum and minimum temperatures. Mean monthly temperatures are less volatile (from 5.3% in summer to 11.8% in winter). The interannual annual temperatures range from 4.1% for mean values to about 8% and 15% for maximum and minimum values, respectively.

The interannual variability of **precipitation** is much higher: by 35-50% in the seasonal context, being higher in the autumn-winter period and the lowest in summer. The typical for Moldova is alternation of wet and dry years. For example, in the Baltata basin only 282 mm of precipitation were observed in the extremely dry 1994 against 659 mm – in the wettest 2001.

### 1.3.4 The Baltata River flow

At present, due to intensive anthropogenic load, the Baltata River is completely transformed. Its natural flow has significantly changed and practically all accumulates in four artificial ponds: three – directly in the riverbed and one – in its right tributary (the Recea River) near Balabanesti village. As a result, the river channel has actually turned into a shallow watercourse, including in the mouth, where it ends into the Dniester River (Photo 3.1). Today a water intake for serious practical needs can really be carried out only from these artificial reservoirs.

Regular instrumental observations of the Baltata runoff were carried out at the hydrological post, located near of the same name village, but only between 1954 and 2012. Therefore, the available series of observations made it possible to carry out some purely research estimates of the historical river flow (e.g., Sirodoev at al., 2022), which is practically impossible to do for the to-date flow.





The comparison of the seasonal and annual Baltata water discharge in two previous comparable in time periods (Table 1.4) clearly demonstrates its decrease in all seasons, except in autumn months when some increase is observed. In particular, in 1996-2012 vs. 1961-1976 the spring flow has decreased by more than 40%; similarly, in winter and summer it decreased by 15-20%. This decrease has not been compensated by an autumn increase (~17%), and the resulting annual flow decreased by above 20%.

**Table 1.4** The Baltata flow in two observation periods

Season	Period		Flow change	
	1961-1976	1996-2012	Abs., l/sec	Related %
<i>Winter</i>	49.0	41.7	-7.3	-15.0
<i>Spring</i>	77.9	46.4	-31.5	-40.4
<i>Summer</i>	49.3	38.7	-10.6	-21.4
<i>Autumn</i>	35.6	41.8	6.2	17.4
<b>Year</b>	<b>53.0</b>	<b>42.2</b>	<b>-10.8</b>	<b>-20.5</b>

On a monthly basis, the maximum flow occurs in March and February that is especially clearly visible in the first period of its registration (Fig. 1.5). In those years, the second, much smaller flow peak was observed in June-July. However, in 1996-2012 the February-March peak of the Baltata flow significantly decreased, as well as the summer maximum. Against the general background of diagram alignment the monthly mean values, the share of autumn runoff has increased.

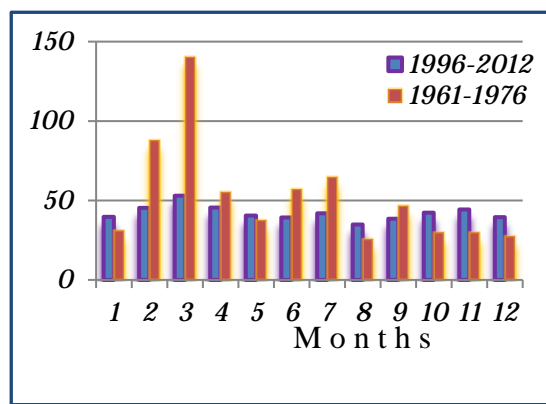


**Fig. 1.5** The annual dynamic of Baltata flow (l/sec) in two periods

It can be assumed the observed changes in the Baltata runoff are associated with a new temperature and humidity regime in the region. In particular, since the air temperature increase is not compensated by a proportional increase in precipitation, the adequate increase in climate aridity takes place and consequently – a corresponding reduction in the surface runoff and river flow.

## **2 Hydrological modeling of the rivers streamflow and sedimentation**

### **2.1 Hydrological modeling as a concept**

The movement and storage of water at watershed scales is a complex system affected by climatic, geologic, soil, land use, anthropogenic and other factors. A nature of the processes inherent in surface and subsurface hydrology is best investigated by the hydrologic models simulating these processes over different spatial and time intervals, and in different physiographical conditions.

By definition, any hydrologic model is certain simplification of a real-world water system (surface and soil waters, wetland, groundwater, estuary, etc.); such simplification aids in understanding, predicting and management of water resources. In recent years, a number of conceptual hydrological simulation models have been developed and increasingly used by hydrologists and water resource managers to understand and address the extensive array of water resource problems, including those related to watersheds, streamflow and reservoir management, as well as to human activities that affect water systems. Numerous review studies that provide comparisons either of specific components or complete hydrologic modeling packages, with varying levels of input/output data and their structure complexity, have been done by different authors (e.g., Beven, 2019; Daniel et al., 2011; Refsgaard et al., 2010; Van Liew et al., 2005 and 2007; Zhang et al., 2008).

However, while hydrology as a science has a long history, Singh (2018) attributes the birth of hydrologic modeling to the second half of the 1850s. Then, until the 1960s, many advances took place in modeling the different components of a hydrologic cycle, which were based mainly on mathematical physics, laboratory and field experiments. In the post-1960s decades, due to the computer revolution, the hydrologic modeling made a giant progress, and new branches of hydrology, such as a digital or numerical hydrology, statistical or stochastic hydrology were born. Finally, we are witnessing how a computing power is exponentially increasing, promoting the maturing of hydrological modeling, in particular, permitting to process huge quantities of raster and vector data in the Geographical Information Systems (GIS) environment.

The last point is especially important because many new research areas have emerged in the latest decades, in particular, the hydrological modeling

under the global environmental change – a domain, which has been receiving a lot of attention in public due to the increased frequency of hydrometeorological extremes and significant variability in the spatial and temporal distribution of precipitation. Sediment and pollutant transport in reservoirs, rivers and other water bodies have culminated into a new field of sedimentation engineering and its prevention, especially since the 1970s with the establishment of the Environmental Protection Agency (EPA, 2022).

Hydrologic models usually study a water flow and water quality, but are also used in decision-making at different scales. These models perform very well in long-term assessments of surface runoff, soil erosion and sediment yield for a wide range of soil types, land uses and climatic conditions (Dutta and Sen, 2018). Watershed, basinwide or other hydrologic modeling is considered as the best because it is economic and less time consuming. Singh (2018) highlighted several major advances and opportunities of hydrological modeling:

- ✚ Simulation of the entire hydrology;
- ✚ Development of research techniques that form a basis for reservoirs management as well as river basin simulation and hydrologic models calibrating;
- ✚ Creation of possibilities for two- and three-dimensional modeling;
- ✚ Simulation of liquid flow's different phases that result in simulation of a water flow and sediment/pollutant transport;
- ✚ Modeling at large spatial scales, such as a river basin, and at small temporal scales.

Integration of hydrology with allied sciences, for example, with climatology, includes climate change issues in hydrologic analysis.

The selection of a hydrological model depends on the research objectives, the availability of input data for its running and the uncertainty in interpreting the outputs obtained. Moreover, if to date many developed countries have their own hydrologic models, the developing countries are objectively limited in hydrologic modeling capabilities due to such factors as the maintenance, computational costs and technical capacity needed to develop and run up-to-date models. In this situation they are forced to use the well-proven foreign models, with appropriate validation and calibration for their regions. World experience shows that hydrological modeling for small catchments is most successfully solved, using hydrological models SWAT and WEPP. Both these models, which were used in this project, will be presented below. Their use solved three main problems: modeling the Baltata River runoff, estimating the transfer and accumulation of sediments in its catch-

ment and assessing the anthropogenic load on its flow. Although these tasks were solved in relation to one river of Moldova, the used approaches are quite acceptable for other small rivers of the country, which due to anthropogenic transformation (uncontrolled pollution, low farming cultures, illiterate land use, etc.), intensified by climate change, are catastrophically degraded or even disappear as watercourses.

## **2.2 SWAT modeling of the Baltata runoff under different climates**

### **2.2.1 SWAT model: history, initial validation and calibration**

Soil and Water Assessment Tool (SWAT) is among the most widely known models used for basin-wide research. In our study the ArcSWAT interface for SWAT2012 was used, which evolved from AVSWAT2000, which was developed for the earlier versions of ArcView (Winchell et al., 2013) and represents multiple decades of its components development (Gassman et al., 2014). The first version of SWAT appeared in the early 1990s, being further enhanced and improved (Arnold et al., 2012). Due to its comprehensive nature, strong technical support, and open-access status, the SWAT model has proven to be highly flexible in addressing a wide range of water resource problems. Hundreds of SWAT-related papers have been presented at numerous scientific meetings and in dozens of articles published in peer-reviewed journals. A good review of SWAT's extensive testing at different spatial scales was provided by Zhang et al. (2008); the widespread use of SWAT in comparison with several other leading models was demonstrated by Refsgaard et al. (2010). With quite a few input data, such as hydrological, geomorphological, soil and land use categories, this model, described in detail by various authors (Winchell et al., 2013; Arnold et al., 2012; Neitsch et al., 2011), is an extremely effective tool for assessing water resource availability for a wide range of scales and environmental conditions across the globe.

Nevertheless, certain weaknesses encountered in some of the SWAT outputs clearly show that expanded testing of this model, initially developed and adapted to specific conditions of the USA, is needed. As Gassman et al. (2014) noted, the SWAT users are to bear in mind that the modeling results should reasonably reflect the actual hydrologic processes. Due to this circumstance, any applied use of this model is preceded by its validation and calibration.

Validation of the SWAT was carried out through a comparison of the Baltata flow field measurements with the results of its modeling outputs. Given the presence in the Baltata riverbed three artificial reservoirs, for the SWAT validation the upper part of its basin upstream from the hydrological post where flow measurements were carried out was selected (Fig. 2.1). The length of this reach is 5.9 km, the drainage area – about 54.5 sq.km. In detail the validation procedure was published in Sirodoev et al. (2022), and here only its results are described.



**Fig 2.1** The upper part of the Baltata basin where SWAT validation was carried out

Following the main purpose of SWAT validation, the research approach included its use to simulate monthly and annual water inflows into the river mainstream and their subsequent comparison with the observed streamflow at the hydrological post Baltata. The study period included five years: from 1 January 2006 to 31 December 2010 when hydrological observations were the most reliable. The results of the SWAT simulation for each year are shown in Table 2.1. It contains information about each run of the model, including the corresponding statistics at the sub-catchment level, and allows the preliminary assessment of the representativeness of obtained estimates.

**Table 2.1** Results of the SWAT simulation in the Upper Baltata watershed

Year	SWAT Output Data, mm								WATER YIELD
	PREC	Runoff in the main stream			Infiltration in soil		Evapotranspiration		
		SURQ	LATQ	GWQ	LATE	SW	ET	PET	
2006	542	109.7	177.5	40.0	59.0	3.8	118.3	738.8	329.0
2007	466	94.5	148.6	30.3	48.5	3.8	110.0	741.5	274.9
2008	466	93.2	151.1	30.6	49.0	3.7	109.7	741.1	276.4
2009	426	85.5	134.4	25.9	43.8	3.8	104.3	742.7	247.1
2010	501	101.3	161.5	34.4	53.0	3.8	114.6	740.9	298.9
Average	480	96.8	154.6	32.2	50.6	3.8	111.4	741.0	285.2

**Abbreviations:** *RREC* – average amount of simulated precipitation; *SURQ* – surface runoff contribution to streamflow; *LATQ* – lateral flow contribution to streamflow; *GWQ* – ground water contribution to streamflow; *LATE* – water percolation past bottom of soil profile; *SW* – water amount stored in soil profile; *ET* – actual evapotranspiration; *PET* – potential evapotranspiration; *WATER YIELD* – water yield to streamflow.

The analysis of simulation results gives certain grounds to consider them as quite correct from a physical point of view. In particular, the total water

inflow into the main channel on average exceeds the infiltration into the soil by about 5.2 times, and the average ratio of real evapotranspiration to precipitation is 0.24. Nevertheless, SWAT, like any other complex hydrological model, contains a large number of input parameters and assumptions that lead to inevitable errors in the results. As one can see from Table 2.2, the relative discrepancies between observed and simulated runoff are too large to be negligible.

**Table 2.2** The ratio of the observed and simulated Baltata flow (m<sup>3</sup>)

Year	Months												Year
	1	2	3	4	5	6	7	8	9	10	11	12	
The ratio of the observed to simulated flows													
2006	–	0.129	2.298	0.154	0.139	0.278	0.207	0.019	0.027	0.112	0.174	0.035	0.086
2007	–	0.203	2.727	0.235	0.151	0.312	0.142	0.010	0.023	0.137	0.248	0.470	0.094
2008	–	0.128	1.475	0.153	0.129	0.247	0.201	0.012	0.022	0.108	0.218	0.325	0.075
2009	–	0.143	2.766	0.230	0.151	0.337	0.265	0.013	0.023	0.120	0.248	0.429	0.084
2010	–	0.240	1.180	0.157	0.111	0.242	0.144	0.014	0.021	0.105	0.165	0.327	0.079

For example, if to express the observed annual runoff as a percentage of the simulated one, then it will be only about 8-9% of the latter. The monthly values showed a different, more complex picture: from a more than two-fold excess of the observed values over the modelled ones in March to 1-2% values during the low-water period (August-September). Obviously, such discrepancies require the model calibration.

Typically, the calibration process boils down to achieving the best fit between modeling results and coupled instrumental observations, which is achieved by changing the SWAT certain parameters (Arnold et al. 2012; Van Liew et al. 2005; Zhang et al. 2008). In Moldova the first such calibration was carried out in the framework of another BSB project where the runoff of another small watercourse (the Cogilnic River) was modeled (Corobov et al., 2016). However, in the current work the calibration was performed in accordance with the recommendations of Dutta and Sen (2018) who conducted a special extensive study on this issue.

### 2.2.2 The SWAT model run

Unlike to SWAT validation, the assessment of surface runoff in the study area was carried out for the entire Baltata watershed, taking into account its above discussed significant anthropogenic transformation. Due to this fea-

ture, the modeling of current and potential surface runoff included also the volume of water entering the ponds.

Key procedures of SWAT modeling included the Baltata River watershed delineation, formation of the relevant database with input information, defining the Hydrological Representative Units (HRUs), directly the SWAT model run and its outputs analysis.

The *watershed delineation* included identification of the Baltata reaches and corresponding sub-watersheds. The delineation was carried out in the ArcSWAT environment, using the Digital Elevation Model (DEM) developed in the project framework. Its scale (1:25000) was suitable for hydrological analysis, and maps vectorization, based on this DEM, provided pixel size 10x10 m sufficient for a hydrological analysis.

The *Baltata reaches* were defined as lengths of its channel where drainage areas were more than a set threshold, or critical value that defines the minimum catchment area of upstream tributaries required to form a source of flow (Winchell et al., 2013). In particular, the division of the entire Baltata basin, with a total area of 153.9 km<sup>2</sup> and selected threshold value of 300 ha, resulted in 27 sub-basins (Fig. 2.2). The length of reaches is from 0.22 km to 7.70 km (2.27 km on average); the mean, maximum and minimum areas of sub-basins are 5.86, 26.19, and 0.23 km<sup>2</sup>, respectively (Table 2.3).

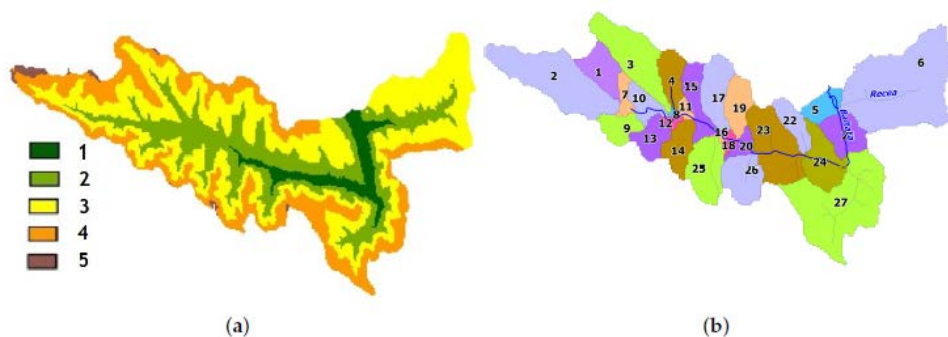


**Fig. 2.2** The Baltata River basin: (a) on a digital elevation model, given in color altitudes, m: 1 – > 50, 2 – 50-100, 3 – 100-150, 4 – 150-200, 5 – > 200); (b) the numbered sub-basins

*Input information* for SWAT simulation includes data on the basin's soil, landuse, slopes and climate. In Fig. 2.3 the *landuse* is represented by settlements – 733.7 ha, arable land – 10,103 ha, pastures – 93.7 ha, perennial plantations – 2067.9 ha, forests – 232.5 ha and surface waters – 66.5 ha.



The *soils* layer, based on maps of 1: 50.000 scale, was vectorized and converted to raster format and classified in accordance with the FAO Global Reference Soil Resources Database (IUSS, 2014). All soils were grouped into four types: black-earth (*Cernosiom*) – 14834.4 ha; alluvial soils (*Fluvisol*) – 596.8 ha; chernozem-like soils (*Gleysol*) – 826.8 ha and merged soils (*Vertisol*) – 391.4 ha.

The *slopes* were broken down by the degree of their erosion hazard into five categories (less than  $2^0$ , from  $2.0^0$  to  $7.0^0$ , from  $7.0^0$  to  $12.0^0$ , from  $12.0^0$  to  $15^0$  and more than  $15^0$ ), occupying respectively 34.3%, 31.9%, 16.6%, 15.8%, 1.4% and 0.1% of the entire Baltata catchment area.

Reclassification of land use, soil, and slope angle maps into SWAT formats allowed their overlap, resulting in the new SWAT's layer, called *Full HRU*, which was added to its DBs.

Table 2.2 Area of the Baltata river's sub-basins

N <sup>o</sup>	S, ha	N <sup>o</sup>	S, ha	N <sup>o</sup>	S, ha
1	465,75	10	286,74	19	419,58
2	1577,07	11	82,62	20	153,09
3	1009,26	12	62,37	21	474,66
4	382,32	13	366,93	22	341,01
5	289,17	14	411,48	23	997,92
6	2597,67	15	452,79	24	631,80
7	168,48	16	23,49	25	656,10
8	23,49	17	575,91	26	566,19
9	324,00	18	77,76	27	1969,92

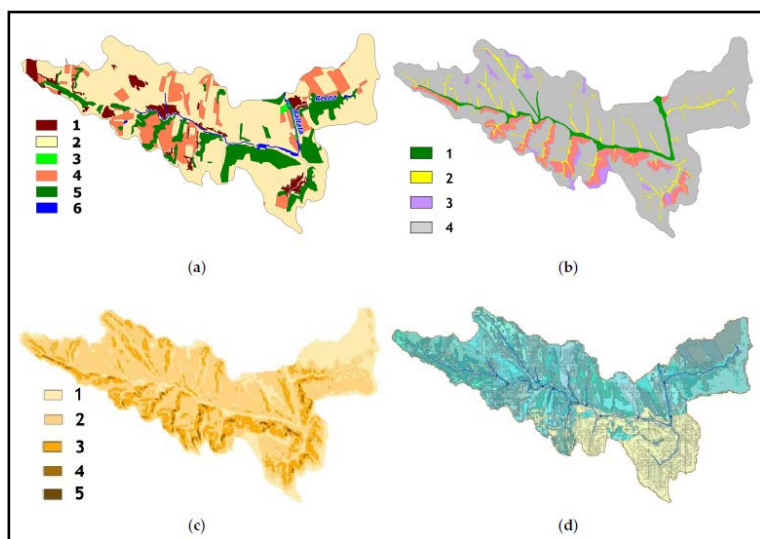


Fig. 2.3 Thematic layers for identification of hydrologic response units (HRU) in the Baltata River Basin:

- (a) Land use types: 1 – urban fabric, 2 – cropland, 3 – pastures, 4 – orchards, 5 – forests, 6 – water;  
 (b) Soil types: 1 – fluvisols, 2 – vertisols, 3 – gleysols, 4 – chernozems;  
 (c) Slope angles: 1 –  $< 2^0$ , 2 –  $2-7^0$ , 3 –  $7-12^0$ , 4 –  $> 12^0$ ; (d) Overlapping layer (*Full HRU*).



### 2.2.3 The Baltata River runoff under current climate

The key parameters of the Baltata basin climate in 1981-2010 – a period chosen by the IPCC as the baseline thirty years for projecting climate change expected in the 21st century – are shown in Table 2.3. The selected statistics include data, which serve as input parameters for runoff simulation in the SWAT. Other climatic variables, required for modeling, were calculated by a weather generator, which is one of the SWAT tools.

The basic spatial distribution of a modeling annual surface runoff in the Baltata watershed in current climate is shown in Fig. 2.4. As we can see, the maximum annual runoff (> 324 mm) occurs in the extreme northwestern part of the basin, and the minimum (<315 mm) – in its southwestern part, south of Budeshti. However, over a large part of the territory, the runoff is in the range of 318-324 mm.

**Table 2.3** Mean monthly maximum ( $T_{max}$ ) and minimum ( $T_{min}$ ) air temperatures, their standard deviation ( $Sd$ ) and precipitation ( $P$ ) at Baltata weather station

Climatic variable	Months											
	1	2	3	4	5	6	7	8	9	10	11	12
$T_{max}$ , °C	1,3	3,0	8,7	16,3	22,7	25,8	28,0	27,8	22,2	15,7	7,9	2,6
$Sd$	3,1	4,0	3,6	2,2	2,0	1,7	1,9	1,9	2,1	1,4	2,9	2,6
$T_{min}$ , °C	-5,2	-4,6	-0,9	4,5	9,5	13,4	15,2	14,4	9,8	4,9	0,5	-3,7
$Sd$	3,2	3,2	2,0	1,4	1,2	0,9	1,3	1,1	1,1	1,4	3,0	2,7
$P$ , mm	28	25	30	37	43	71	63	56	45	38	32	32

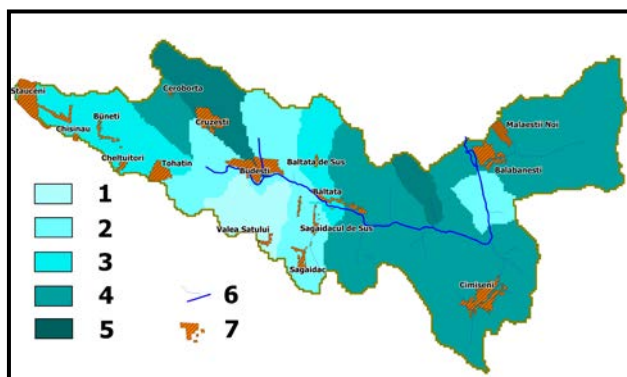


**Fig. 2.4** Spatial distribution of annual surface runoff (mm) in the Baltata River basin in 1981-2020

**Note:** 1 – < 315, 2 – 315-318, 3 – 318-321; 4 – 321-324, 5 – > 324 mm.  
6 – main river and its tributaries; 7 – settlements.

Multiplying the runoff per unit area in mm by the catchment area has given its total monthly values in km<sup>3</sup> (Table 2.4). The minimum runoff is observed in winter and spring; the maximum – in summer. The modeling or potential annual runoff in the Baltata basin can reach 0.048 cubic kilometers. However, given an undoubted bias in these estimates due to an anthropogenic load on the watershed, these results should be considered with some caution. At the same time, they provide a certain basis for assessing other impacts on the runoff, for example, caused by climate change.

**Table 2.4** SWAT modeling of monthly runoff in the Baltata River basin and its accumulation in the reservoirs in 1981-2010

Reservoirs	S e a s o n s				Annual runoff	
	Winter	Spring	Summer	Autumn	mm	km <sup>3</sup>
<i>Baltata</i>	14,15	5,29	22,3	15,2	44,94	0,004349
<i>Baltata</i>	4,49	11,2	42,0	30,0	87,89	0,009341
<i>Cimiseni</i>	6,84	17,4	64,1	45,2	133,54	0,017197
<i>Balabanesti</i>	1,62	2,86	12,3	10,6	27,18	0,000393
<b>Total runoff:</b>						
<i>into reservoirs</i>	14,7	36,75	140,7	101,0	<b>293,55</b>	<b>0,03128</b>
<i>in the basin</i>	15,9	40,9	148,3	106,5	<b>311,8</b>	<b>0,04799</b>

In addition to modeling the potential total runoff from the Baltata entire watershed, its potential inflow into existing here reservoirs was also modeled. These reservoirs accumulate water to provide the purely economic needs of local population, first of all, for irrigation of agricultural fields and household plots, as well as fish farming, recreation, etc. This annual water accumulation can be now from amount up to ~ 0.0004 km<sup>3</sup> in the reservoirs near Balabanesti to 0.017 km<sup>3</sup> near Chimiseni, and more than 0.031 km<sup>3</sup> on the whole, or about 65% of the watershed total runoff.

Since a surface runoff is the main factor determining the pollutants and sediments transfer, it can be assumed that, in accordance with its annual distribution, their accumulation in reservoirs will also be formed.

## 2.2.4 The Baltata River runoff under likely future climate

### 2.2.4.1 Climate change modelling

Modeling of the possible future surface runoff in the Baltata watershed was based on the projections of expected changes in local climate. In general, assessing the impacts of these changes requires their high-resolution scenar-



tion of the Baltata basin in the net of *CORDEX*'s nodes is shown in Fig. 2.5. In more detail the RCPs description and this part of research description can be found in Sîrodoev et al., 2022.

#### 2.2.4.2 Projections of likely future air temperature and precipitation

The projections of future mean air temperatures in the study area, developed according to the *CORDEX* methodology, are shown in Table 2.5.

A short analysis of the obtained results shows that in case of the radiative load stabilization (scenario RCP2.6), the average annual air temperature will increase here slightly: within 0.1°C by the middle of this century and by 0.2°C by its end. The largest increase will occur along the pathway of the high radiation load (RCP8.5). At the same time, if in the first half of the century an annual temperatures increase will still be within the permissible interval of 2°C, amounting to 1.6 °C, then by the late century this "tolerance" will be exceeded by more than 2 times and the temperature increase can reach 4.4°C. The pathway of intermediate stabilization (RCP4.5) begins to take adverse irreversible effect (up to 2.5°C) only in 2071-2100.

**Table 2.5** Projections of mean air temperatures change in the Baltata basin, °C

Season	1971 - 2000	Time horizon (years)					
		2021-2050			2071-2100		
		Representative Concentration Pathways (RCPs)					
		RCP2.6	RCP4.5	RCP8.5	RCP2.6	RCP4.5	RCP8.5
Winter	-2.0	0,5	1,9	2,0	0,8	2,8	5,1
Spring	9.4	-0,2	1,2	1,6	0,4	2,4	3,8
Summer	19.7	0,2	1,7	1,5	-0,3	2,7	4,8
Autumn	9.1	0,1	1,1	1,5	-0,2	2,1	3,8
Year	9.1	0,1	1,5	1,6	0,2	2,5	4,4

The greatest, in absolute values, warming is expected in winter, when it can amount, depending on a RCP, from 0.5 °C to 2 °C by the middle of the century and from 0.8 °C to 5.1 °C – by its end. A fairly high, albeit somewhat less, increase in temperatures is also expected in the summer: to 1.5-1.7°C by the first period and 4.8°C in the last thirty years. In transitional seasons, the temperature increase is slightly lower.

To estimate the probable changes in maximum and minimum air temperatures, which serve as input parameters to SWAT modeling, there were used their high and statistically significant relationship with mean tempera-

tures. In particular, the correlation coefficient  $r$  of maximum temperatures with mean ones is about 0.97-0.98 for monthly and 0.95 for annual values. The relationship between minimum and mean temperatures is somewhat lower; nevertheless, it is also quite sufficient for reliable statistical prediction of changes in this parameter.

Results of transition from mean temperatures to their maximum and minimum values are shown in Table 2.6. The absolute change in maximum temperatures will be slightly higher than expected changes in mean temperatures, while the change in minimum temperatures will be slightly lower. However, the statistical analysis, which essentially presupposes a synchronous change in all temperature parameters, is to a certain extent applicable only under conditions of a stationary climate that ensures immutability of climate variability over time. Undoubtedly, under conditions of anthropogenic climate change, these statistical dependencies can be violated.

**Table 2.6** Projections of the maximum ( $T_{max}$ ) and minimum ( $T_{min}$ ) air temperatures ( $^{\circ}\text{C}$ ) changes in Baltata basin relative to 1971-2000 by seasons

Season	Time horizons (years)											
	2021-2050						2071-2100					
	Representative concentration pathways (RCPs)											
	RCP2.6		RCP4.5		RCP8.5		RCP2.6		RCP4.5		RCP8.5	
	T <sub>max</sub>	T <sub>min</sub>	T <sub>max</sub>	T <sub>min</sub>	T <sub>max</sub>	T <sub>min</sub>	T <sub>max</sub>	T <sub>min</sub>	T <sub>max</sub>	T <sub>min</sub>	T <sub>max</sub>	T <sub>min</sub>
Winter	2.6	-4.1	4.2	2.1	4.3	2.1	3.0	-3.7	5.2	-1.5	7.6	0.6
Spring	15.1	4.3	17.1	0.9	17.5	1.1	15.7	4.6	18.7	6.0	20.5	6.9
Summer	26.6	14.1	28.4	1.4	28.1	1.2	26.2	13.9	29.7	16.3	31.9	17.9
Autumn	15.1	4.9	16.1	1.0	16.5	1.4	14.9	4.8	17.2	6.8	19.0	8.2
Year	14.9	4.7	16.5	1.3	16.6	1.4	15.0	4.8	17.8	6.7	19.9	8.1

The results of CORDEX modeling of likely changes in precipitation, expressed in absolute and relative values, are shown in Table 2.7. They allow drawing two principal conclusions.

1. Changes in precipitation depend directly on the level of radiative load. In particular, by the middle of this century, given the load will be stabilized (scenario RCP2.6), the annual precipitation sum in the Baltata basin will decrease by 5.1%, however in the late century it will increase by 7%, primarily due to its increase in spring. According to intermediate (RCP4.5) and high radiative load (RCP8.5) in the middle century the total annual precipitation is expected to be practically at the level of 1971-2000 (decrease

by 1-2%), and later – slightly increases (~by 5%). Thus, on the whole, we can expect that in the current century changes in precipitations will be by  $\pm 5\%$ .

**Table 2.7** Projectiond of precipitation change in absolute (*Abs*, *mm*) and relative (%) expression in the Baltata basin relative to 1971-2000

Season	1971-2000	Time horizons (years)											
		2021-2050						2071-2100					
		Representative Concentration Pathways (RCPs)											
		RCP2.6		RCP4.5		RCP8.5		RCP2.6		RCP4.5		RCP8.5	
		<i>A<math>\delta</math>c</i>	%	<i>A<math>\delta</math>c</i>	%	<i>A<math>\delta</math>c</i>	%	<i>A<math>\delta</math>c</i>	%	<i>A<math>\delta</math>c</i>	%	<i>A<math>\delta</math>c</i>	%
<i>Winter</i>	85	4	4.7	21	24.7	12	16.6	4	4.7	19	22.4	10	11.8
<i>Spring</i>	117	30	21.9	8	5.8	5	4.3	30	25.5	15	12.8	8.5	14.6
<i>Summer</i>	193	-49	-25.4	-44	-22.8	-32	-16.6	-15	-7.8	-26	-13.5	-53	-27.5
<i>August</i>	118	-12	-10.2	6	5.1	2	1.7	17	5.7	17	14.4	6	5.1
<b><i>Year</i></b>	<b>512</b>	<b>-26</b>	<b>-5.1</b>	<b>-7</b>	<b>-1.4</b>	<b>-12</b>	<b>-2.3</b>	<b>36</b>	<b>7.0</b>	<b>26</b>	<b>5.1</b>	<b>25</b>	<b>4.9</b>

2. Seasonally, the greatest changes in precipitation are expected in the summer when under all scenarios they decrease by 25-27% and more from their baseline values. Also, it is expected certain precipitation shift in the warm period to earlier dates. The smallest precipitation changes are expected in autumn.

#### 2.2.4.3 The Baltata runoff under future climate

According to the SWAT simulation (Tables 2.8), a possible change in surface runoff from the Baltata watershed due to new temperature and humidity conditions may be, depending on the time horizon and radiative load, from an increase by 7-8% at moderate and strong loads in the first half of 21th century to a decrease from about 8% to more 25% at the late century. On average, an increase in runoff can reach about 2% in 2021-2050, and a decrease – up to 17% in 2071-2100. Correspondingly, the volumes of water entering the basin's reservoirs will change (Table 2.9).

If we use the gradation of risks from a runoff decrease, proposed by the US Department of Agriculture (USDA FS, 2013), the obtained values of runoff change of less than 20% can be considered as a low risk, from 20 to 40% as a moderate, and more than 40% as a high risks.

Of course, the obtained results, due to the presence of a number of uncertainties, should be considered only as some rough estimates. At the same time, there are no doubts that the correct use of SWAT hydrological modeling allows, on the one hand, to calculate correctly the potential water re-

sources even of a small river, and on the other hand, to account for the flow losses due to various kinds of anthropogenic loads on their state, sometimes caused by the poor water management. The lack of such accounting, combined with climate change, negatively affects the quantity and quality of water, including sediments and pollution accumulation, provided by the Baltata River and its potential for self-purification.

**Table 2.8** Modeling projections of changes in the Baltata watershed surface runoff in absolute (*Abs*, *mm*) and relative expression (%) relative to 1981-2010

Month		Time horizons, years											
		2021-2050						2071-2100					
		Representative Concentration Pathways (RCPs)											
		RCP2.6		RCP4.5		RCP8.5		RCP2.6		RCP4.5		RCP8.5	
1981-2010	Abs.	%	Abs.	%	Abs.	%	Abs.	%	Abs.	%	Abs.	%	
January	0,4	0,2	46,3	0,7	158,5	0,6	136,6	-0,4	-100	-0,4	-100	-0,4	-100
February	15,1	2,6	17,0	7,6	50,1	7,3	48,1	-10,2	-67,5	-8,8	-58,1	-9,5	-62,9
March	27,4	1,2	4,2	6,0	21,8	5,8	21,2	-9,4	-34,4	-4,4	-15,9	-8,0	-29,2
April	8,9	13,5	152,1	5,6	63,4	5,2	58,9	-8,9	-99,9	-8,8	-98,6	-8,9	-99,8
May	4,6	6,8	148,5	1,7	36,5	1,5	32,2	-4,6	-99,8	-4,6	-99,6	-4,6	-99,8
June	23,1	4,6	20,0	-2,1	-9,0	-2,8	-11,9	-22,1	-95,8	-21,4	-92,5	-22,0	-95,3
Ju/ly	62,2	-17,0	-27,4	-6,3	-10,1	-6,8	-10,9	-53,6	-86,2	-47,4	-76,2	-51,7	-83,1
August	63,0	-20,2	-32,0	-4,8	-7,7	-5,2	-8,2	-43,1	-68,4	-36,4	-57,7	-41,1	-65,2
September	40,4	-8,6	-21,2	-1,7	-4,2	-1,8	-4,5	-21,8	-53,9	-14,8	-36,6	-19,7	-48,8
October	21,6	-6,1	-28,3	-3,2	-14,9	-3,3	-15,4	-7,2	-33,1	-1,2	-5,3	-5,4	-25,0
Noember	44,5	-9,0	-20,2	23,1	52,0	22,5	50,6	97,8	219,9	115,7	260,1	104,1	234,1
December	0,5	-0,1	-12,5	0,0	-2,1	0,0	-2,1	4,4	917	5,7	1196	4,8	991,7
Year	311,8	-32,0	-10,3	26,5	8,5	23,0	7,4	-79,2	-25,4	-26,6	-8,5	-62,4	-20,0

**Table 2.9** Modeling projections of changes in the Baltata watershed runoff into artificial reservoirs/ponds in absolute (*Abs*, *mm*) and relative expression (%) as to 1981-2010

P o n d	1981-2010	Time horizons, years											
		2021-2050						2071-2100					
		Representative Concentration Pathways (RCPs)											
		RCP2.6		RCP4.5		RCP8.5		RCP2.6		RCP4.5		RCP8.5	
		Abs	%	Abs	%	Abs	%	Abs	%	Abs	%	Abs	%
Baltata	44,9	-4,6	-10,3	3,8	8,5	3,3	7,4	-11,4	-25,4	-3,8	-8,5	-9,0	-20,0
Baltata	87,9	-9,1	-10,3	7,5	8,5	6,5	7,4	-22,3	-25,4	-7,5	-8,5	-17,6	-20,0
Cimisheni	133,5	-13,8	-10,3	11,4	8,5	9,9	7,4	-33,9	-25,4	-11,5	-8,5	-26,7	-20,0
Balabanest	27,2	-2,8	-10,3	2,3	8,5	2,0	7,4	-6,9	-25,4	-2,3	-8,5	-5,4	-20,0
Runoff into ponds	293,6	-30,2	-10,3	24,9	8,5	21,7	7,4	-74,6	-25,4	-24,9	-8,5	-58,7	-20,0

## 2.3 WEPP modeling of soil erosion and sediment deposition

### 2.3.1 Soil erosion as a global challenge

Serious environmental and economic problems, generated by soil erosion, are a global phenomenon that is considered as one of the most significant processes related to surface hydrology. At the same time, erosion is a complex process, which causes losses of soil fertility, land degradation, sedimentation in the rivers, lakes and reservoirs. Ultimately, it leads to the loss of agricultural resources and threatens built facilities. In recent decades, we are witnessing how land use, previously considered as an environmental issue of local importance, has become a global driver with various effects (EPA, 2022; Foley et al., 2005). A land degradation is also one of the major problems in the continental and regional context. In particular, the Seventh Pan-European Environmental Assessment (UN, 2022), describing the land use and land-use change in the pan-European region, considers land erosion as one of the negative land-use dynamics results, although with different characteristics throughout the region. According to this assessment, the field measurements in EU countries show an average rate of soil erosion of  $0.2\text{--}3.2 \text{ t ha}^{-1} \text{ year}^{-1}$  on a per-country basis. Over the past 30 years the average rate of soil erosion has especially decreased in Eastern Europe, following massive cropland abandonment and climate change. Moreover, as Is-saka and Ashraf (2017) revealed in their review, the erosion processes cause on-site and off-site effects not only on land but also on water, thereby affecting its quality.

Several large-scale studies made in Moldova have highlighted the unfavourable evolution of the great majority of its natural and socio-economic parameters, causing an increased risk for sustainable agriculture (Sirodoev et al., 2019). The intensity of soil erosion manifestation in the country is largely determined by the relief of its area where the degree of surface dissection, depth of erosion's local bases and length and shape of slopes form such a complex system that it becomes almost impossible to give a single characteristic to relief. On the rather gentle slopes (starting from  $5^\circ$ ) the ravines and landslides are intensively developing as the most widespread erosion forms. Moreover, this unique combination of natural factors is not limited to Moldova national borders, but is characteristic of a wider regional context, including neighbouring territories of Ukraine or Romania (Prefac et al., 2016). Due to these circumstances a differentiated



approach is required, for example, for each river catchment and even a slope, and a strong need for their comprehensive understanding and detailed assessment persists.

Generally, to conclude on the level and size of erosion impacts on soil problems the quantitative assessments are required. On this way, modeling of soil loss and sedimentation caused by erosion, along with field measurements, are a permanent challenge in natural resources and environmental planning. A special place in these studies belongs to hydrological processes, which cause and accelerate soil erosion. The movement and storage of water at watershed scales is a complex system affected by climatic, geologic, soil, land use, anthropogenic and other factors. The sediment and pollutant transport in reservoirs, rivers and other water bodies have culminated into a new field of sedimentation engineering and its prevention, especially since the 1970s with the establishment of the Environmental Protection Agency (EPA, 2022). This point is also especially important because in the latest decades many new research areas have emerged, in particular, the hydrological modeling under global warming – a domain that receive a lot of attention due to the increased frequency of hydrometeorological extremes (IPCC, 2013).

As it has been noted above (see Sub-section 2.1) the nature of processes inherent in surface and subsurface hydrology is best investigated by the hydrologic models simulation of these processes over different spatial and time intervals, and in different physiographical conditions. The *Water Erosion Prediction Project* model (usually and hereafter referred as WEPP), along with the SWAT, is one of such models.

### **2.3.2 GeoWEPP as a new modeling tool**

The *Water Erosion Prediction Project* model is the results of erosion process researches in the U.S., aimed to develop a process-based soil erosion model in contrast to the previous empirical approaches (Flanagan and Nearing, 1995; Flanagan et al., 2007). WEPP model incorporates the fundamentals of soil hydrologic and erosion science that consolidates climate, soil infiltration, water balance, plant growth and residues decomposition to predict finally a soil loss and sediment delivery and deposition over a range of time-scales, averaging the annual monthly and yearly totals for several decades.

The WEPP software, available at the time of its release (1985–1995), was written in FORTRAN and a rudimentary DOS-based interface (Flanagan et

al., 2013). However, further the model has been improved continuously, and in the late 1990s the GIS-linked and web-based model applications were developed. As present the WEPP has a number of customized interfaces developed for common applications such as a sediment yield and runoff (Yüksel et al., 2008), forests (Elliot, 2013), rangelands and so on, as well as for different scenarios of cropland soils and vegetation, describing a given erosion concern in great detail (Minkowski and Renschler, nd).

The first geospatial interface to the WEPP was GeoWEPP (Renschler, 2003), which was originally an extension of ArcView 3.2 and subsequently updated to function within the ArcGIS 9 system (Minkowski and Renschler, nd). GeoWEPP allows a user to access and import commonly available topographic, soils, and land use/land cover data layers to preprocess input information and conduct different scenario simulations. The linkage of environmental assessment tools and GIS, with their capability in handling geospatial information at various spatial and temporal scales, is very effective in soil erosion and sediment yield estimations (Manoj and Kothyari, 2000).

Generally, WEPP uses physically-based equations to describe hydrological soil loss and sediment generation as well as processes of their transport, thus addressing two fundamental tasks: runoff modeling and erosion and/transport modeling. *Runoff modeling* is required to obtain infiltration and surface runoff's volumes, which are a driving force in the soil detachment by flowing water in rills and channels. The *erosion processes*, represented in the WEPP, are limited to sheet and rill erosion, and erosion occurring in channels due to hydraulic shear; through its erosion components all three stages of erosion (detachment, transport and deposition) are quantified (Flanagan and Nearing, 1995).

GeoWEPP generates the watershed and channel network based on a corresponding DEM and so-called outlet point. Its application includes four essential steps (Minkowski and Renschler, nd; Renschler and Flanagan, 2002):

1. *Import of the DEM and its preprocessing for the WEPP database scale;*
2. *Channel and watershed delineation and discretization for modeling scale;*
3. *Input of the model's parameters and model run for the prediction scale;*
4. *Mapping model results and post-processing for the assessment scale.*

In this sequence the DEM is used to delineate the channel network, determine sub-catchments in the selected watershed, and generate information for WEPP running. All input data are prepared into UTM's coordinates and converted into ASCII files. After the DEM ASCII files preparation stage has been completed, the WEPP simulations can start.

As concern erosion and sediment simulating, the WEPP provides two alternatives: Watershed Method and Flowpath Method (Minkowski and Renschler, nd). The difference between these two methods is the following.

The *watershed method*, also called *offsite assessment*, uses only one soil and one management for each sub-catchment, thus losing the spatial variability of the entire catchment for these parameters; the *Flowpath method*, also called *onsite assessment*, retains the catchment diversity. Moreover, the first method reports a sediment yield of the entire study area; the second method shows *a soil loss* for its each portion.

For simulating soil loss and sediment yield in the Baltata River basin both methods were employed.

### 2.3.3 Preparing the GeoWEPP input information

The input information for a GeoWEPP simulation basically includes data on the DEM based watershed topography, soil, landuse/land cover and local climate.

The DEM in GeoWEPP is used to delineate the watershed's channel network, determine its sub-watersheds and generate hillslopes for the model running. As with working in the SWAT model, the DEM of the Baltata River basin was developed in the framework of this project (Fig. 2.6).

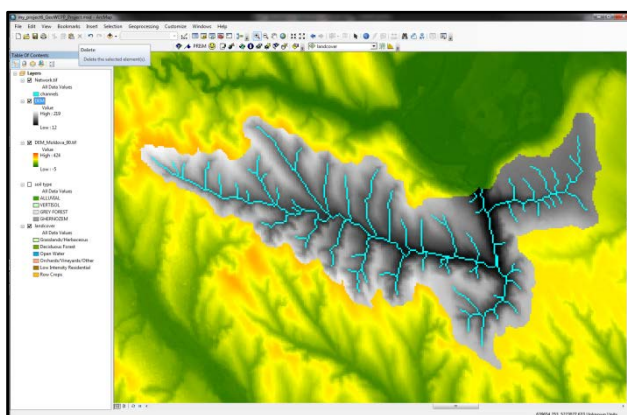


**Fig. 2.6** DEM of the Baltata River watershed, loaded into ArcMap, with overlaid its channel network

The main types of landuse in the Baltata basin were presented in Fig. 1.2 and for clarity of the GeoWEPP technology is duplicated here (Fig. 2.7). However, because the landuse data stored in that figure as a shape image cannot be projected properly when loaded into ArcMap, they were convert-

ed to an ASCII raster text file. Converting the landuse layer to ASCII has also required two text files that are needed to link the GIS data with the WEPP parameter files used in the simulation process. One of these files links the raster cell values with the landuse description; the second fail – with their attributes (Fig. 2.7).

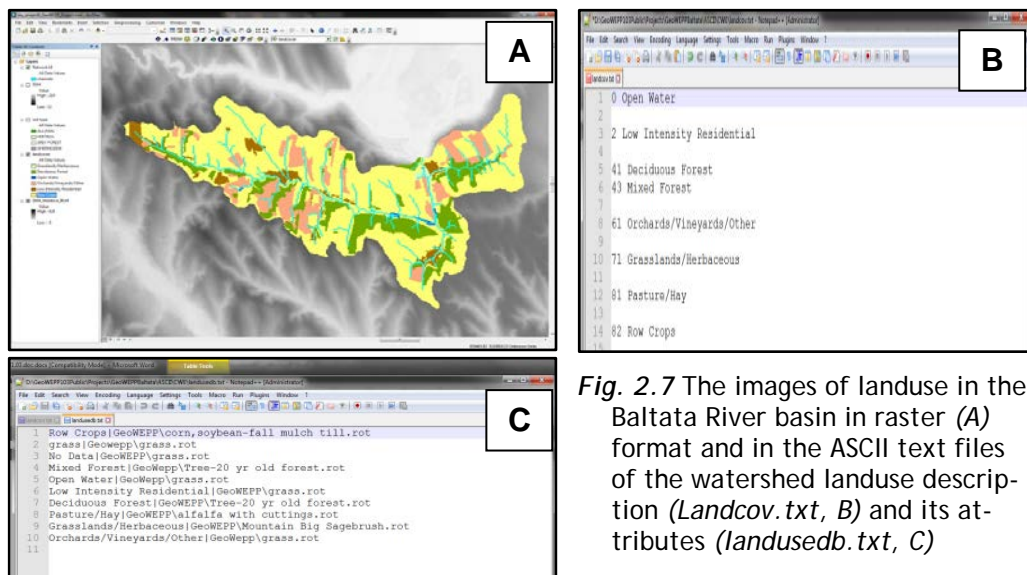


Fig. 2.7 The images of landuse in the Baltata River basin in raster (A) format and in the ASCII text files of the watershed landuse description (*Landcov.txt*, B) and its attributes (*landusedb.txt*, C)

Just like for the landuse, the soil data, stored as a shape image, to be projected properly when loaded into ArcMap were converted to ASCII raster file and two ASCII text files to link the soil GIS data with the WEPP soil parameter files (Fig. 2.8).

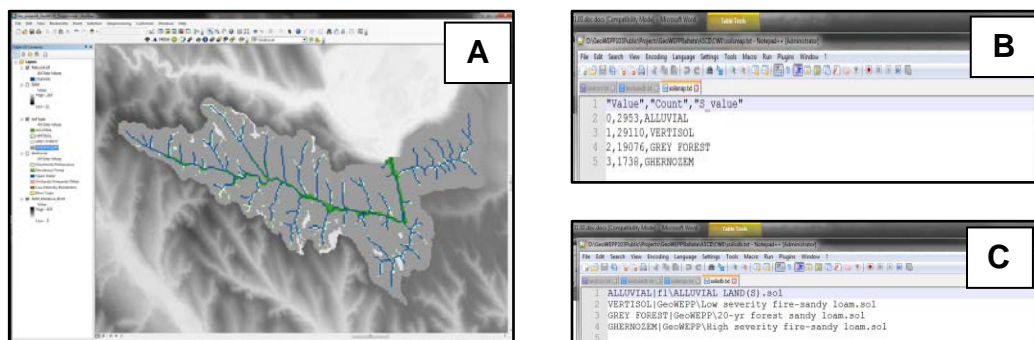


Fig. 2.8 The image of soils in the Baltata River basin in the raster format (A) and ASCII text files of their description (*soilsmap.txt*, B) and their attributes (*soilsdb.txt*, C)

As concerns the climate information, for a GeoWEPP simulation there is sufficient to have data on monthly mean maximum and minimum temperatures, precipitation and number of wet days. In our case, it was used observations at the Baltata weather station, averaged for 1991-2020 years (the last climatic period) and converted to Fahrenheit units according to the WEPP requirements (Table 2.10). Imputing the climate information, needed for WEPP simulation, is realized by the *Parameter-Regressions on Independent Slopes Model (PRISM)*. The model<sup>2</sup> allows modifying the available climate data for their use in WEPP (Fig. 2.9).

**Table 2.10** Mean (*Tmean*), maximum (*Tmax*), minimum (*Tmin*) air temperatures, precipitation (*P*) and wet days at the Baltata weather station in 1991-2020 in their initial (*upper table*) and modified for WEPP units (*lower table*)

Climatic parameter	Month											
	1	2	3	4	5	6	7	8	9	10	11	12
<i>Tmean</i> , °C	-1.8	-0.2	4.4	10.8	16.4	20.3	22.3	21.8	16.3	10.1	4.8	-0.1
<i>Tmax</i> , °C	1.6	3.9	9.9	17.2	23.1	26.8	29.1	29.0	23.0	16.1	8.7	3.2
<i>Tmin</i> , °C	-5.1	-3.9	-0.5	4.5	9.6	13.7	15.6	14.6	10.0	5.0	1.3	-3.3
<i>P</i> , mm	29	24	30	33	50	68	63	48	45	40	37	34
<i>Wet days</i>	3.5	3.4	4.3	5.5	6.4	7.4	6.3	5.3	4.4	4.2	4.2	4.4

Climatic parameter	Month											
	1	2	3	4	5	6	7	8	9	10	11	12
<i>Tmean</i> , °F	28.8	31.7	40.0	51.4	61.5	68.6	72.2	71.2	61.3	50.2	40.7	31.9
<i>Tmax</i> , °F	34.83	39.03	49.78	62.98	73.52	80.26	84.32	84.16	73.42	60.91	47.69	37.70
<i>Tmin</i> , °F	22.75	24.91	31.16	40.17	49.26	56.73	59.99	58.35	49.98	40.98	34.25	26.12
<i>P</i> , inch	1.13	0.96	1.18	1.30	1.98	2.69	2.48	1.88	1.78	1.58	1.46	1.33

The screenshot shows the PRISM Climate Modification software interface. At the top, there are input fields for 'Climate Parameters for' (SALT LAKE) and 'Modified Climate Name' (Baltata weather station). Below these, there are fields for 'W' (40.77) and 'N' (111.97) with a 'feet elevation' of 4220. To the right, there are fields for 'W' (29.03) and 'N' (47.05) with a 'feet elevation' of 259. The main part of the interface is a table with 12 columns representing months (January to December) and 4 rows representing climate parameters: Mean Maximum Temperature (°F), Mean Minimum Temperature (°F), Mean Precipitation (in), and Number of Wet Days. The table is organized into two columns, with the first column showing data for the original location and the second column showing modified data. The bottom of the window has buttons for 'Accept These Values', 'Clear All Changes', 'Help', and 'Exit', along with a checkbox for 'Adjust temperature for elevation by lapse rate'.

Mean Maximum Temperature (°F)	Mean Minimum Temperature (°F)	Mean Precipitation (in)	Number of Wet Days	Month	Mean Maximum Temperature (°F)	Mean Minimum Temperature (°F)	Mean Precipitation (in)	Number of Wet Days
36.58	19.76	1.19	9.92	January	34.83	22.72	1.13	3.50
43.40	24.54	1.16	8.26	February	39.03	24.91	0.96	3.40
51.97	31.08	1.69	9.94	March	49.78	31.16	1.18	4.30
61.71	37.90	2.04	9.26	April	62.98	40.17	1.30	5.50
71.91	45.67	1.74	8.72	May	73.52	49.26	1.98	6.40
83.15	54.13	0.85	5.32	June	80.26	56.73	2.69	7.40
92.52	62.34	0.73	4.55	July	84.32	59.99	2.48	6.30
90.09	60.82	0.83	5.56	August	84.16	58.35	1.88	5.30
79.47	50.82	1.06	5.57	September	73.42	49.98	1.78	4.40
66.10	39.88	1.30	5.90	October	60.91	40.98	1.58	4.20
50.08	29.73	1.40	8.22	November	47.69	34.25	1.46	4.20
35.32	22.00	1.35	9.64	December	37.70	26.12	1.33	4.40

**Fig. 2.9** PRISM modification of the Baltata basin climate in 1991-2020

<sup>2</sup> <https://prism.oregonstate.edu/>

### 2.3.4 GeoWEPP simulations and results

The GeoWEPP modeling starts from generation of a channel network in the watershed. This process, based on the basin's DEM, use two parameters: the *Critical Source Area* (CSA) and *Minimum Source Channel Length* (MSCL). CSA is a minimum source area needed to generate a channel; MSCL is the shortest distance the first order channel needs to travel before it converges with another channel. For the Baltata watershed delineation these parameters were setting of 100 ha and 3000 m, respectively (Fig. 2.10).

The watershed delineation ends with selecting an outlet point as a cell with only one channel flowing into it. Based on the selected outlet point, GeoWEPP generates the so called subcatchments. Each channel within this subcatchment has three hillslopes: *left*, *right*, and *source*. An example of this step is shown in Fig. 2.11.

Soil losses and sediments simulation in the Baltata watershed were estimated using the two above discussed approaches.

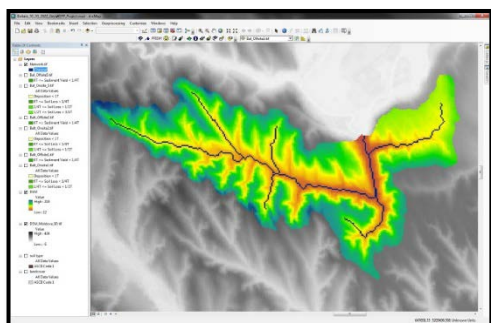


Fig. 2.10 The Baltata watershed network with Critical Source Area of 100 ha and Minimum Source Channel Length of 3000 m

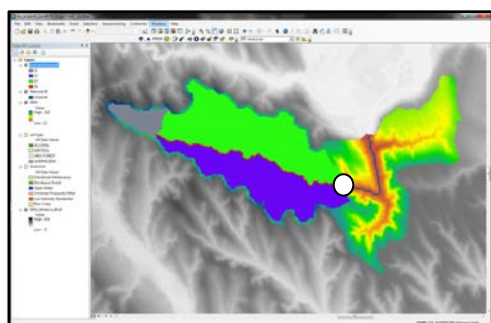


Fig. 2.11 The selected outlet point (white circle) and corresponding hillslopes in the Baltata watershed upper part

#### 2.3.4.1 Results of the WEPP offsite (watershed) simulation

The *offsite method* and its report provide the WEPP simulation results measured at the watershed outlet point, reflecting modeled values contributed by the catchment's hillslopes and channels. The offsite report focuses only on *sediment yields* delivered through channels to the outlet point from representative hillslopes. The soil losses on the hillslopes are mainly shown in the onsite report.



The results of the WEPP offsite simulation for the Baltata watershed, with its total contributing area to outlet equal 14062 ha, are shown in Tables 2.11 and 2.12.

**Table 2.11** Average annual sediment values in the Baltata watershed

Hill slopes	Runoff volume, m <sup>3</sup>	Subrunoff volume, m <sup>3</sup>	Soil loss, kg	Sediment, kg	
				deposition	yield
<i>1</i>	15148.00	23.19	0.00	20587.0	200590.65
<i>2</i>	14783.67	36.24	0.00	18231.3	18231.28
<i>3</i>	7140.20	5.67	0.00	0.00	0.00
...	...	...	...	...	...
<i>28</i>	13780.34	34/44	0/00	17367.0	17366/8

Column definition: *Hillslopes*: the WEPP hillslope being reported; *Runoff and Subrunoff Volumes*: the amount of runoff from each hillslope; *Soil Loss*: the amount of soil loss recorded for each hillslope; *Sediment Deposition*: the amount of soil deposition recorded for each hillslope; *Sediment Yield*: the amount of sediment yield recorded for each hillslope at the outlet point.

**Table 2.12** Average annual sediments values from 10 reliable channel outlets

Channels	Discharge value, m <sup>3</sup>	Sediment yield, ton	Soil loss, ton	Upland charge, m <sup>3</sup>	Subsurface flow, m <sup>3</sup>
<i>1</i>	36777.9	11.0	0.0	36668.6	0.0
<i>2</i>	105847.8	40.6	0.0	107167.0	0.0
<i>3</i>	221955.5	32.5	0.0	224715.4	0.0
...	...	...	...	...	...
<i>10</i>	116060.9	8.7	0.0	117209.8	0.0

Column definition: *Channels*: the WEPP channel being reported; *Discharge Volume*: the amount of water, discharged from the WEPP channel; *Sediment Yield*: the sediment yield from the channel; *Soil loss*: soil loss from channel; *Upland charge*: the amount of water entering the canal from hillslopes; *Subsurface flow*: underground water flow.

Distribution (fragments) of primary particles and organic matter (OM) in the eroded sediment is the follows: *clay* – 0.063; *silt* – 0.124; *sand* – 0.813; *organic matter* – 0.038. Index of specific surface (SSA), which expresses a property of solids and defined as the total surface area of a material per unit of mass, amounts 34.63 m<sup>2</sup>/g of total sediment. Enrichment ratio of specific surface = 2.50.

Average annual deliveries from the Baltata catchment area, contributed to outlet amounted:

- water discharge from outlet – 0.001 km<sup>3</sup>
- sediment discharge from outlet – 5432.2 ton/yr
- sediment delivery per unit area – 0.4 t/ha/yr
- sediment delivery ratio for watershed – 0.880.
- total hillslope soil loss – 2314.6 ton/yr
- total channel soil loss – 3855.8 ton/yr.

Thus, according to the modeling results, about 90% of the sediments, formed in the Baltata catchment in 1991-2010, enter the Dniester River. However, in our case, this figure reflects only a certain hypothetical situation, when the Baltata flow would be determined only by the purely physical and geographical conditions of its catchment, not disturbed by anthropogenic interference. A real situation, as noted in the description of the study area, is completely different, and can be expected that most sediments settle in reservoirs created in the Baltata riverbed. This is confirmed by additional estimates, demonstrated in the subsequent section.

WEPP offsite simulation of annual sediment delivery (0.4 t/ha/yr) has resulted in its fairly even distribution by territory (Fig. 2.12). In most of the watershed, the annual sediments per hectare are less than 1/4 t, followed by areas with sediments from 1/4 to 1/2 t, and only in the lower part of the riverbed they reach 1-2 tons.

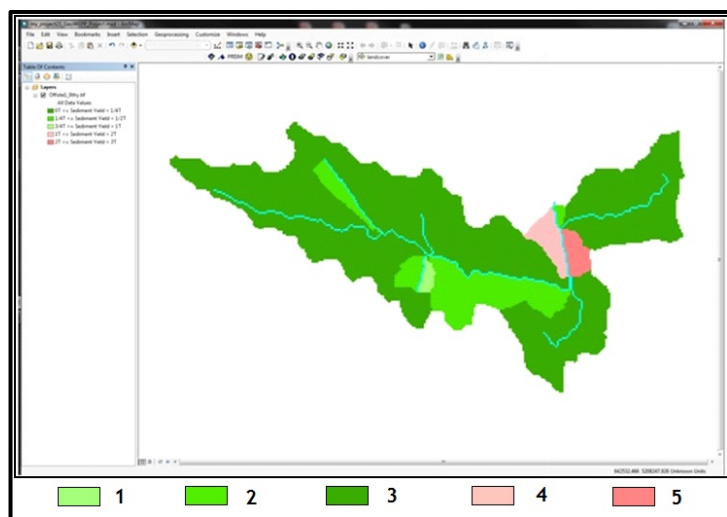


**Fig. 2.12** Map of WEPP offsite simulation of average annual sediments distribution in the Baltata River basin

**Sediment Yield (ton):**

1.  $0 \leq \text{Yield} < \frac{1}{4}$
2.  $\frac{1}{4} \leq \text{Yield} < \frac{1}{2}$
3.  $\frac{1}{2} \leq \text{Yield} < 1$
4.  $1.0 \leq \text{Yield} < 2.0$
5.  $2.0 \leq \text{Yield} < 3.0$

#### 2.3.4.2 Results of the WEPP onsite (flowpath) simulation

The results of WEPP *onsite*, or flowpath approach (Table 2.13) are focused on the *soil loss* occurring within each hillslope of the watershed. Estimation of the sediment yield, not simulated here, was shown in the offsite report. The total value of hillslopes soil loss (~21542 ton/yr) is a lot more than that, obtained by watershed method (~6170 ton/yr). Moreover, in this case, we obtain a high degree of soil loss detail across the basin; the corre-



sponding map of soils loss in the Baltata watershed, identified by WEPP flowpath simulation, is shown in Fig. 2.13.

**Table 2.13** Flowpass summary of soil loss simulation in the Baltata watershed

Hill slope	Area, ha	Runoff, m <sup>3</sup> /yr	Soil loss, ton/yr	Sediment yield, ton/yr	Mapping, ton/ha/yr	
					Soil loss	Sediment
<b>Left</b>	1185	113425	14167	n/a/	12.0	n/a/
<b>Right</b>	337	80496	6276	n/a/	18.6	n/a/
<b>Source</b>	147	24181	1099	n/a.	7.5	n/a.

Column definition: As in Table 2.3

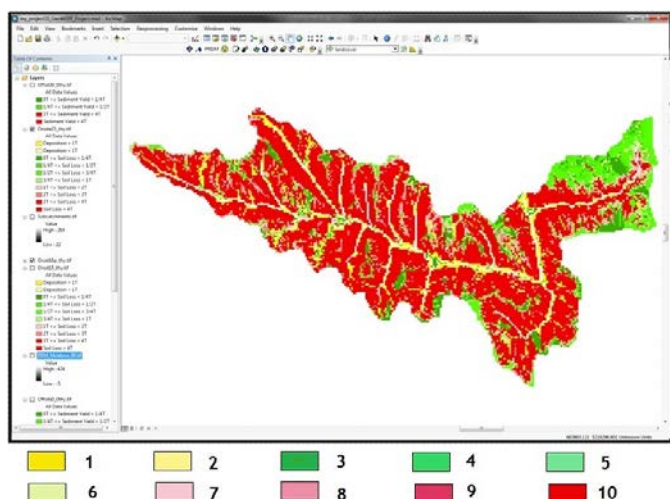


**Fig. 2.13** Map of the WEPP onsite simulation of average annual soil loss and sediment deposition in the Baltata River basin

**Sediment deposition, ton**

1. > 1.0; 2. < 1.0

**Soil loss, ton**

3.  $0 \leq \text{Loss} < \frac{1}{4}$
4.  $\frac{1}{4} \leq \text{Loss} < \frac{1}{2}$
5.  $\frac{1}{2} \leq \text{Loss} < \frac{3}{4}$
6.  $\frac{3}{4} \leq \text{Loss} < 1$
7.  $1.0 \leq \text{Loss} < 2.0$
8.  $2.0 \leq \text{Loss} < 3.0$
9.  $3.0 \leq \text{Loss} < 4.0$
10. > 4 ton

As a certain *conclusion* of the carried out study one can say that it has clearly demonstrated the enormous potential of hydrological modeling for assessing the scale and spatial distribution of soil and sediments accumulation resulted from erosion processes in small river basins. The further development and wide use of this method can not only supplement, but sometimes replace the existing expensive and labor-intensive field experiments, which is especially important under the current state of national science. However, the wide use of this model in the Moldova conditions is possible only with the creation of appropriate and freely accessible databases on soils, landuse and climate for the country entire territory. Without the WEPP adaptation to specific national conditions its practical application will remain only at the level of individual experiments.

### **3 Using the remote sensing techniques to identify and map erosion-prone areas in the small river watersheds**

#### **3.1 Introduction**

Since the 1960s there has been developed set of models to assess the soil erosion and land degradation risks, including the above-described SWAT and WEPP modelling tools. However, surface erosion mapping on large, river-basin-wide areas remains a challenge. That is why, medium-resolution satellite images, which in the early 1980s became available to a large scientific community, started to be widely used in erosion assessment (Vrieling, 2007). Initially, satellite images had been applied for visual interpretation and detection of eroded areas, but later, with the development of digital indexes, the various remotely sensed data were used for erosion assessment. Since the very beginning, satellite images have been applied in erosion research both independently and as one of inputs in the classical soil erosion models to substitute some standard parameters (e.g., vegetation cover) or the newly elaborated ones, in which remotely sensed information is included as a separate factor (Vrieling, 2007; Aiello et al., 2015; Langat et al., 2019; Mhangara et al., 2012; Petropoulos et al., 2015; Sepuru and Dube, 2018; Žížala et al., 2019).

However, the great majority of these studies, while using classical or modern modelling tools, employ remotely sensed data to a very limited extent. Knowing the added value that satellite remote sensing brings to mapping, analyzing and modelling surface erosion (Vrieling, 2007; Sepuru and Dube, 2018), such a gap should be covered to obtain a more detailed and accurate assessment of surface erosion. The purpose of the presented here study was to identify the erosion-prone areas in the Baltata River basin, using the historical satellite monitoring of the Earth's surface as well as ancillary information to analyze how these areas are distributed among the structural drivers, such as land use types, soil types and slope angles. The proposed methodology can be extrapolated at larger scales, while the expected outputs could be incorporated in the models that assess climate change impact within large river basins or nationwide.

## 3.2 Implementation of Vegetation Indexes to map areas the most vulnerable to soil erosion

### 3.2.1 Using the normalized difference indexes for determination of erosion-prone areas

Typically, a normalized index is a single number, which quantifies the presence of a certain material entity in a remote sensing image based on the differences in this entity's reflectance in different spectral intervals. It has also been proved that a quick and rough assessment of surface erosion can be made solely on the remote sensing information provided by the Normalized Difference Vegetation Index (NDVI), which assesses the fraction of a vegetation cover within a pixel (Rouse et al., 1974), or by the Normalized Difference Water Index (NDWI), which reflects water content in soil and vegetation (Gao et al., 1996).

NDVI assumes that the lowest values of spectral brightness are observed in its red band (*R*), the highest – in its near-infrared (*NIR*) band, and thus it is calculated according to the following equation:

$$NDVI = (NIR - R) / (NIR + R) \quad 3.1$$

This rationale is based on the intense absorption of chlorophyll in the spectrum's red band and the high reflectivity of green leaves' pigments – in the NIR band. In turn, dead and dormant vegetation, as compared to live vegetation, has a higher reflectance in the spectrum visible domain and a lower one – in its NIR band. And, at last, the soil has a higher reflectance than green vegetation and a lower reflectance than dead vegetation in the spectrum visible part, and usually a lower reflectance than vegetation in the near-infrared one. Thus, the values of surface cover reflectance are determined by the complex combination of live and dead vegetation, as well as by presence of areas with bare soil.

The NDWI index was proposed in 1996. Today its primary use is detecting and monitoring the slight changes in the water content of plants. Thus, NDWI is computed through a combination of the *NIR* and short-wave infrared (*SWIR*) bands:

$$NDWI = (NIR - SWIR) / (NIR + SWIR) \quad 3.2$$

The range of NDWI values is from -1 to 1. Generally, NDWI values below -0.1 point to water stress in plants (Gao, 1996).

### 3.2.2 Initial data and methods

The approach used to identify erosion hot spots in the Bălța River basin was based on the freely available satellite images and analysis tools, with the contribution of some ancillary information, such as land use and soil types as well as gullies and landslides obtained as a result of manual interpretation of satellite images and field research.

At the first phase of research, there were used satellite images, acquired using Thematic Mapper (TM) and MultiSpectral Instrument (MSI) sensors on the board of Landsat 5 and Sentinel-2 missions, accordingly (Fig.3.1). To better detect erosion-prone areas, the early spring and late autumn images, when vegetation cover is less developed, were used. Another criterion of image selection was cloud coverage, which was less than 5% in all images. On the whole, six scenes were acquired, by three for each season, covering the period between 1986 and 2020, with one intermediate date in the middle, which differs for spring and autumn datasets due to scene availability (Table 3.1). Additionally, some corrections in the images to remove cross-platform differences were made (Flood, 2017; Claverie et al, 2018; Vogeler et al., 2018). The NDVI and NDWI indexes were calculated, using the "RStoolbox" package (Leutner et al., 2019) developed for *R* statistical computing environment (R Core Team, 2020).



**Fig. 3.1** Thematic Mapper Landsat 5 (*left*) and Multi-Spectral Instrument Sentinel-2 (*right*) used to receive satellite images for the Baltata River basin

**Table 3.1** Characteristics of the satellite images

Scene ID		Sensor	Scene acquiring date	
Type of identifier	No.		Spring	Autumn
path/row	181/027	TM	22 Apr 1986	15 Oct 1986
			28 Apr 2000	28 Sep 2003
UTM grid tile	35TPN	MSI	2 Apr 2020	22 Oct 2020

For the determination of erosion-prone areas, using vegetation and water indexes, the threshold values should be established. According to the reviewed literature, the generally accepted NDVI value threshold for the bare ground is 0.2 (Rouse et al., 1974), while NDWI values below -0.1 point to water stress in plants (Gao et al., 1996). That is, it is much more likely that pixels having  $NDVI \leq 0.2$  are covered with sparse vegetation or have no vegetation at all (Fig. 3.2a). Because we are rather interested in erosion than in plant stress, the NDWI threshold value less than -0.2 was adopted (Fig. 3.2b). In such a way, these areas become the most exposed to surface erosion processes.

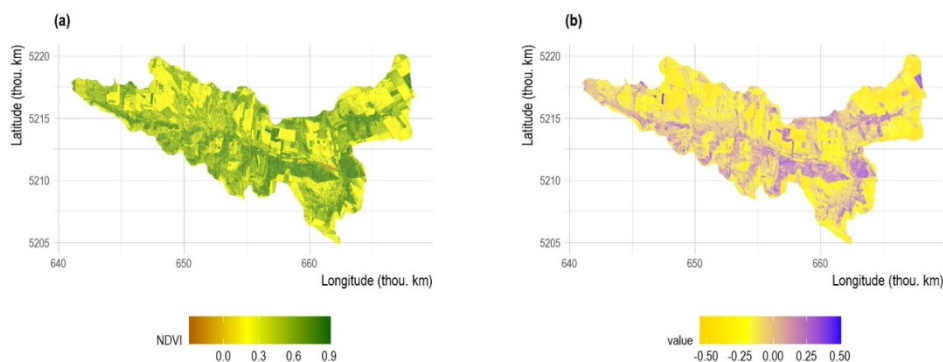


**Fig. 3.2** Examples of NDVI (April 2020) and NDWI (October 2020) distributions within the Baltata River basin

To determine any confinement between the indexes and lands exposed to degradation the ancillary information (soil and land use types) was used. The continuous DEM-derived slope-angle outputs were grouped into four discrete types: flatlands with slope angles less than  $2^\circ$ , gentle slopes areas with slope angles between  $2^\circ$  and  $5^\circ$ , moderate slopes areas with slope an-

gles between 5° and 7°, and steep slopes areas with slope angles more than 7°. Additionally, a 30x30 m square grid, whose spatial resolution is comparable to that of a Landsat-5 scene, was prepared. All input information (gullies, landslides, digital indexes, and ancillary data) were overlaid on the grid and the appropriate values were assigned to each grid cell, in which the analyzed variables are located. Thus, a matrix with 187438 rows (grid cells) and 19 columns (17 variables + cell ID + cell area in sq. m) resulted, which was used in further analysis.

Based on the two indexes distribution, a multi-step approach was developed for the determination of erosion-prone areas. This approach uses exclusively remotely sensed data with the involvement of ancillary information for filtering out inappropriate areas. Because practically no erosion is observed within the urban environment and in water-covered areas, these land-use types were removed from the analysis, and the area of interest represented about 94% of the Baltata River watershed. The remaining types included four land-use types (croplands, forests, orchards, and pastures), four soil types (chernozems, fluvisols, gleysols, and vertisols), and four slope angle areas (flatlands, gentle slopes, moderate slopes, and steep slopes).

The direct processing of space information included the following steps:

1. Selection of grid cells, in which gullies and landslides were observed, and their labelling as “erosion”.

2. Determination of grid cells with critical values of NDVI and NDWI below 0.2 and -0.2, respectively, for each analyzed year and separately for spring and autumn.

3. Labelling the cells with critical values in both seasons and with any combination of the two out of three analyzed years as “high probability” of erosion, while those having critical values just in one of the seasons – as “moderate probability” of erosion. Thus, two parallel assessments of “erosion probability” within the grid cells by NDVI and NDWI were obtained.

4. Combination of these two assessments according to the following schema: (a) cells with the “high probability” of erosion according to both indexes were labelled “high exposure” to erosion; (b) cells with the “high probability” of erosion according to either of the indexes were labelled as “moderate exposure”; (c) cells with “moderate probability” according to both indexes were labelled “low exposure” to erosion. In such a way, there was obtained a map, in which the entire basin’s area was divided into five categories (Fig. 3.3). In this figure no exposure to erosion is shown as a

transparent area and cells, in which gullies and landslides are present, are labelled as “erosion”.

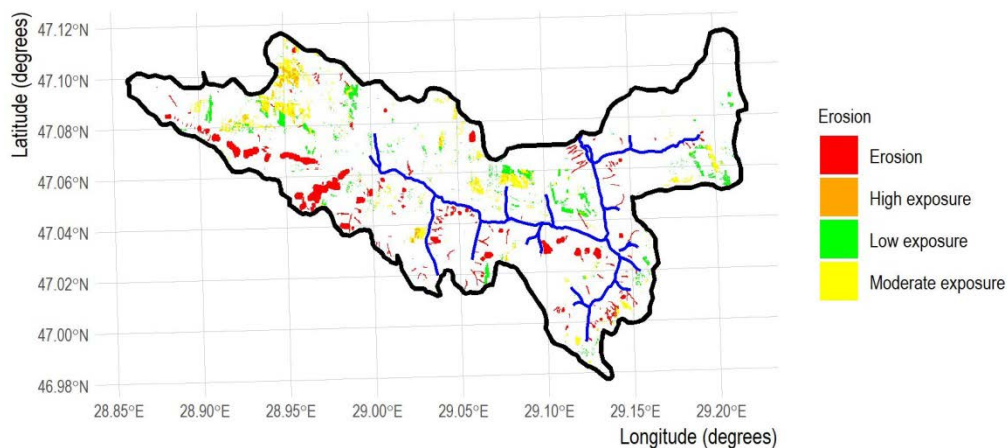


**Fig. 3.3** Erosion-prone areas in the Baltata River basin

### 3.2.3 Spatial distribution of erosion-prone areas

Analysis of the research outputs has shown that just 8.37% of the Baltata entire basin’s area is affected by erosion or exposed to it (Table 3.2). The dominant erosion forms are landslides, which cover two times larger areas than gullies. At the same time, these two forms occupy 40% of the erosion-prone area. Moderate exposure is the next category (32%), low exposure accounts for 23%, and high exposure is the least important category with its share slightly above 4%.

The distribution of slope angles (Table 3.3) is not quite equal: gentle slopes occupy more than 36% of the entire basin area, while the other two slope categories and the flatlands oscillate between 18% and 23% each. The gentle slopes' dominance can explain also why they have the highest share (44%) in the total areas affected by erosion, followed by steep and moderate slopes. The share of slopes affected by erosion is more balanced: for each category this figure falls within an interval of 10-13%. No erosion was detected on flatlands, which means that these lands have not influenced the further analysis and final results.



**Table 3.2** Types of erosion in the Baltata River basin

Type of erosion/exposure	Area (ha)	Share (%) in:	
		basin's area	affected by erosion area
Low exposure	322.83	1.91	22.84
Moderate exposure	453.33	2.69	32.08
High exposure	61.20	0.36	4.33
Erosion, including:	575.82	3.41	40.75
<i>Gully</i>	<i>184.05</i>	<i>1.09</i>	<i>13.02</i>
<i>Landslides</i>	<i>359.73</i>	<i>2.13</i>	<i>25.46</i>
<i>Gully and landslides</i>	<i>32.04</i>	<i>0.19</i>	<i>2.27</i>
<b>Total affected by erosion</b>	<b>1413.18</b>	<b>8.37</b>	<b>100.0</b>

**Table 3.3** Distribution of erosion by slope angles

Slope angle type	Basin		Affected by erosion		Share of slopes affected by erosion (%)
	area (ha)	share (%)	area (ha)	share (%)	
Steep slopes	3643.11	21.6	460.26	32.6	12.6
Moderate slopes	3078.54	18.2	329.94	23.3	10.7
Gentle slopes	6129.54	36.3	622.98	44.1	10.2
Flatlands	4018.23	23.8	—	—	—
<b>Total</b>	<b>16869.42</b>	<b>100.0</b>	<b>1413.18</b>	<b>100.0</b>	<b>—</b>

The distribution of erosion by soil types is very unbalanced: although chernozems occupy almost 90% of the basin's area, their contribution to the areas affected by erosion even exceeds this figure (Table 3.4). Because of this extremely imbalanced situation, chernozems will dominate all erosion types. At the same time, vertisols are remarkable for their share of erosion-affected soils, more than 12%. Fluvisols are located at the other extreme, with just 2%. We should also emphasize that gleysols and vertisols have a higher share in eroded areas than their share in the total basin area, by 2



and 5 times, accordingly. That makes them more vulnerable to erosion than the two other soil types.

**Table 3.4** Distribution of erosion by soil types

Soil types	Basin		Affected by erosion		Share of soils affected by erosion (%)
	area (ha)	share (%)	area (ha)	share (%)	
Chernozems	15028.47	89.1	1275.75	90.3	8.5
Fluvisols	600.03	3.6	12.15	0.9	2.0
Gleysols	832.95	4.9	75.60	5.3	9.1
Vertisols	407.97	2.4	49.68	3.5	12.2
<b>Total</b>	<b>16869.42</b>	<b>100.0</b>	<b>1413.18</b>	<b>100.0</b>	—

*Land-use type distribution* is not as imbalanced as the soils, but croplands still dominate the basin on more than 2/3 of its area (Table 3.5). Forests and orchards follow them far behind, with 13.4% and 12.5%, accordingly. The impact of croplands on soil erosion is also proved by their share in the erosion-affected areas: almost 70% of erosion or exposure to erosion occurs on croplands. Forests contribute to erosion twice more than their share in the basin's area (26.2% vs. 13.4%). This seeming "abnormal" situation is explained by land protection measures taken in the second half of the 20th century when the majority of landslides were afforested for the sake of land stabilization. That is why many forest plots are located on landslides, being almost exclusively confined to the active erosion type. Unlike forests, orchards are much less exposed to erosion. Pastures are poorly presented in the basin; they are confined exclusively to active erosion developed on chernozems and fluvisols. Due to this feature, they are overrepresented in the degraded areas: their share here is 11 times higher than the same figure in the entire basin. The same situation happens with the forests; however, this ratio is much smaller, just 1.2 times.

The active erosion type is confined to steep slopes: 2/3 of its area is located on slopes with angles greater than 7°. Moreover, about 65% of this erosion category is confined to afforested areas (50% on steep slopes), which represent stabilized landslides. Another 30% are located on croplands (including 14% on steep slopes, the highest figure). The other three exposure types (high, moderate, and low) are exclusively confined to croplands, in a

proportion that varies from 95% to 99%. About 16% of the steep slopes with erosion are affected by this type of exposure vs. 2/3 of moderate slopes. Gentle slopes are affected by erosion to an even greater extent (87%).

**Table 3.5** Distribution of erosion by land-use types

<b>Land use types</b>	<b>Basin</b>		<b>Affected by erosion</b>		<b>Share of lands affected by erosion (%)</b>
	<i>area (ha)</i>	<i>share (%)</i>	<i>area (ha)</i>	<i>share (%)</i>	
Croplands	11369.7	67.4	983.07	69.6	8.6
Forests	2260.98	13.4	370.71	26.2	16.4
Orchards	2113.47	12.5	54.36	3.8	2.6
Pastures	91.89	0.5	5.04	0.4	5.5
Urban	980.73	5.8	—	—	—
Water	52.65	0.3	—	—	—
<b>Total</b>	<b>16869.42</b>	<b>100.0</b>	<b>1413.18</b>	<b>100.0</b>	<b>—</b>

Thus, the analysis of satellite information confirmed that diminishing an erosion risk can be done by changing the landuse types. In particular, the lands occupied by crops, which are highly exposed to surface erosion, can be converted into other landuse types that present a smaller risk of degradation, such as forests. Such a conversion brings multiple benefits by not just protecting lands from degradation but also helping to increase the share of forests, thus meeting the need for forested water protection belts.

### **3.3 Satellite images in the assessment of trends in stream bank erosion**

#### **3.3.1 Introduction**

Stream bank erosion (SBE) is a complex natural process, which is a main factor of long-term changes in river courses (Dragicevic et al., 2017). This form of erosion occurs because of changes in hydrologic regimes due to variability of its natural triggers or human activity (Zaimes et al., 2021). SBE modifies the cross-sectional shape of the river channel, which, in turn, leads to hydro-morphodynamic adjustments seeking the new dynamic equilibrium of the river channel (Castro-Bolinaga and Fox, 2018). During readjustments, the

changes in flow depth, bed-material composition and sediment transport capacity occur at various rates and, for example, according to Fox et al. (2016) stream bank erosion is responsible for up to 92% of sediment load in rivers and streams. In recent years, human activities have the most impact on SBE among other drivers (Hawley et al., 2020), significantly influencing the natural conditions of streams and rivers (Saleem et al., 2020). Land use changes and increasing crop production, especially based on old technologies, are among the drivers with high influence on the nature of runoff, streamflow and finally – on the SBE intensity (Zaimes et al., 2019).

Although in the past 15 years, erosion processes have represented a subject of analysis and modelling at various scales, from local (e.g., Boboc et al., 2011) to regional (Ercanoglu et al., 2009) and national (Shaker et al., 2011), none of the abovementioned studies treated the problem of stream bank erosion. Therefore, taking into account the limited knowledge of this process in Moldova (Sirodoev et al., 2019], as well as knowing the added value of satellite remote sensing in erosion mapping and spatial modeling (Senanayake et al., 2020; Ouma et al., 2022), such a gap must be 'closed' to create a more comprehensive representation of SBE in the country.

The purpose of the current study was to determine and map the potential SBE areas within a small agricultural watershed, using a long-term series of satellite images. On the other hand, mapping and monitoring of this form of erosion in a basin-wide area is a difficult task, especially from a long-term perspective (Dragicevic et al., 2017). In our opinion, the medium-resolution satellite images represent an optimal balance between the scale of analysis, its duration and time consumed for data collecting and processing. Moreover, in the below presented SBE analysis we could not identify any previous applications of this image type; they have been mainly involved in assessing the erosion impacts on other linear objects, such as roads (Zhao et al., 2018) and railroads (Ouma et al., 2022) infrastructure.

As in the previous Chapters, the proposed erosion mapping methodology was developed and tested within the Baltata River basin.

### **3.3.2 Data and methods**

In the research, there were used the satellite images acquired by Thematic Mapper (TM) and Operational Land Imager (OLI) sensors on the board of Landsat 5 and Landsat 8 missions, accordingly. Involving Landsat images allowed for increasing the study period from 1985 to 2022, as well as the rela-

tive compatibility of the two instruments: a quite coarse spatial resolution of Landsat scenes (30 m) is compensated by the longest sample available at this resolution (37 years). In selecting the appropriate scenes we took into consideration the period when the study area had no snow cover. Although due to climate change impacts the period of stable snow cover has been shrinking, for the sake of uniformity we used the same period (between March, 15 and October, 15) for the entire analyzed time span of 37 years. The selected scenes were processed, including subsetting, radiometric and geometric correction, in the cloud using Google Earth Engine (Gorelick et al., 2017). For avoiding a noise in data and focusing on the main trends in the changes on Earth's surface, we replaced real digital numbers of each spectral band with their median values. Thus, 37 images have been got: 27 TM yearly scenes for the period 1985-2011 and 10 OLI yearly scenes for 2013-2022. Each spectral band in the scenes contains median values for the period March, 15 – October, 15 for each year (Fig. 3.4).

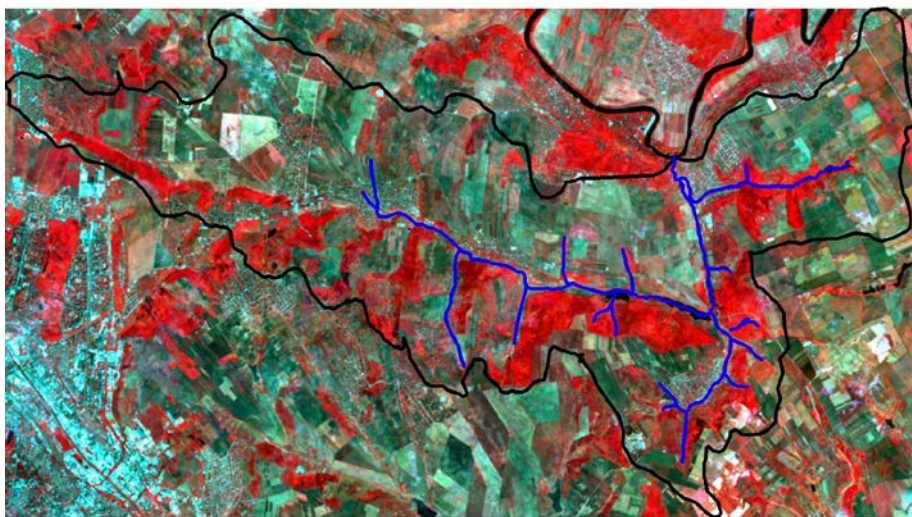


**Fig. 3.4** An example of a false-colored OLI scene (Near Infrared - Red - Green bands), containing median values for March 15 - October 15, 2022

*Note:* Baltata basin boundary is given in black; main streams are shown in blue

The image processing also included two additional steps. Firstly, there were selected just those pixels that are intersected by river channels. This approach would include in the analysis a buffer zone of up to 15 m, on average, from the river course on each side. The size of the buffer zone is conditioned by the spatial resolution of satellite images: the disadvantage of the

relatively large width is compensated by the length of the time period included in the analysis. Secondly, the image processing included also the calculation of the Modified Normalized Difference Water Index (MNDWI) (Xu, 2006) to build a water mask and exclude water-covered areas from further analysis. Because the analyzed river basin is overwhelmingly rural, for the determination of water-covered areas, we used the same threshold (MNDWI = 0) for both sensors (Zhai et al., 2015). These two operations resulted in a set of 1955 pixels, which represent the study area for further analysis.

Next, for each scene, we computed the Normalized Difference Railway Erosivity Index (NDReLI, Eq. 3.3) (Ouma et al., 2022), which represents a modification of the Normalized Difference Road Landside Index (NRDLI) (Zhao et al., 2018). Since both indexes were developed to assess erosion along linear objects, e.g. road or railway infrastructures, they are considered here as a good proxy for assessing temporal trends of stream bank erosion.

$$NDReLI = \left[ \frac{\rho_{SWIRi} - \rho_{blue}}{\rho_{SWIRi} + \rho_{blue}} - \left( \frac{\rho_{SWIRi} - \rho_{green}}{\rho_{SWIRi} + \rho_{green}} - \frac{\rho_{NIR} - \rho_{red}}{\rho_{NIR} + \rho_{red}} \right) \right] \quad 3.3$$

In the *NDReLI* equation,  $\rho_{SWIRi}$  is a spectral reflectance in the short-wave infrared band (SWIR band in TM and SWIR1 in OLI),  $\rho_{NIR}$  – spectral reflectance in the near-infrared band, while  $\rho_{red}$ ,  $\rho_{green}$  and  $\rho_{blue}$  are the reflectance in the corresponding spectral bands of the visible spectrum. *NDReLI* falls within the range [-1; +1]; the higher the figure, the higher the erosivity (Ouma et al., 2022). Finally, all yearly values for each pixel were collected in a single table. As a result, up to 37 *NDReLI* values for each pixel we got, depending on the data availability for each year.

In the next phase, a linear regression model *NDReLI* vs. time was ran for each pixel. As a preliminary step, there were removed outliers, which exceeded 2 standard deviations from the mean, as well as pixels with less than 30 values considered as non-significant data. The obtained 1312 valid pixels represented 67% of the study area total pixels, with sample sizes ranging from 33 to 37.

A positive trend in the regression (Fig. 3.5) for all valid pixels is a result of increasing *NDReLI* over time and suggests a growing trend of stream bank erosion. Accordingly, a negative slope would point to decreasing erosion. The regression modeling, assessed with 95% confidence (p-value  $\geq 0.05$ ), produced three types of the output: pixels with a positive trend, a negative trend and non-significant pixels (Table 3.6).

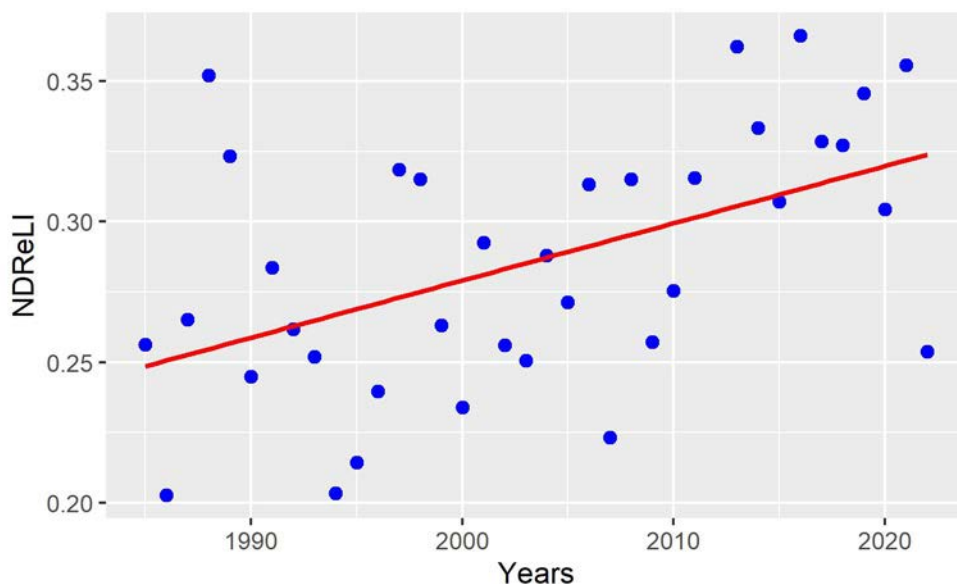


Fig. 3.5 Example of linear regression model NDReLI vs. time for a valid pixel

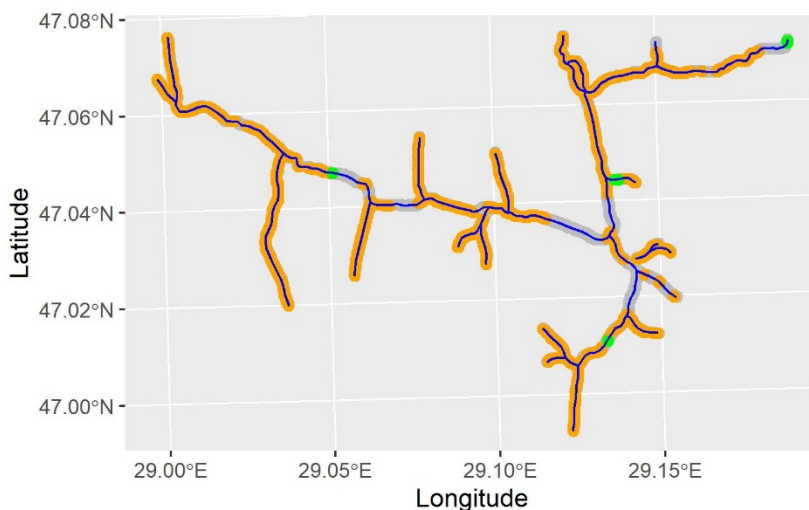
Note: The model equation:  $y = 0.002x - 3.79$ ;  $r^2 = 0.23$ ;  $p\text{-value} = 0.002$

Table 3.6 The output of regression modeling NDReLI vs. Time

	For entire study area	Non-significant pixel	Valid pixels	Trends		
				not significant	positive	negative
Number of pixels	1955	643	1312	262	1043	7
Share of total, %	100	32.9	67.1	13.4	53.4	0.3
Share of valid, %	–	–	100	20	79.5	0.5

The modeling output highlights a significant increasing trend in stream bank erosion: almost 80% of the valid pixels and more than half of all subjected to this process. Very few sectors, accounting for just 0.3% of the main streams length, have a significant positive trend, which represents a decrease in bank erosion in the analyzed period.

The spatial distribution of stream bank erosion shows that increasing trends can be met in all river sectors, from source to mouth, while decreasing trends are located in four sectors: in the source and middle course of bigger streams and close to the mouth of small ones (Fig. 3.6). The sectors with non-significant model outputs tend to concentrate in the middle course of larger streams; in some source areas they are also present.



**Fig. 1.6 Time trends in stream bank erosion of Baltata River, 1985-2022**

Note: The erosion is given: *increasing* – in orange; *decreasing* – in green.

Sectors with non-significant model output are given in grey.

### 3.3.3 Results and discussions

The Baltata River flow has an unstable character over the year, which can be very low or even completely disappear during the summertime. Nonetheless, more than half of its course is affected by erosion processes. As can be seen from Fig. 3.7, the strength of the above discussed relationship in the majority of cases is quite low (though significant). But in 155 cases out of 1050 significant pixels (15%), more than 50% of erosion is explained by the time variable; in 10 cases, time is responsible for more than 75% of changes in the erosion index.

The slope angles of the regression line are very low (Fig. 3.8): its average value equals 0.0024, with a maximum value of 0.0066. It suggests that the response of erosion to change in time is quite weak but stable. However, it should not be a surprise since stream bank erosion is a continuous process (Zaimes et al., 2021).

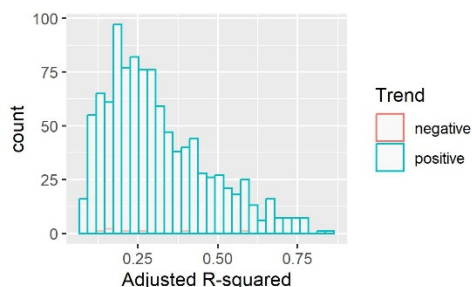


**Fig. 3.7 Histogram of adjusted  $R^2$  of linear regression models for significant erosion trends**



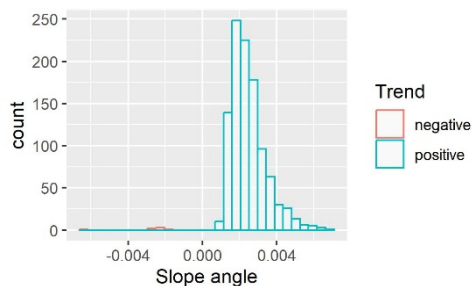


**Fig. 3.8. Histogram of slope angles of linear regression models for significant erosion trends**

Sectors with a strong relationship between increasing erosion and time variable are predominantly located on the small streams or in the mouth areas (Fig. 3.9). It is where heavy rainfalls generate torrents and flow with the highest erosive potential.

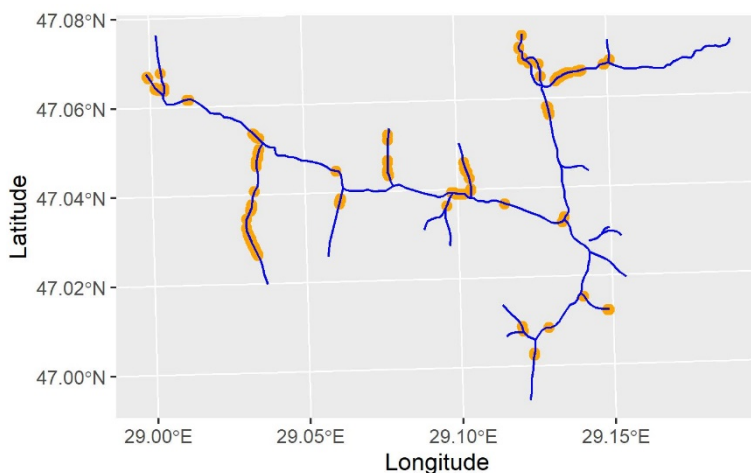


**Fig. 3.9 Sectors (in orange) of streams within the Baltata River basin (in blue) with a strong relationship between the erosion index and time variable**

Regarding land use types, we also analyzed how they impact stream bank erosion through considering the largest share of certain land use categories within the pixel. Obviously, in pixels with dominant water-covered areas, the coefficient of determination (R-squared) is among the highest and the most concentrated around the top values (Fig. 3.10). Croplands also stand out for the highest values; their maximal values (over 75%) are located exclusively here. In addition, negative trends, i.e. erosion accumulation in the area of stream banks, occur just on croplands. Five land use types (croplands, forests, orchards, pastures, and urban fabric) have a more or less similar distribution of R-squared, with the predominance of this coeffi-



cient close to the lower end of the distribution, except orchards, where the middle segment is the largest.

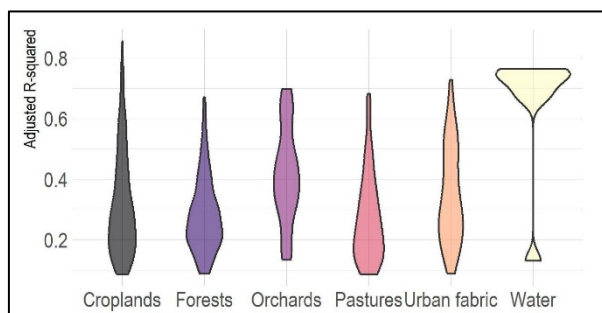


**Fig. 3.10 Violin plot of the distribution of adjusted r-squared for significant erosion trends by land use categories**

The obtained results mean that croplands might have the strongest impact on stream bank erosion over time, but on quite a restricted area. At the same time, relatively large water-covered areas are much more important for increasing erosion than any other land use type. Curiously, while croplands, forests, pastures and urban fabric have the largest plot close to the lower end of the distribution, in orchards the middle segment is the largest. It can be interpreted as orchards being, on average, a more important driver for erosion increase than the other four categories.

The proposed methodology is appropriate for the long-term medium-to-small-scale analysis. However, it has several drawbacks, such as quite coarse spatial resolution. Due to the low intensity of hydro-geomorphological processes in Baltata River and quite coarse spatial resolution of the data sources, in about half of the analyzed pixels (54.7%) there were identified significant erosion trends in 37 years. Nevertheless, it is a good start to highlight the places for a more detailed analysis using other, more detailed methods. One of the approaches to map stream bank erosion in these conditions consists in focusing on the trends, which become visible on a larger scale in a long-term perspective. That is why, we used the longest available set of medium-resolution satellite images, which were processed to reduce intra-yearly variability and noise in data. It is also expected the resulting methodological approach will be extrapolated to be used in other parts of Moldova or other countries with similar geographical and lithological conditions.

## 4. Drone mapping of erosion hotspots

### 4.1 Introduction

The application of unmanned aerial vehicles (UAV), in particular drones, to observe and quantify different forms of soil erosion has become an attractive tool due to its many benefits (Hairston, 2021; Pineux et al., 2017). The UAVs combine the simplicity of aerial surveys and precision of results with an affordable price, while providing a quick erosion measurement at different scales. Being integrated with post processing, for example, with ArcGis software, it is also a promising methodology in terms of data processing automation and cost-effectiveness (Bazzoffi, 2015). UAVs, equipped with regular cameras, can collect images with photogrammetric software to produce three-dimensional models. So, Junwei et al. (2019) have demonstrated better efficiency of drone technology in comparison with traditional technologies in the soil and water conservation monitoring of slag areas on the example of a large hydropower project; a periodic aerial photography and post-modeling, combining with ArcGIS, provided the enhanced support for drone data analysis.

According to Perez et al. (2015), the drones are an emerging tool capable to get the spatial and remote sensing data of high resolution in performing regular site inspections, with opportunity to be pre-programmed with flight patterns to arbitrarily capture necessary information. Austin and Hairston (2019), representing drones' potential in sediment and erosion control as research tools providing new perspectives, along with relatively low-cost and high spatial resolution, note also their "on-demand" information, great efficiency and self-documenting.

In terms of erosion control, the drones provide, for example, many benefits in agricultural management (Rachman et al., 2019) where its enhancing application leads to improving its effectiveness to locate and quantify erosion and deposition, particularly in agricultural watersheds with silt loam soils and a smooth relief (Pineux et al., 2017). Watershed analyses, such as flow direction and flow accumulation, are useful not only to detect gullies and rills but also to delineate the natural geomorphological boundary of soil erosion in the catchment area (Sungchan et al., 2020). This task is especially urgent for Moldova where erosion is still a major cause of land degradation, especially due to intensively cultivated dry agricultural land in steep slope areas (Leah and Kuharuk, 2017). And at last, drones are gaining the approval

and usage for a wide range of natural resources management and geospatial research. A good review on this issue can be found in d'Oleire-Oltmanns et al. (2012).

Sungchan et al. (2020) summarize the latest applications and advances of drone technologies use in soil erosion mapping as follows:

- a) mapping and modeling of the soil surface in a fine spatial resolution;
- b) volumetric estimation of gully and rill erosion;
- c) understanding the sediment transport process, and
- d) prediction of future soil erosion based on surveys data.

Thus, on the whole, drone technologies, allowing the acquisition of high spatiotemporal data, which is difficult to do from traditional remote sensing platforms, provide wide opportunities to understand spatial characteristics and variability of soil erosion and deposition on different scales. Enabling a user-controlled image acquisition, they bridge a gap in scale and resolution between ground observations and imageries acquired from conventional manned aircrafts and satellite sensors.

According to the BSB965 Project's Program, the drones should have been used to map surface erosion in different landscapes at watershed levels. While the large high erosion areas were identified by vegetation indices, the drones provided their further study at small scales through mapping the surface hot spots and evaluating the streambank erosion. In this chapter the survey of erosion prone areas is presented for the Baltata River catchment.

## 4.2 Methodic of a drone survey and mapping

As a rule, organizing the use of a drone survey to capture aerial data with different downward-facing sensors includes the following main stages:

- Planning the survey as an addition to a space one;
- Drone testing and the first pioneer survey;
- Carrying out the survey;
- Processing and analysis of drone's images.

Realization of these stages was partially based on the initial rough assessment of surface erosion in the studied watershed, provided by the satellite remote sensing results, presented in Chapter 3.



*Fig. 4.1 PHANTOM 4 PROSpecs drone, used in the study*

#### 4.2.1 Drone description and testing

The choice of possible unmanned platforms for low-altitude Earth observation is huge and continues to grow, varying greatly around the world (Junwei et al., 2019). For this study a new version of the DJI's smartest drone (Phantom 4 PROSpec; Fig. 4.1) was used. DJI (*Da-Jiang Innovations*) is the world's leader in civilian drones and aerial imaging technology, providing new tools to help businesses and government agencies incorporate this technology into their daily operations. This drone is equipped with two dual rear imaging sensors and infrared sensing systems that detect obstacles in 5 directions and fly around them in 4 directions; its most important characteristics are shown in Table 4.1.

**Table 4.1** Characteristics of the PHANTOM 4 PROSpecs drone

<i>Weight (Including battery)</i>	1388 g	<i>Temperature</i>	0° – 40° C
<i>Maximum altitude speed</i>	6 m/s	<i>Satellite systems</i>	GPS / GLONASS
<i>Maximum rate of decline</i>	3 m/s	<i>Hover Accuracy Range</i>	<i>Vertical:</i>
			±0.1 m (Vision Positioning)
<i>Maximum flight altitude above sea level</i>	6000 m		±0.5 m (GPS Positioning)
			<i>Horizontal:</i>
<i>Maximum flight time</i>	30 minutes		±0.3 m (Vision Positioning)
			±1.5 m (GPS Positioning)

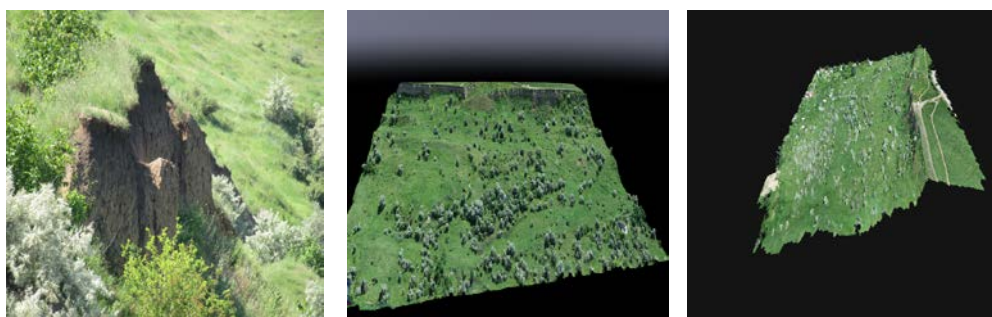


**Fig. 4.2** The photo of a landslide in the Baltata River floodplain (*leftmost*) and its PHANTOM 4 PROSpecs drone 2B and 3D images

As an object for the drone testing, a big landslide in the Baltata basin, with a developing ravine, was selected (Fig. 4.2). In part, a landslide was chosen as the object for testing because ravines and gullies represent a serious erosion and sediment source (e.g., Kaiser et al., 2014).

#### **4.2.2 Drone survey planning and organization**

The DJI Phantom 4 Pro drone mapping of erosion in the Baltata River basin followed the following steps:

- Planning of the drone flight mission aimed to cover all area targeted for mapping and to ensure the drone will fly at a consistent altitude, providing the area complete coverage and its high-resolution images.
- Processing the images through transferring them to a computer and their stitch together by specialized software for creating a high-resolution orthomosaic of the target area.
- Analysis of the orthomosaic, their technical and visual inspection for identifying and mapping areas of erosion, with emphasis on its “hot spots”.
- Interpretation of the results to understand the erosion extent and severity and developing the recommendation for erosion control strategies and land management plans.

Because the drone application was partially based on the results of previous field and satellite observations, the main task of its planning was to identify the erosion manifestations requiring their further detailing, concerning both the surface erosion-prone areas in the Baltata river catchment and bank erosion in its main channel.

The sites that were drone surveyed ranged from individual erosion hot-spots to the individual parts of the Baltata riverbed. Based on the river nature, in particular, the presence of three reservoirs directly in its channel, the drone survey included, first of all, their coastal strips by 100 meters wide on each side. The remaining objects of the survey included manifestations of linear and surface erosion, identified from satellite images and discussed in Chapter 3.

#### **4.2.3 Drone erosion mapping**

Generally, erosion mapping is a technique of using aerial photographs, satellite images, and other data to identify and measure the effects of erosion or soil loss in a given area; these data are further used to create its detailed map that shows the erosion locations and extent. Erosion mapping helps to

understand the causes and effects of erosion, and to inform strategies for preventing and mitigating its effects. The use of drones for detail erosion mapping is particularly beneficial due its efficiency and cost-affectivity, providing important information not only about erosion extent, but also about its severity. Additionally, drones can be used for a quick and easy data collection of large areas in a short amount of time that make them ideal for monitoring, tracking and mapping the erosion effects over time. This drones' feature allows to take a response action accordingly and makes them a powerful tool, which can help to track erosion and better manage and mitigate its effects. Finally, drone mapping can be used to identify areas where erosion risk is especially high – the so called “hot spots”. The analysis of these data and identifying areas where erosion and pollution are most severe, can base the action to better manage and mitigate adverse effects of these environmental threats.

The technique of drone erosion mapping involves capturing drone images of a target area and their processing and analysis using specialized software. For the effective mapping of erosion and pollution, a number of different tools and technologies are used. In particular, the collected high-resolution images are analyzed through a variety of software tools, including GISs, which is need to create detailed maps necessary to identify areas at risk of erosion and pollution and measure their current and potential future adverse effects.

The reported research was based on the DEM of the Baltata River basin, developed in the framework of this project.

## **4.3 Drone erosion survey, data processing and results**

### **4.3.1 Drone survey report**

Usually, all remote sensing methods, used for the detection of eroded areas, include the visual interpretation of aerial images based on the soil color and its changes related to the erosion processes (Žižala et al., 2019).

One drone survey report is demonstrated below on the example of the Baltata river catchment area at the entrance to reservoirs in its floodplain, provisionally named by us the Upper Baltata (Fig. 4.3). The survey covered area has 0.145 km<sup>2</sup> (14.5 ha), with an average ground drone sampling distance (GSD) equal 1.21 cm. From 686 images 438, or 63% were calibrated and geolocated. Initial and computed images positions are shown in Fig. 4.4.

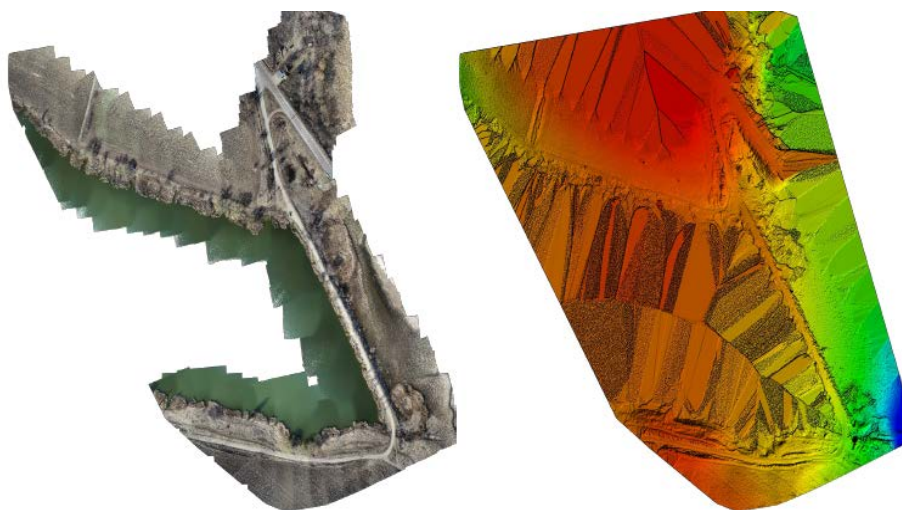


**Fig. 4.3** Orthomosaic (*left*) and the corresponding sparse Digital Surface Model (*right*) of the Upper Baltata catchment area before densification

Overlapping of images that determines a survey quality is shown in Fig. 4.5. Red and yellow areas indicate a low overlap, for which poor results may be generated. Green areas indicate an overlap of over five images for every pixel. Good quality results will be generated also as long as the number of keypoints, or matching homologous features across overlapping images, is sufficient for these areas. In drone surveys the keypoints generate image correspondences; insufficient keypoint matches between image pairs contain large amounts of noise and uncertainty. In the reported example of a survey from total 61598 keypoints per image there were matched 19389; some details of matches are shown in Fig. 4.6. In this figures the darkness of links indicates the number of matched 2D keypoints between the images. Bright links indicate weak links and require manual tie points or more images. Dark green ellipses indicate the relative camera position uncertainty of the bundle block adjustment result.

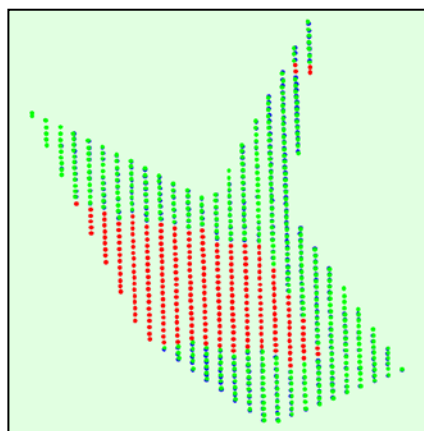


**Fig. 4. 4** Top view of the initial drone images position and offset between their initial (*blue dots*) and computed (*green dots*) positions. Red dots indicate water surface.



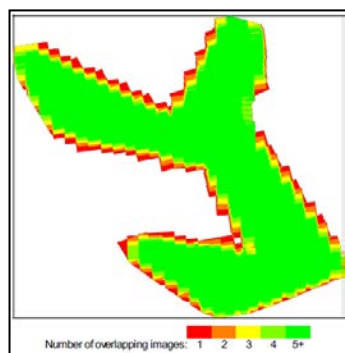


**Fig. 4.5** Number of overlapping images for each pixel of the orthomosaic

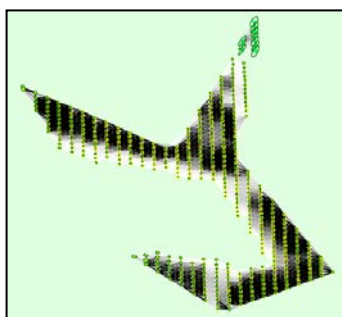
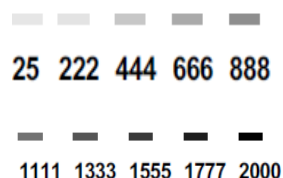


**Fig. 4.6** Computed image positions with links between matched images.

*Number of keypoint matches between images in Fig. 2.11*



### 4.3.2 Drone survey results

#### 4.3.2.1 Stream bank erosion

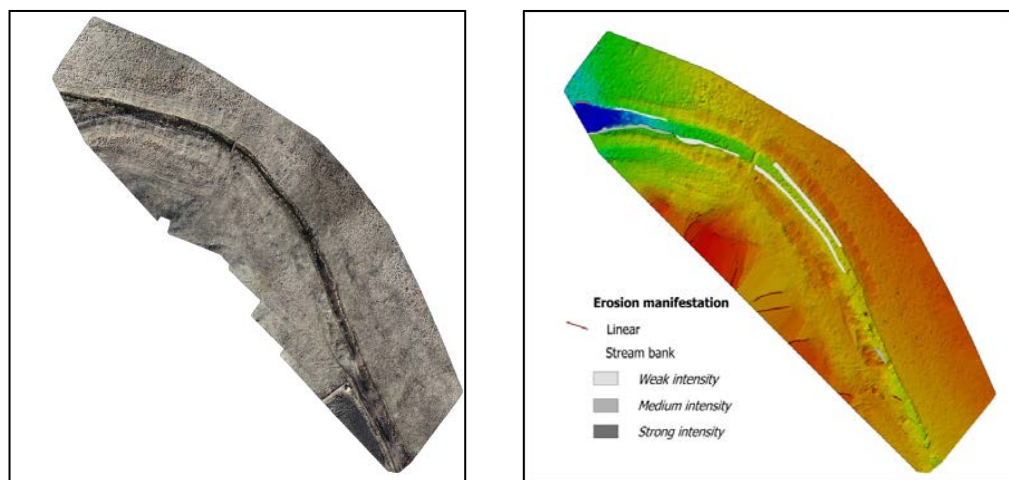
The analysis of drone stream bank erosion, presented in this sub-chapter, aims to detail its general picture in the Baltata River watershed based on long-term satellite imageries, discussed in Chapter 3. The drone survey results are considered on the example of the river watershed's two plots, conventionally named the Middle Baltata and the Lower Baltata - Recea mouth confluence.

*The Middle Baltata plot*, with an area of 1.26 ha, is a fragment of the Baltata River wide floodplain in its middle part (Fig. 4.7, *left*). The territory of this site is relatively flat, with numerous hillocks and depressions, occupied by meadow vegetation and rare shrubs. The river depth here is up to 80 cm; its steep up to 1 m high banks, composed of loamy-argillaceous alluvial formations, are weakly washed away by a slow streamflow. It can be also noted the significant areas of undermining and landslides with a width of 20-40 cm in some places. The survey results are shown in Fig. 4.7 (*right*).

The orthomosaic combines 25 orthophoto images of the study area, with the keypoints's average number of about 73.3 thousand, at a resolution of 1.1 cm/pixel. At the digital model the blue and green colors show subhorizontal surfaces, while the image interpretation results – the erosion areas. In particular, several microerosion forms of linear erosion have been identified in the southwestern part of the study area, mainly in the riverside. Here, there were also identified plots within which a stream bank erosion of



low intensity is manifested. A small area with strong erosion is noted in the northwestern part. It is also seen that right-bank slopes are subject to more intense erosion.



**Fig, 4.7** Orthomosaic of the study area (*left*) and its Digital Surface Model with identified erosion areas (*right*)

In general, areas of low intensity erosion occupy 0.013 ha (1%), medium – 0.0026 ha (0.21%), and strong intensity – less than 0.005% of the entire study area. The length of the bank sections subject to erosion is 55% for the right bank, and 31% – for the left one.

***The Lower Baltata - the Recea mouth*** study area is located in the lower reaches of the Baltata River, in its floodplain adjacent to the western outskirts of the Balabanesti village and the Recea river mouth. This area of 7.6 ha is a fragment of the wide 270-300 m floodplain, relatively flat but with numerous hillocks and depressions, occupied by grassy vegetation. Until the 1980s, this floodplain was swampy, but then it was planned and partially plowed up, and the right banks of the Baltata River and its tributary Recea were leveed. The flow of both rivers here is fast, the channel up to 80 cm deep is strongly winding, and the steep banks up to 1-1.2 m high, composed of loamy-argillaceous alluvial formations and bulk soils, are intensively washed away. The drone 2D image of this area is shown in Fig. 4.8 (left). Its orthomosaic combines 306 orthophoto images, with their mean value of about 68.8 thousand keypoints.

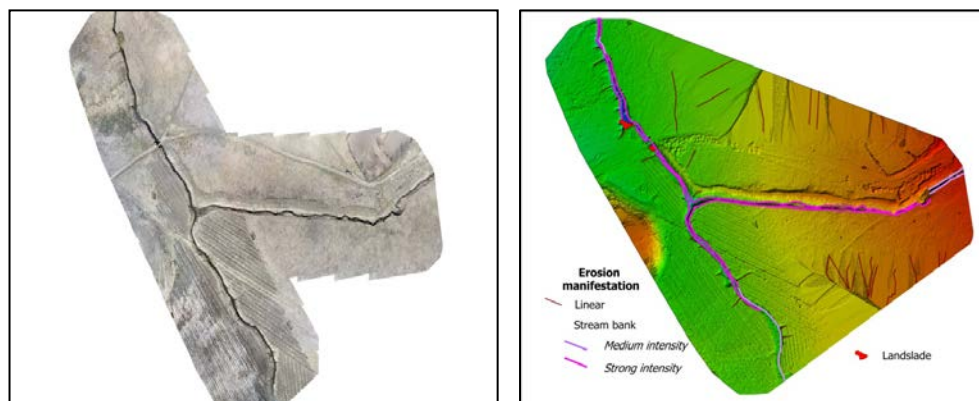


**Fig. 4.8** Orthomosaic of the study area (*left*) and its Digital Surface Model with identified erosion areas (*right*)

The Digital Surface Model (DSM) of this area (Fig. 4.8, *right*) clearly demonstrates its sub-horizontal surfaces – blue and green ones; the interpretation of DSM makes it possible to identify several erosion plots. In particular, practically both banks of the Baltata and Recea rivers are subject to erosion processes; in the eastern and southern parts of the survey area, several microerosive forms of linear erosion were identified, which also occur in areas adjacent to the banks.

The places, within which a bank erosion of predominantly strong intensity is manifested, have been identified over a greater extent of both river-sides, the places of medium intensity – on the Baltata River in its lower reach and also on a small length of the Recea eastern bank. Identification of weak erosion manifestations on drone images turned out to be impossible. In general, the bank erosion on these two rivers is developing along their lengths of about 2800 m and about 2300 m from the mouths, respectively, in a narrow riparian strip. Several landslides resulting from the bank erosion have been also identified. The largest of them (up to 5 m long and 12 m wide) is located near a small bridge across the Baltata River.

#### **4.3.2.2 Surface erosion**

As in the case of coastal erosion, the results of the drone surface erosion survey are demonstrated on two plots, tentatively named North Baltata and Sagaidac.

The **North Baltata** plot of 4.43 ha is located north of the village Baltata, on the right slope of the beam cutting through the left slope of the Baltata river valley. Its area with a steepness of 3-4 degrees, represented mainly by chernozem, is used for growing the tilled and grain crops. The 2D orthomosaic of the upper part of this slope area (Fig. 4.9, left) combines 128 orthophoto images with the mean value of keypoints about 57.07 thousand at 1.57 cm/pixel resolution. This images interpretation made it possible to identify several areas of erosion (Fig. 4.9, right).

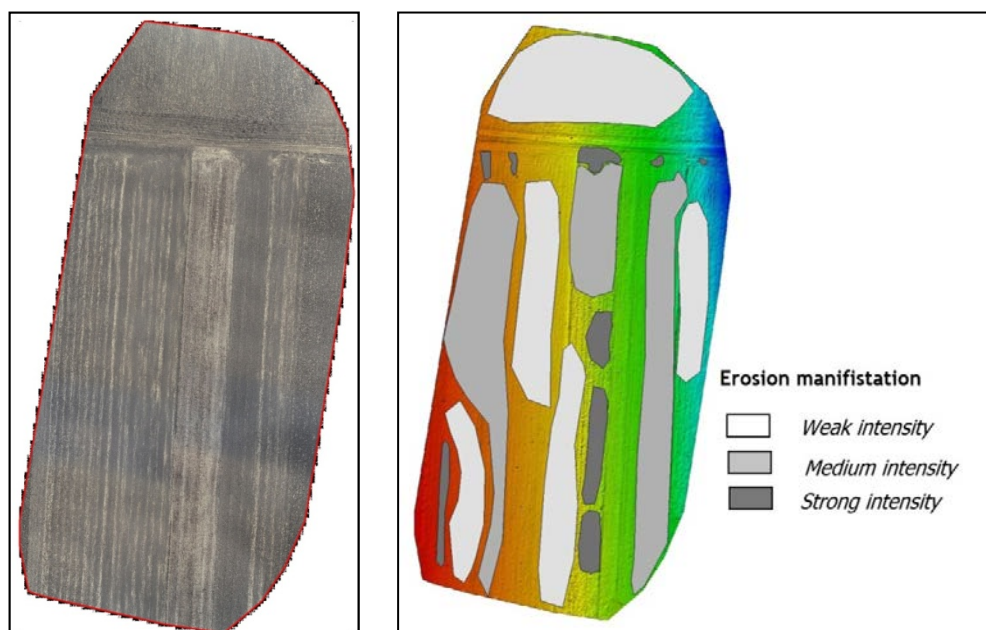


**Fig. 4.9** Orthomosaic of the North Baltata area (*left*) and its Digital Surface Model with identified erosion plots (*right*)

On the whole, this part of the Baltata River watershed is subject to surface erosion of varying intensity. The most affected by erosion processes is its middle, most steep part. Manifestations of the erosion of medium and low intensity occur almost along the entire slope. The total area of identified plots of low erosion intensity is approximately 1.2 ha, or 29.6% with their mean value of 0.24 ha. The total area of medium intensity erosion plots is 0.97 ha (21.9% with their mean value of 0.32 ha) and of high intensity – 0.91 ha (4.3% with a mean value of 0.02 ha).

The **Sagaidac** research plot, with an area of 1.88 ha, is located to the east and southeast of the same name village, on the right slope of one of the

Baltata River tributaries, in its lower part. This slope with a steepness of 3-5 degrees has a landslide genesis and is used for grain crops; partially, the slope is covered with grassy vegetation and is used for poor quality pastures. Its western part is occupied by forests. The slope soils are represented by chernozem interspersed with landslide soils; in the tributary's floodplain the soils are alluvial.

The results of a drone survey of the floodplain and slope of this Baltata right tributary are presented in Fig. 4.10 where the 2D orthomosaic includes 44 orthophoto images with the mean value of keypoints about 56.4 thousand and a resolution of 1.47 cm/pixel. The interpretation of the obtained images made it possible to identify several areas of erosion.

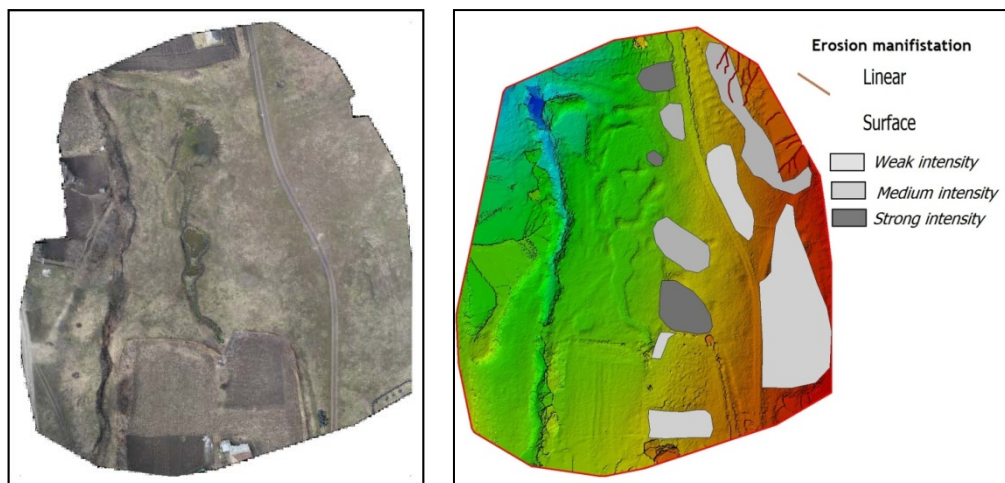


**Fig. 4.10** Orthomosaic of the Sagaidac area (*left*) and its Digital Surface Model with identified erosion plots (*right*)

In particular, this study plot is subject to surface erosion of different intensity, with its predominance in the lower and middle parts of the slope. Manifestations of surface erosion of medium and low intensity are observed almost along the entire slope; in addition, in the northeastern part there are noted manifestations of linear erosion. The total area of identified areas of low intensity erosion is 0.013 ha, or 9.8%, with their mean value of 0.003 ha. The total area of areas with medium intensity erosion is 0.006 ha (4.7% with a mean value of 0.002 ha) and of strong intensity – 0.003 ha (2.3% with a mean value of 0.001 ha).

## 5. Fingerprinting method for identifying the suspended sediments sources

### 5.1 Introduction

The so-called method of fingerprinting is successfully used to identify sources of suspended sediments in water bodies (Collins et al, 2007; Koiter et al, 2013; Lamba et al, 2014; Walling, 2013). To address this task this method links the physical or geochemical properties of suspended sediments to their corresponding sources within the watershed (Walling et al., 2008; Walling, 2013), based on two major assumptions: (a) the potential sources of suspended sediment are distinguishable based on selected fingerprinting properties, for example, physical or geochemical, and (b) the relative source contributions of different sources to suspended sediment can be determined through the comparison of their fingerprinting properties with those in source material samples (Collins and Walling, 2002). The common approach used in sediment fingerprinting studies is to select as much as possibly fingerprinting properties and apply statistical procedures to optimize them in order to best apportion suspended sediment to different potential sources (Davis and Fox, 2009; Walling et al., 2008]. The different types of sediment fingerprinting properties, which have been used to identify their sources, include heavy metals, radio and stable isotopes, nutrients, sediment structure (particle size) and magnetic properties of minerals [Collins et al. 2017; Franz et al., 2014; Huisman et al., 2013; Malhotra et al., 2018; McKinley et al., 2018; Moore and Semmens, 2008). Inorganic tracers can be also used to prioritize sediment sources, but since numerous factors control their distribution, it is difficult to develop a predictive approach to do this across the landscape (Collins and Walling, 2007). Multiple fingerprinting properties and multivariate statistical techniques are used to determine the relative source contribution of different sources to suspended sediments. Geochemical fingerprinting properties are the most used factors in the analysis of different sources of river in-stream sediment with a less uncertainty (*ibid*).

The available studies show that stream banks and agriculture lands are important sources of suspended sediment in a river watershed. The land use type and watershed size are also important factors for their formation in surface water bodies and the river bank erosion influence on this process (Abbas et al., 2023). Identification of suspended sediment sources gives good

results during periods of rivers intensive runoff, snowmelt, heavy rains, etc. (Franz et al., 2014).

## 5.2 Fingerprinting methods overview

Fingerprinting technique works best when long-term data on sediment dynamics are available, notably from bank erosion assessments, sediment budgets and other sources. Sediment source fingerprinting results are also change if sediment dynamics vary over time. This method is quite sensitive to rainfall and the duration of preceding dry periods, as was demonstrated by the marked variation in sediment source apportionment among rainfall events and across entire dry periods (Devereux et al, 2009; Poletto et al., 2009). A schematic description of the fingerprinting method is provided in Fig. 5.1 (Poletto et al., 2009). Its use for the assessment of the river sediment sources includes several tracers: fallout radionuclides ( $^{137}\text{Cs}$ ,  $^7\text{Be}$ ,  $^{40}\text{K}$ ,  $^{210}\text{Pb}$ ,  $^{226}\text{Ra}$ ,  $^{234}\text{Th}$ ), mineral magnetism spectrocolumetry, compound-specific stable isotopes ( $^{13}\text{C}$ ,  $^{15}\text{N}$ ,  $^{18}\text{O}$ ), spectral fingerprinting (VNIR-SWIR spectral information), environmental DNA, and geochemical parameters Collins et al., 2020).

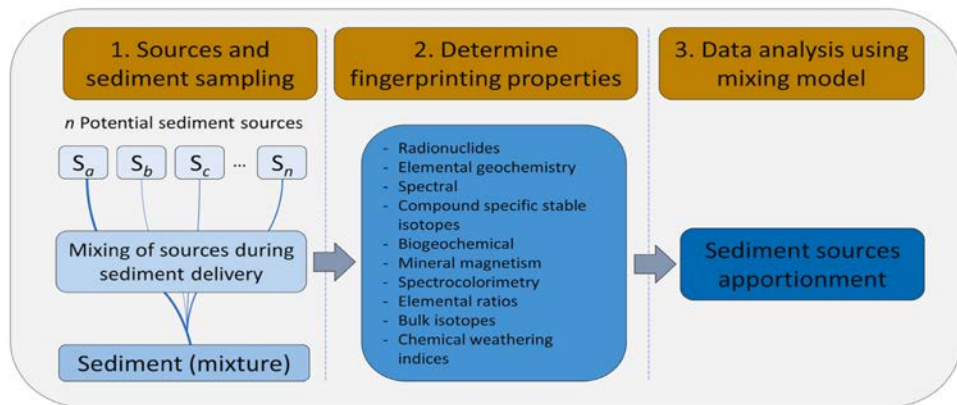


**Fig. 5.1** Schematic diagram of the sediment source fingerprinting method  
Source: Poletto et al., 2002 modified from Walling and Collins, 2000.

The widespread use of sediment source fingerprinting has been limited because of the cost and efforts involved in preparing samples for radionuclide and elemental geochemistry analyses, as well as of the needs for expensive analytical equipment and specially trained staff. The spectral fingerprint can be used as a rapid and cost-effective alternative (Brosinsky et



al., 2014). It has been also determined that mid-infrared (MIR) spectroscopy is fast, inexpensive, and non-destructive when the objective is to identify sediment sources in rural catchments with a view to developing targeted mitigation strategies.

Any physical or chemical indicators are environmentally sustainable; that is, they should not change during transport within the watershed. Fall-out radionuclides, geochemical elements and organic matter properties are the most used tracers in traditional methods, including the MIC-based method. A combination of traditional and alternative tracers can be useful to improve the distribution of sediment sources and obtain the best simulation results (Collins and Walling, 2002). The selection of an appropriate set of tracers for a particular system can represent an extensive and resource intensive watershed-specific trial-and-error exercise.

The main objective of a fingerprinting mixing model is to compute the proportional contributions of all sources to suspended sediment loads at the catchment scale, which is achieved by a minimizing error. During this process, the following two conditions must be respected: the contribution must have a value between 0 and 1, and the sum of all contributions must equal 1. Apportionment results from the sediment mixture combinations that have the highest goodness of fit (GOF) based on the sum of squares of relative error are [14]:

$$GOF = 1 - \frac{1}{n} \left( \sum_{i=1}^n \frac{\left| b_i - \sum_{j=1}^m \omega_j a_{i,j} \right|}{\Delta_i} \right), \quad 5.1$$

where  $GOF$  is the goodness of fit;  $\Delta_i$  is the value range of normalized tracer  $i$ ;  $a_{i,j}$  is the value of tracer  $i$  in sediment source  $j$ ;  $b_i$  is the value of tracer  $i$  in the sediment;  $\omega_j$  is the unknown relative contribution from sediment source  $j$ ;  $n$  is the number of tracers used, and  $m$  is the number of sediment sources used. Mixing models are computationally challenging to use and thus normally require a fair amount of expertise and familiarity with specific statistical programs.

There are several programs for the calculation of various sources contribution to sediments formation. Free, user-friendly software (e.g., R package: FingerPro) has been developed for users with limited or no experience with sediment source fingerprinting (Malhotra et al., 2018). In recent years,



the programs IsoSource (Phillips and Gregg, 2003) and MixSIR (Moore and Semmens, 2008) were created for ecological applications. Other open-source software (Sediment Fingerprinting Tool, or SIFT) has been developed using the R programming language and is structured to better guide end-users in applying the fingerprinting approach (Collins et al., 2017). Like SIFT, the Sed\_SAT (Sediment Source Assessment Tool) (Franz et al., 2014) was created with methodological fundamentals in mind. A commonly used tool for field-level prioritization, using average annual soil erosion rate, is the RUSLE 2 (Revised Universal Soil Loss Equation 2 (USDA-ARS, 2006), which is available and fairly easy to use in comparison to other complex models. Therefore, combined use of RUSLE 2 with sediment fingerprinting could be effective in identifying specific fields (Lamba et al, 2014).

The sediment source fingerprinting can quantify *the sediment budget*, which includes the evaluation of sediment contributions from three primary sources: hillslopes, gullies, and riverbanks. This information provides a valuable framework for understanding sediment behavior at large scales and thus can inform management strategies on sediment mobilization, transfer and storage at the catchment scale, revealing the extent of erosion and deposition rates (Walling and Collins, 2008). The integrated approach to developing sediment budgets is based on the monitoring of sediment yield and fingerprinting sediment source with using radionuclides to estimate soil erosion and deposition (Abbas et al., 2023). The sediment budget of a catchment consists of three main components: (1) sediment load, which corresponds to net erosion in the catchment and can be quantified, using suspended sediment measurements and turbidity sensors; (2) gross erosion within the catchment that can be determined using, for example, the RUSLE model or radionuclide tracers; (3) sediment source fingerprinting that calculates the fraction of each sediment source (Abbas et al., 2023; Walling, et al., 2021). Sediment budgets can be used to calculate valuable metrics, like the sediment delivery ratio (SDR), which expresses the relationship between total erosion and quantities of exported sediments within catchments.

Data on water-mediated soil erosion are available at the European scale with a resolution of 100 m, calculated using high-resolution input data files in a modified version of the Revised Universal Soil Loss Equation (RUSLE) (<https://esdac.jrc.ec.europa.eu/resource-type/soil-threats-data> ). The contribution of riverbanks to the sediment budget is in the range of 3-25%, and that of surface sources tended to occur in the range of 75-97%, which sug-

gests that these figures could be taken as general values for river catchments (Abbas et al., 2023). Sediment budgets can be used to estimate the sediment delivery ratio (Walling et al., 2008).

### 5.3 Sampling methods

The recommended sediment sampling is to be carried out, using a time integrated trap sampler (Lamba et al., 2014), which collect fine suspended sediment ( $< 63 \mu\text{m}$ ). But due to the lack of appropriate equipment the sediment samples in the Baltata River's basin were collected by grab samplers to the depth of 5.0 cm from three sources: at the outlets of its watershed and one sub-watershed, and at the beginning of reservoirs in the Baltata riverbed. The sampling was carried out in September 2022 after intensive precipitation events in the month beginning. One water sample was collected in the river outlet area. Soil samples were collected from surface up to 5.0 cm depth in riverbanks near different landuse, preferably without plant coverage and with erosion marks. The complex soil samples were collected using standard methodology (ISO 10381-1:2002) on plots measuring 10 x 10 m. Each complex sample has 10-15 subsamples. The sampling location is presented in Fig. 5.2.

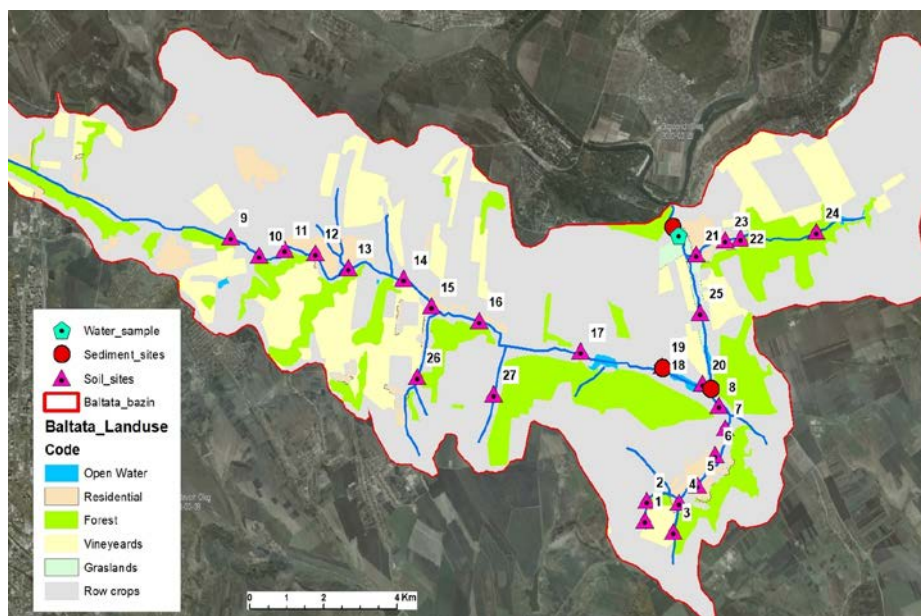


Fig. 5.2 The location of samples collected for the sediment fingerprinting in the Baltata River basin

The sediment fingerprinting properties must possess conservative behavior during sediment transport within a watershed. The mass-conservative test should be used after the analysis of trace elements to determine if the concentrations of fingerprinting properties in the suspended sediment samples fall within the range of the source samples' fingerprinting property concentrations at each site (Franz et al. 2014). Therefore, the fingerprinting properties after passing this test were subjected to a statistical selection procedure. Specifically, a Kruskal-Wallis H test and the multivariate discriminate function analysis (DFA) were proposed to select composite fingerprints (Collins and Walling, 2007). In our study, the first test was used for the analysis of individual properties power to discriminate between sediment sources, and the properties with  $P > 0.05$  were excluded. The stepwise DFA, based on minimization of Wilks' lambda, was applied to the fingerprinting properties that passed Kruskal-Wallis H-test to identify the optimum set of fingerprinting properties providing an optimum discrimination between sediment sources (Collins and Walling, 2002).

A multivariate mixing model was used to estimate relative contributions from four principal land uses: cropland, forests, orchards and vineyards localities (Walling, 2005; Walling et al., 2015). This model minimizes the sum of the squares of the relative errors (RDs) as:

$$RDs = \sum_{i=1}^m \left\{ \left[ C_i - \left( \sum_{s=1}^n P_s S_{Si} \right) \right] / C_i \right\} \quad 5.2$$

where  $m$  is the number of fingerprint properties selected in the optimal combination of fingerprinting properties,  $C_i$  – the concentration of fingerprint property  $i$  in the sediment,  $n$  – the number of sources,  $P_s$  – the proportional contribution from the source, and  $S_{Si}$  – the concentration of fingerprint property  $i$  in source  $s$ .

The boundary conditions of this model are presented by the following equations:

$$\sum_{s=1}^n P_s \times S_{Si} = C_i \quad 5.3$$

$$\sum_{s=1}^n P_s = 1 \quad (0 \leq P_s \leq 1) \quad 5.4$$

If the RDs are minimal, the proportion of the contribution of each potential sediment source can be determined. To assess model performance and optimization results, a goodness-of-fit (GOF) metric (Eq. 1) is commonly used. Generally, the mixing model is considered satisfactory to explain the contribution of sediment sources when the GOF value is  $>0.8$ .

## 5.4 Results and discussion

The example of statistical data for different land uses and sediments in the study area are presented in Table 5.1.

**Table 5.1** The descriptive statistics of seven fingerprinting elements in source material and sediment samples for each studied plot

Statistics	Fingerprinting elements						
	Cu, mg/kg	Cr, mg/kg	Mn, mg/kg	Fe, mg/kg	Ni, mg/kg	Pb, mg/kg	Zn, mg/kg
<b>Forest land use</b>							
<i>Average</i>	9.72	10.71	360.42	5777.69	11.70	16.82	17.49
<i>Median</i>	9.76	10.80	364.55	5564.00	11.90	17.60	17.97
<i>SD</i>	1.00	0.87	35.04	3978.33	2.42	6.30	3.99
<i>CV, %</i>	10.31	8.16	9.72	68.86	20.66	37.44	22.80
<i>Min</i>	9.20	10.24	341.20	3904.00	10.40	13.35	15.30
<i>Max</i>	10.20	11.10	375.50	7865.00	12.79	19.50	19.20
<b>Arable land use</b>							
<i>Average</i>	12.31	12.90	428.95	9543.23	15.20	14.10	19.45
<i>Median</i>	12.48	12.95	455.50	9895.00	15.80	14.60	19.20
<i>SD</i>	0.45	0.09	57.07	719.43	1.60	1.01	0.63
<i>CV, %</i>	3.63	0.67	13.30	7.54	10.50	7.18	3.26
<i>Min</i>	11.80	12.80	363.50	8716.00	13.40	12.90	19.00
<i>Max</i>	12.60	13.00	467.90	10019.00	16.40	14.80	20.20
<b>Settlement</b>							
<i>Average</i>	21.36	21.31	415.97	10992.31	19.61	20.36	47.66
<i>Median</i>	20.20	17.24	400.20	10135.00	20.25	20.40	49.35
<i>SD</i>	3.32	8.34	41.94	1608.91	2.16	2.20	8.91
<i>CV, %</i>	15.56	39.12	10.08	14.64	11.01	10.80	18.70
<i>Min</i>	18.80	15.80	384.20	9994.00	17.20	18.10	38.00
<i>Max</i>	25.10	30.90	463.50	12848.00	21.40	22.50	55.60

	Sediments						
<i>Average</i>	10.30	16.95	435.88	9741.45	16.82	17.07	22.93
<i>Median</i>	10.40	16.41	460.42	9685.00	16.50	16.25	22.50
<i>SD</i>	1.96	1.25	62.37	516.99	1.45	1.86	1.69
<i>CV, %</i>	19.02	7.37	14.31	5.31	8.60	10.92	7.37
<i>Min</i>	8.30	16.10	365.00	9255.00	15.60	15.80	21.50
<i>Max</i>	12.20	18.40	482.30	10284.00	18.40	19.20	24.80

*Note:* *SD* – Standard Deviation; *CV* – Coefficient of Variation

Three principal land uses were considered for this analysis: forest, arable lands and settlement, for different sediments sites. As example, the box plots in Fig. 5.3 demonstrate the statistical characteristics of selected trace elements for selected land uses. Before using the fingerprinting approach for discriminating sediment sources, all data were checked for univariate and multivariate outliers. The criterion of the mean  $\pm 1$  SD (standard deviation) was used to identify univariate outlier data. However, given the nature of geochemical data, this rule could not deliver a relevant threshold estimate for the study variables. Therefore, the median  $\pm 3$  Median Absolute Deviation (MAD) criterion was used:

$$\text{MAD} = 1.482 \text{ Median } (|x_i - x_{\text{median}}|) \quad 5.5$$

Because for using the multivariate Discriminant Function Analysis (DFA) the enough number of samples per category is recommended, the selected minimum ratio of sample size to the number of tracers was approximately 5 and at least 15 to 20 observations per category were considered.

The two-stage statistical procedure proposed and used by Collins et al. (2002, 2007, 2017 and 2020) was employed to confirm the potential sediment sources discrimination in the watershed. Using the Kruskal-Wallis H test, the power of individual properties to discriminate between sediment sources was examined, and properties with  $P > 0.05$  were excluded. Based on the results of the Kruskal-Wallis H test, the discriminate function analysis (DFA) was used to examine the ability of the tracer properties to confirm the existence of inter-category contrast and to assess the discriminatory power of those tracer properties, which determined the optimal group (Collins and Walling, 2007). By minimizing Wilks' lambda, DFA selects an optimum composite fingerprint with the minimum number of tracer properties that supply the greatest discrimination between the analyzed source materials.

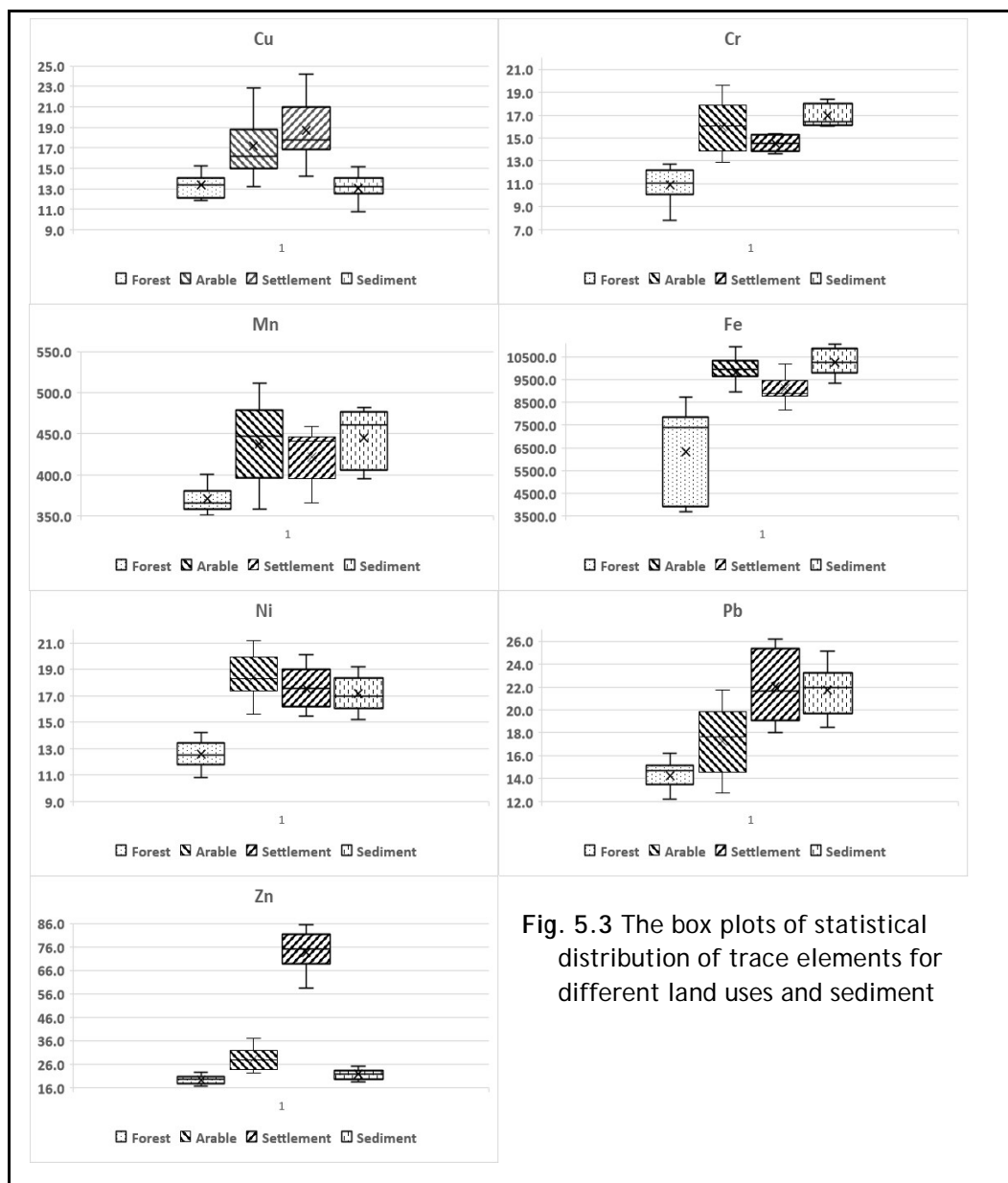


**Fig. 5.3** The box plots of statistical distribution of trace elements for different land uses and sediment

The results of applying ANOVA (Analysis of Variation) test for one site are given in Table 5.2. Obtained results show that, out of seven studied elements, just Zinc with  $p$ -values below 0.05 were capable of discriminating erosion types as a source of sediment for all land uses. On the other hand, forest lands use showed statistically significant differences by  $p$ -values prac-

tically for all fingerprinting parameters except Cu. Arable land use has *p*-values below 0.05 for Cu, Pb and Zn. Settlement land use has *p*-values below 0.05 for Cu, Cr, Fe and Zn.

Table 5.2 An example of the results of One-Way ANOVA test applied to the three principal sediment sources

Fingerprinting property	Forest land use		Arable land use		Settlement	
	F-value	P-value	F-value	P-value	F-value	P-value
Cu	0.7447	0.2955	0.0269	<b>0.0010</b>	0.0479	<b>0.0001</b>
Cr	0.1190	<b>0.0000</b>	0.0254	0.1254	0.3223	<b>0.0002</b>
Mn	0.0535	<b>0.0002</b>	0.3525	0.2840	0.9998	0.0838
Fe	0.0008	<b>0.0002</b>	0.1491	0.0743	0.6420	<b>0.0003</b>
Ni	0.7003	<b>0.0000</b>	0.3703	0.0858	0.6299	0.2397
Pb	0.4193	<b>0.0000</b>	0.4948	<b>0.0019</b>	0.2210	0.4082
Zn	0.8291	<b>0.0123</b>	0.0199	<b>0.0033</b>	0.0001	<b>0.0000</b>

Note: In *bold italic* the properties with statistically significant differences in means (*p*-value > 0.05) for studied sources

And at last, Table 5.3 presents the results of the Discriminant Function Analysis (DFA) for the Baltata watershed two plots. The optimum composite fingerprints selected by DFA, Cr, Fe, Ni, Zn could correctly distinguish only 65 % for site 1 and 70 % for site 2 of the source type samples.

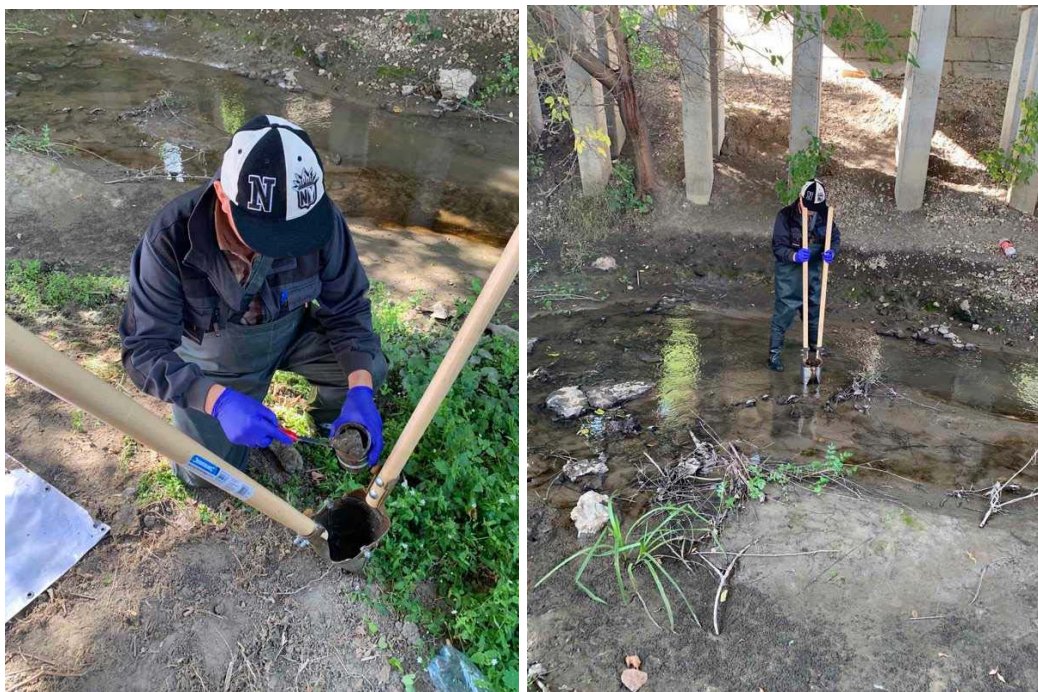
Table 5.3 Final results of the stepwise Discriminant Function Analysis for the Baltata watershed's two studied sites

Site	Fingerprinting property	Wilks lambda	Cumulative percentage source samples classified correctly
Site 1	Cr	0.525	52.0
	Ni	0.415	54.5
	Zn	0.728	65.0
Site 2	Cr	0.615	55.0
	Fe	0.745	60.0
	Ni	0.225	64.0
	Zn	0.660	70.0



## Conclusion

Undoubtedly, due to limited analytical capacities of this research team the limited number of fingerprinting properties was used by Moldavian team for the more detailed investigation of the sediment fingerprinting. Nevertheless, the presented study has demonstrated that this approach can be successfully used for assessing the type, location and "provenance" of the source of sediments transported through a river watershed, while the utilization of other fingerprinting properties is required for more valid results of this a completely new research tool for Moldova. The widespread implementation of fingerprinting into the everyday practice of mitigating the river basins erosion and pollution, along with this method further adoption, requires modern special equipment for both sampling and laboratory analysis.



Soil and water sampling in the bank zone of the Baltata River

## **Litter traps as a tool to prevent the rivers pollution**

The presented below litter trap to absorb river debris, plastic and other physical pollutants and to prevent their subsequent entry into the Black Sea was developed as part of this project activity by its subcontractor NGO “Re-nașterea Rurală” (Chisinau). The trap is composed of two absorption tubes connected with heavy anchors on the river’ bottom. The absorbed litter is collected in a metal net cage. The trap allows free passage on the river for boats and kayaks. The trap is installed on the Răut River, on the territory of the “Old Orhei” National Park, which took responsibility for its periodic cleaning. The trap collects about one ton of litter per month, preventing it's coming to the Dniester River and later – to the Black Sea.



**General view of the litter trap and its information board**

## References

- Abbas G., Jomaa S., A. Bronstert, Rode M., 2023: Downstream changes in riverbank sediment sources and the effect of catchment size. *Journal of Hydrology: Regional Studies* 46:101340
- Aiello, A., Adamo, M., & Canora, F., 2015: Remote sensing and GIS to assess soil erosion with RUSLE3D and USPED at river basin scale in southern Italy. *Catena*, 131, 174-185. DOI: 10.1016/j.catena.2015.04.003
- Arnold, J.G.; Moriasi, D.N.; Gassman, P.W., et al., 2012: SWAT: Model Use, Calibration, and Validation, *Trans. ASABE* 55, 1491-1508.
- Bazzoffi P., 2015: Measurement of rill erosion through a new UAV-GIS methodology. *Italian Journal of Agronomy* 10(s1):708. Available at: <https://www.agronomy.it/index.php/agro/article/view/708/685>
- Beven K., 2019: How to make advances in hydrological modeling, *Hydrology Research* 50.6: 1481-1494. doi: 10.2166/nh.2019.134
- Boboc, N., Bejan, I., Sirodoev, I., 2011: Landslide distribution and land use within the Calarasi key sector. *GEOREVIEW: Scientific Annals of Stefan cel Mare University of Suceava. Geography Series*, 20(1), 17-23.
- Brosinsky, A., Foerster, S., Segl, K., Lopez-Tarazn, J.A., Pique, G., Bronstert, A., 2014. Spectral fingerprinting: characterizing suspended sediment sources by the use of VNIR-SWIR spectral information. *J. Soils Sediment.* 14 (12), 1965-1981. <https://doi.org/10.1007/s11368-014-0927-z>
- Castro-Bolinaga, C. F., & Fox, G. A., 2018: Streambank erosion: Advances in monitoring, modeling and management. *Water*, 10, 1346.
- Claverie, M., Ju, J., Masek, J. G., Dungan, J. L., Vermote, E. F., Roger, J.-C., Skakun, S. V., Justice, C. (2018). The Harmonized Landsat and Sentinel-2 surface reflectance data set. *Remote Sensing of Environment*, 219, 145-161
- Collins, A.L.; Walling, D.E. 2002 Selecting fingerprint properties for discriminating potential suspended sediment sources in river basins. *J. Hydrol.* 261, 218-244.
- Collins, A.L., Blackwell, M., Boeckx, P., et al., 2020: Sediment source fingerprinting: benchmarking recent outputs, remaining challenges and emerging themes. *J. Soils Sediment.* 20 (12), 4160-4193
- Collins, A.L., Pulley, S., Foster, I.D.L., Gellis, A., Porto, P., Horowitz, A.J., 2017: Sediment source fingerprinting as an aid to catchment management: a review of the current state of knowledge and a methodological decision-tree for end-users. *J. Environ. Manag.* 194, 86-108. <https://doi.org/10.1016/j.jenvman.2016.09.075>
- Collins, A. L., & Walling, D. E., 2007: Sources of fine sediment recovered from the channel bed of lowland groundwater-fed catchments in the UK. *Geomorphology*, 88, 120e13.
- Corobov R., G. Syrodoev, I. Trombitsky, 2016a: Anthropogenic and Climate Change Contributions to Uncertainties in Hydrological Modeling of Small Rivers Watershed Runoff. *Advances in Ecological and Environmental Research*, 1(1):14-34.
- Corobov R., G. Syrodoev, I. Trombitsky and D. Galupa, 2016b: Anthropogenic factors as an element of uncertainty in hydrological modelling of water yield with SWAT. *Journal of engineering science and technology review* 9(2): 138 - 145.



- Gao, B. C., 1996: NDWI—A normalized difference water index for remote sensing of vegetation liquid water from space. *Remote sensing of environment*, 58(3), 257-266. DOI: 10.1016/S0034-4257(96)00067-3
- Gassman, P.W.; Sadeghi, A.M.; Srinivasan, R., 2014: Applications of the SWAT Model Special Section: Overview and Insights. *J. Environ. Qual.* 43, 1-8.
- Daniel, E.B., J.V. Camp, E.J. LeBoeuf, J.R. Penrod, J.P. Dobbins, and M.D. Abkowitz, 2011: Watershed modeling and its applications: A state-of-the-art review. *Open Hydrol. J.* 5:26-50.
- Davis, C.M., Fox, J.F., 2009. Sediment fingerprinting: review of the method and future improvements for allocating nonpoint source pollution. *J. Environ. Eng. ASCE* 135 (7), 490-50
- Devereux, O.H., Prestegard, K.L., Needelman, B.A., Gellis, A.C., 2010. Suspended-sediment sources in an urban watershed, Northeast Branch Anacostia River, Maryland. *Hydrol. Process.* 24 (11), 1391-1403.  
<https://doi.org/10.1002/hyp.7604>
- D'Oleire-Oltmanns S., I. Marzolf, K.D. Peter and J.B. Ries, 2012: Unmanned Aerial Vehicle (UAV) for Monitoring Soil Erosion in Morocco. *Remote Sens.* 2012, 4:3390-3416; doi:10.3390/rs4113390
- Dragicevic, S.; Pripuzic, M.; Živkovic, N.; Novkovic, I.; Kostadinov, S.; Langovic, M.; Milojkovic, B.; Cvorovic, Z., 2017: Spatial and Temporal Variability of Bank Erosion during the Period 1930-2016: Case Study—Kolubara River Basin (Serbia). *Water*, 9, 748.
- Dutta S. and D. Sen, 2018: Application of SWAT model for predicting soil erosion and sediment yield. *Sustain. Water Resour. Manag.* 4:447-468.  
<https://doi.org/10.1007/s40899-017-0127-2>
- Elliot W.J., 2013: Erosion processes and prediction with WEPP technology in forests in the northwestern U.S. *Transactions of the ASABE* 56(2): 563-579.
- EPA, 2022: *Climate Adaptation and Erosion & Sedimentation*. Available at: <https://www.epa.gov/arc-x/climate-adaptation-and-erosion-sedimentation>
- Ercanoglu M., Boboc N., Sirodoev I., Temiz F.A., Sirodoev G., 2009: Landslide susceptibility assessment in the Central Part of the Republic of Moldova. In: *Geophysical Research Abstracts*, Vol. 12, EGU2010-0 EGU General Assembly 2010.
- Flanagan D.C. and M.A. Nearing (eds), 1995: USDA-Water Erosion Prediction Project Hillslope Profile and Watershed Model Documentation. NSERL Report No. 10, USDA-ARS National Soil Erosion Research Laboratory, West Lafayette, 298 p.
- Flanagan, D. C., J. E. Gilley, T. G. Franti (2007): Water Erosion Prediction Project (WEPP): Development history, model capabilities, and future enhancements. *Transactions of the ASABE*, 50(5): 1603-1612
- Flanagan D. C., J. R. Frankenberger, T. A. Cochrane, C. S. Renschler, W. J. Elliot, 2013: Geospatial Application of the Water Erosion Prediction Project (WEPP) Model. *Transactions of the ASABE* 56(2): 591-601
- Flood, N. (2014). Continuity of reflectance data between Landsat-7 ETM+ and Landsat-8 OLI, for both top-of-atmosphere and surface reflectance: a study in the Australian landscape. *Remote Sensing*, 6(9), 7952-7970.
- Foley J.A., DeFries R., Asner G.P., Barford C., Bonan G., Carpenter S.R., Chapin F.S., Coe M.T. et al., 2005: Global consequences of land use. *Science*, 309(5734): 570-574.

- Fox, G.A., Purvis, R.A., Penn, C.J., 2016: Streambanks: A net source of sediment and phosphorus to streams and rivers. *Journal of Environmental Management*, 181, 602-614.
- Franz, C., Makeschin, F., Weiß, H., Lorz, C., 2014: Sediments in urban river basins: identification of sediment sources within the Lago Paranoá catchment, Brasília DF, Brazil – using the fingerprint approach. *Sci. Total Environ.* 466-467, 513-523
- Gorelick, N., Hancher, M., Dixon, M., Ilyushchenko, S., Thau, D., & Moore, R., 2017: Google Earth Engine: Planetary-scale geospatial analysis for everyone. *Remote sensing of Environment*, 202, 18-27. DOI: 10.1016/j.rse.2017.06.031
- Hawley, R.J., MacMannis, K.R., Wooten, M.S., Fet, E.V., Korth, N.L., 2020: Suburban stream erosion rates in northern Kentucky exceed reference channels by an order of magnitude and follow predictable trajectories of channel evolution. *Geomorphology* 352, 106998.
- Hulme M., 2020: Climates Multiple: Three Baselines, Two Tolerances, One Normal. *Academia Letters*, Article 102. <https://doi.org/10.20935/AL102>.
- IPCC, 2013: Summary for Policymakers. In: *Climate Change 2013: The Physical Science Basis. Contribution of Working Group I to the Fifth Assessment Report of the Intergovernmental Panel on Climate Change* [Stocker, T.F., D. Qin, G.-K. Plattner, et al.]. Cambridge University Press, Cambridge, United Kingdom and New York, NY, USA.
- Junwei Z., Z. Yi, C. Zhou, L. Chang, F. Chen, Z. Zhao, G. Gao 2019: Application of UAV and ArcGIS in Soil and Water Conservation Monitoring of slag area—Taking a slag area of hydroelectric power station in Dadu River as an example. *IOP Conf. Ser., Earth Environ. Sci.* 376 012045. doi:10.1088/1755-1315/376/1/012045
- Jacob D., J. Petersen, B. Eggert *et al.*, 2013: EURO-CORDEX: new high-resolution climate change projections for European impact research. *Reg Environ Change*, DOI 10.1007/s10113-013-0499-2
- Kaiser A., F. Neugirg, G. Rock *et al.*, 2014: Small-Scale Surface Reconstruction and Volume Calculation of Soil Erosion in Complex Moroccan Gully Morphology Using Structure from Motion. *Remote Sens.* 6, 7050-7080; doi:10.3390/rs6087050
- Koiter, A.J., Owens, P.N., Petticrew, E.L., Lobb, D.A., 2013: The behavioural characteristics of sediment properties and their implications for sediment fingerprinting as an approach for identifying sediment sources in river basins. *Earth Sci. Rev.* 125, 24-42
- Lamba J., Karthikeyan K.G., Thompson A.M. (2014) Apportionment of suspended sediment sources in an agricultural watershed using sediment fingerprinting. *Geoderma* 239-240 (2015) 25-33
- Leah T. and E. Kuharuk, 2017: Investigation of factors affecting the development of erosion processes in the soil of Moldova. *Technological and ecological safety* 1:50-55 (in Russian)
- Leutner B., Horning N., Schwalb-Willmann J. (2019). RStoolbox: Tools for Remote Sensing Data Analysis. R package version 0.2.6 <https://CRAN.R-project.org/package=RStoolbox>
- Malhotra K., Lamba J., Srivastava P. Shepherd S. 2018 Fingerprinting Suspended Sediment Sources in an Urbanized Watershed Water, 10, 1573; doi:10.3390/w10111573

- Manoj K.J. and U.C. Kothyari, 2000: Estimation of soil erosion and sediment yield using GIS, *Hydrological Sciences Journal*, 45:5: 771-786, DOI: 10.1080/02626660009492376
- McKinley, R., Radcliffe, D., Mukundan, R., 2013. A streamlined approach for sediment source fingerprinting in a Southern Piedmont watershed, USA. *J. Soils Sediments* 13 (10), 1754-1769
- Mhangara, P., Kakembo, V., & Lim, K.J., 2012: Soil erosion risk assessment of the Keiskamma catchment, South Africa using GIS and remote sensing. *Environmental Earth Sciences*, 65(7), 2087-2102. DOI: 10.1007/s12665-011-1190-x.
- Minkowski M. and C. Renschler, nd: *GeoWEPP for ArcGIS 9.x Full Version Manual (for GeoWEPP Version 2.2008 or earlier)*. Department of Geography, The State University of New York at Buffalo. 129 p. Available at: [https://moam.info/queue/geowepp-for-arcgis-9x-full-version-manual\\_599b6c761723dd0e40b19023.html](https://moam.info/queue/geowepp-for-arcgis-9x-full-version-manual_599b6c761723dd0e40b19023.html)
- Moore, J.W., Semmens, B.X., 2008. Incorporating uncertainty and prior information into stable isotope mixing models. *Ecol. Lett.* 11 (5), 470-480. <https://doi.org/10.1111/j.1461-0248.2008.01163.x>
- Neitsch, S.; Arnold, J.; Kiniry, J.; Williams, J., 2011: Soil and Water Assessment Tool—Theoretical Documentation. Version 2009; Technical Report; Blackland Research Center—Texas Agricultural Experiment Station; Grassland, Soil and Water Research Laboratory — USDA Agricultural Research Service: Temple, TX, USA, 618p.
- Ouma, Y. O., Lottering, L., & Tateishi, R., 2022: Soil erosion susceptibility prediction in railway corridors using RUSLE, soil degradation index and the new normalized difference railway erosivity index (NDReLI). *Remote Sensing*, 14(2), 348.
- Perez M.; W.C. Zech; W.N. Donald, 2015: "Drones": Revolutionizing erosion and sediment control site inspections. Available at: [https://www.researchgate.net/publication/282189144\\_Drones\\_Revolutionizing\\_erosion\\_and\\_sediment\\_control\\_site\\_inspections](https://www.researchgate.net/publication/282189144_Drones_Revolutionizing_erosion_and_sediment_control_site_inspections)
- Petropoulos, G. P., Kalivas, D. P., Griffiths, H. M., & Dimou, P. P., 2015: Remote sensing and GIS analysis for mapping spatio-temporal changes of erosion and deposition of two Mediterranean river deltas: The case of the Axios and Aliakmonas rivers, Greece. *International Journal of Applied Earth Observation and Geoinformation*, 35, 217-228. DOI: 10.1016/j.jag.2014.08.004
- Phillips, D.L., Gregg, J.W., 2003. Source partitioning using stable isotopes: coping with too many sources. *Oecologia* 136, 261-269. <https://doi.org/10.1007/s00442-003-1218-3>
- Pineux N., J. Lisein, G. Swerts, C.L. Bielders, P. Lejeune, G. Colinet, A. Degré, 2017: Can DEM time series produced by UAV be used to quantify diffuse erosion in an agricultural watershed? *Geomorphology* 280: 122-136. <https://doi.org/10.1016/j.geomorph.2016.12.003>
- Poleto, C., Merten, G.H., Minella, J.P., 2009. The identification of sediment sources in a small urban watershed in southern Brazil: an application of sediment fingerprinting. *Environ. Technol.* 30 (11), 1145-1153. <https://doi.org/10.1080/09593330903112154>

- Prefac, Z., Dumitru, S., Chendeş, V., Sirodoev, I., & Cracu, G., 2016: Assessment of landslide susceptibility using the certainty factor model: Râşcuţa catchment (Curvature Subcarpathians) case study. *Carpath. J. Earth Environ. Sci.*, 11: 617-626.
- Perez M.; W.C. Zech; W.N. Donald, 2015: "Drones": Revolutionizing erosion and sediment control site inspections. Available at:  
[https://www.researchgate.net/publication/282189144\\_Drones\\_Revolutionizing\\_erosion\\_and\\_sediment\\_control\\_site\\_inspections](https://www.researchgate.net/publication/282189144_Drones_Revolutionizing_erosion_and_sediment_control_site_inspections)
- Rachman L.M., Muhammad B. D., Purwakusuma P.W., Rasyid A.R, 2019: The role of drones for supporting precision agricultural management, Proc. SPIE 11372, Sixth International Symposium on LAPANIPB Satellite, 1137202 (24.12. 2019.doi: 10.1117/12.2538417
- R Core Team, 2020; R: A language and environment for statistical computing. R Foundation for Statistical Computing, Vienna, Austria. Accessed:  
<https://www.R-project.org/>.
- Refsgaard, J.C.; Storm, B.; Clausen, T., 2010: Système Hydrologique Européen (SHE): Review and perspectives after 30 years development in distributed physically-based hydrological modelling. *Hydrol. Res.* 41, 355-377. Available online:  
<https://iwaponline.com/hr/article-pdf/41/5/355/371012/355.pdf>
- Rouse, J.W., R.H. Haas, J.A. Schell, D.W. Deering, 1974: Monitoring vegetation systems in the Great Plains with ERTS, In: S.C. Freden, E.P. Mercanti, and M. Becker (eds) Third Earth Resources Technology Satellite-1 Symposium. Volume I: Technical Presentations, NASA SP-351, NASA, Washington, D.C., pp. 309-317.
- Sepuru, T. K., & Dube, T., 2018: An appraisal of the progress of remote sensing applications in soil erosion mapping and monitoring. *Remote Sensing Applications: Society and Environment*, 9, 1-9. DOI: 10.1016/j.rsase.2017.10.005
- Saleem, A., Dewan, A., Rahman, M.M., Nawfee, S.M., Karim, R., Lu, X.X., 2020: Spatial and temporal variations of erosion and accretion: a case of a large tropical river. *Earth Syst. Environ.* 4, 167-181.
- Senanayake, S., Pradhan, B., Huete, A., & Brennan, J., 2020: A review on assessing and mapping soil erosion hazard using geo-informatics technology for farming system management. *Remote Sensing*, 12(24), 4063.
- Shaker, R. R., Sirodoev G., Sirodoev, I. (2011). Landslide susceptibility in the Republic of Moldova: a landscape and multivariate approach for regional assessment. In *Applied Geography Conferences* (Vol. 34, pp. 288-299).
- Shrestha B., M. S. Babel, S. Maskey, A. van Griensven, S. Uhlenbrook, A. Green, and I. Akkharath, 2013: Impact of climate change on sediment yield in the Mekong River basin: a case study of the Nam Ou basin, Lao PDR. *Hydrol. Earth Syst. Sci.*, 17, 1-20, doi:10.5194/hess-17-1-2013
- Singh V.P., 2018: Hydrologic modeling: progress and future directions. *Geosci. Lett.* 5:15. doi.org/10.1186/s40562-018-0113-z
- Șirodoev Gh., Mițul E., Gherasi A. Canțîr A. (2019). Geomorphological factors. In: Nedeaľcov M. (ed.). Atlas. The Republic of Moldova: Natural and anthropogenic risk factors. Institute of Ecology and Geography, Chişinău, pp. 9-40. (in Romanian)
- Șirodoev, I.; Corobov, R.; Șirodoev, G.; Trombitsky, 2022: Modelling Runoff within a Small River Basin under the Changing Climate: A Case Study of Using SWAT in



- the Baltata River Basin (The Republic of Moldova). *Land* 11, 167.  
<https://doi.org/10.3390/land11020167>
- Sungchan O., A. Chang, J. Jung, et al., 2020: Recent Advances in UAS based Soil Erosion Mapping. *Mod Concep Dev Agrono.* 7(2). MCDA. 000657.  
DOI: 10.31031/MCDA.2020.07.000657
- Yüksel A., , Abdullah E., Akay 1, Recep G., Mahmut R., and Muzaffer C. Application of GeoWEPP for Determining Sediment Yield and Runoff in the Orcan Creek Watershed in Kahramanmaraş, Turkey. *Sensors* 2008, 8, 1222-1236
- Ursu A. (Ed.), 2000: Degradarea solurilor și deșertificarea, p. 209, Chişinău (in Romanian)
- USDA FS (U.S. Department of Agriculture, Forest Service), 2013: *Assessing the Vulnerability of Watersheds to Climate Change*. General Technical Report, PNW-GTR-884, 32 p.
- Van Liew, M.W., Arnold, J.G., and Bosch, D.D., 2005: Problems and potential of autocalibrating a hydrologic model. *Transactions of the ASAE*, 48(3):1025-1040.
- Vogeler, J. C., Braaten, J. D., Slesak, R. A., & Falkowski, M. J., 2018: Extracting the full value of the Landsat archive: Inter-sensor harmonization for the mapping of Minnesota forest canopy cover (1973-2015). *Remote sensing of environment*, 209, 363-374.
- Vrieling A., 2007: Mapping erosion from space. Doctoral Thesis. Wageningen University
- Winchell, M.; Srinivasan, R.; Di Luzio, M.; Arnold, J., 2013: ArcSWAT Interface for SWAT2012: User's Guide; Technical Report, Blackland Research Center—Texas Agricultural Experiment Station; Grassland, Soil and Water Research Laboratory—USDA Agricultural Research Service: Temple, TX, USA,.
- Walling, D.E., Collins, A.L., Stroud, R.W., 2008: Tracing suspended sediment and particulate phosphorus sources in catchments. *J. Hydrol.* 350 (3-4), 274-289
- Walling, D., 2013: The evolution of sediment source fingerprinting investigations in fluvial systems. *J. Soils Sediments* 13 (10), 1658-1675.
- Walling, D.E., Collins, A.L., 2000: Integrated assessment of catchment sediment budgets: A technical manual. University of Exeter, Exeter, UK
- Walling, D.E., Collins, A.L., 2008: The catchment sediment budget as a management tool. *Environ. Sci. Policy* 11 (2), 136-143.  
<https://doi.org/10.1016/j.envsci.2007.10.004>
- Walling, D.E., Collins, A.L., Sickingabula, H.M., Leeks, G.J.L., 2001: Integrated assessment of catchment suspended sediment budgets: a Zambian example. *Land Degrad. Dev.* 12 (5), 387-415. <https://doi.org/10.1002/ldr.461>
- Walling, D. E., 2005: Tracing suspended sediment sources in catchments and river systems. *The Science of the Total Environment*, 344, 159e184
- Walling, D. E., Owens, P. N., & Leeks, G. J. L., 2015; Fingerprinting suspended sediment sources
- Xu H., 2006: Modification of Normalised Difference Water Index (NDWI) to Enhance Open Water Features in Remotely Sensed Imagery. *International Journal of Remote Sensing*, 27(14): 3025-3033.
- Zaimes, G. N., Tamparopoulos, A. E., Tufekcioglu, M., & Schultz, R. C., 2021: Understanding stream bank erosion and deposition in Iowa, USA: A seven-year

- study along streams in different regions with different riparian land-uses. *Journal of Environmental Management*, 287, 112352.
- Zaimes, G. N., Tufekcioglu, M., & Schultz, R. C., 2019: Riparian land-use impacts on stream bank and gully erosion in agricultural watersheds: What we have learned. *Water*, 11(7), 1343.
- Zhai, K., Wu, X., Qin, Y., & Du, P., 2015: Comparison of surface water extraction performances of different classic water indices using OLI and TM imageries in different situations. *Geo-spatial Information Science*, 18(1), 32-42.
- Zhang, X., Srinivasan, R., Van Liew M., 2008: Multi-site calibration of the SWAT model for hydrologic modelling. *Transactions of the ASABE* 51(6): 2039-2049.
- Zhao, Y., Huang, Y., Liu, H., Wei, Y., Lin, Q., & Lu, Y., 2018: Use of the Normalized Difference Road Landside Index (NDRLI)-based method for the quick delineation of road-induced landslides. *Scientific Reports*, 8(1), 17815.
- Žížala, D., Juřicová, A., Zádorová, T., Zelenková, K., Minařík, R. (2019). Mapping soil degradation using remote sensing data and ancillary data: South-East Moravia, Czech Republic. *European Journal of Remote Sensing*, 52(sup1), 108-122. DOI: 10.1080/22797254.2018.1482524



## Rezumat

Proiectul „Protecția cursurilor de apă pentru o Mare Neagră curată, prin monitorizarea inovatoare cu instrumente comune de control și practici bazate pe natură în vederea reducerii sedimentelor și poluării cu deșeuri din plastic (BSB963)” cu acronimul „Protect-Streams-4-Sea” a început pe 20 iulie 2020. Durata totală a proiectului este de 36 luni. Proiectul este finanțat în cadrul UE INTERREG IV „Programul operațional comun 2014 pentru bazinul Mării Negre 2014-2020”. Bugetul total al proiectului este de 907.135,00 €, unde contribuția UE este de 834.543,41 €. Partenerul principal este succesorul legal al Universității Elene Internaționale a Technologiko Ekpedefitiko Idryma Anatolikis Makedonias kai Thrakis. În implementarea proiectului mai sunt implicate patru instituții din regiunea Mării Negre, și anume: Administrația Apelor Buzău-Ialomița din România, ONG-ul Uniunea Pădurarilor Tineri din Armenia, Asociația Internațională a Păstrătorilor Râului Eco-TIRAS din Republica Moldova și Universitatea Artvin Coruh din Turcia. Pentru a viețui de-a lungul unei Mări comune, este necesară o gestionare durabilă a apei, și anume, țările din vecinătate să adopte metode și practici comune. Acesta este unul dintre punctele forte ale proiectului, deoarece sunt parteneri de implementare din cinci țări diferite, iar activitățile se desfășoară în toate țările participante. Obiectivul general al „Protect-Streams-4-Sea” este protecția mediului, reducerea poluanților și a deșeurilor în Marea Neagră. Acest lucru se poate realiza concentrându-se asupra poluanților interiori și deșeurilor, în special din bazinele hidrografice ale râurilor ce se varsă în Marea Neagră. Broșura propusă prezintă rezultatele principale ale proiectului, în special cele obținute în urma activităților în Republica Moldova.

Prin urmare, ideea prezentului proiect constă în reducerea poluanților și deșeurilor din sursele nepunctiforme ca să nu ajungă în râuri și, în consecință, în Marea Neagră. Acest obiectiv a fost atins în principal prin utilizarea diferitor metode inovatoare, dintre care majoritatea au fost aplicate în R.Moldova practic pentru prima dată. Pe lângă R.Moldova, partenerii proiectului au fost universitățile și ONG-urile din Grecia, România, Armenia și Turcia.

*Obiectivul general* al proiectului a fost protecția mediului și reducerea poluanților și deșeurilor în Marea Neagră. *Obiectivele sale specifice* au inclus dezvoltarea de noi instrumente pentru monitorizarea comună a poluanților și deșeurilor, identificarea surselor și volumelor acestora, precum și

dezvoltarea și propunerea celor mai bune practici de management. Durata proiectului este de 36 luni: de la 20.07.2020 până la 19.07.2023.

Scopul principal al acestei broșuri este de a informa publicul larg despre derularea proiectului în R.Moldova și rezultatele obținute. La prezentarea rezultatelor cercetărilor efectuate se pune accent pe aplicarea tehnologiilor inovatoare, ținând cont de inovația și utilitatea acestora.

Ca zonă de studiu pentru îndeplinirea sarcinilor Proiectului în R.Moldova a fost selectat râul Bălțată - un curs de apă mic și destul de tipic pentru R.Moldova. Acest râu este un afluent de dreapta al fluviului Nistru, unde pătrund direct toți poluanții de suprafață și deșeurile care ajung în cursul său principal. Pe lângă aceasta, Bălțata oglindește situația ecologică generală din alte mici bazine hidrografice analoge ale regiunii date. Suprafața bazinului său constituie 153,9 km<sup>2</sup>, lungimea - 27,47 km, lățimea - 7,74 km și are pe maluri 13 localități rurale. Din punctul de vedere al proiectului au fost importanți doi factori: nivelul sporit de degradare și procesele intensive de eroziune a solurilor (peste 29%).

Ca atare, Proiectul s-a concentrat asupra monitorizării mediului, poluanților și deșeurilor din sursele nepunctiforme care ajung în Marea Neagră, iar eforturile de salubritate a acestui râu sunt utile nu numai mării, dar și de-a lungul zonelor riverale, unde numeroși poluanți și deșeuri sunt ajung în bazinele hidrografice ale râurilor.

Studiul acestor procese a inclus:

### ***1. Modelarea hidrologică a debitului și sedimentării râului Bălțata.***

Deoarece scurgerea și stocarea apei în bazinele hidrografice este un proces complex și influențat de factorii climatici, geologici, pedologici, de utilizarea terenului, antropici, etc., natura acestor factori cel mai bine este investigată prin modele hidrologice care se simulează pentru diferite intervale spațio-temporale și în diferite condiții fiziografice. În cadrul proiectului au fost utilizate două modele hidrologice: SWAT (Soil and Water Assessment Tool) și WEPP (Water Erosion Prediction Project). Implementarea lor a urmărit câte o sarcină specifică pentru fiecare: SWAT având ca scop estimarea debitului actual și preconizat al r. Bălțata, pe când modelarea WEPP a vizat stimularea pierderii de sol și a producției de sedimente în bazin.

În special, modelarea SWAT a potențialului scurgerii anuale a r. Bălțata în condițiile climatice actuale (1981-2020) poate ajunge la 0,048 km<sup>3</sup>. Toto-

dată, având în vedere o părtinire incontestabilă a acestor estimări din cauza presingului antropic asupra bazinului hidrografic, aceste rezultate ar trebui luate în considerare, cu o oarecare prudență, ele oferind o bază pentru evaluarea impacturilor așteptate din cauza schimbărilor climatice. Modelarea SWAT a arătat că, în funcție de orizontul de timp și sarcina radiativă, debitul r. Bălțata se poate schimba de la o creștere cu 7-8% în prima jumătate a secolului al XXI-lea la o scădere de la aproximativ 8% și peste 25% în perioada 2071-2100. În medie, o creștere a scurgerii poate ajunge la circa 2% în aa. 2021-2050 și o scădere până la 17% în aa. 2071-2100. Mai mult decât atât, SWAT a simulat acumularea de apă în trei rezervoare din albia râului. Această acumulare anuală de apă poate atinge 65% din scurgerea totală a bazinului hidrografic.

Modelarea WEPP a stimulat pierderile de sol și producția de sedimente în bazinul r. Bălțata, cauzate de eroziunile plăcilor și malurilor albiei în urma modificărilor hidraulice. Pentru evaluarea lor au fost utilizate abordările: la distanță și la fața locului. Metoda offsite a bazinului hidrografic a oferit rezultate de simulare concentrate pe randamentul de sedimente livrat prin canale către un anumit punct de evacuare. În general, conform acestei abordări deversarea de sedimente din Bălțata a fost de aproximativ 5430 tone/an (0,4 t/ha/an), cu o distribuție teritorială destul de uniformă. În majoritatea bazinelor hidrografice sedimentele anuale la hectar sunt mai mici de 1/4 t, urmate de zonele cu sedimente de la 1/4 până la 1/2 t, și doar în albia mai mică ajungând la 1-2 t. Valoarea totală a pierderii de sol, estimată prin abordarea onsite, s-a ridicat la circa 21542 t/an). Pe lângă aceasta, metoda dată a oferit un grad sporit de detaliere a pierderilor de sol în bazin.

Studiul efectuat a demonstrat în mod clar potențialul enorm al modelării hidrologice pentru evaluarea dimensiunii și distribuției spațiale a solului și acumulării de sediment, rezultate în urma proceselor de eroziune. Dezvoltarea ulterioară și utilizarea pe scară largă a acestei metode poate nu numai să suplimenteze, dar uneori să înlocuiască experimentele practicate pe teren, costisitoare și cu volum mare de muncă. Cu toate acestea, utilizarea pe scară largă în R.Moldova a acestei metode este posibilă doar prin crearea bazelor relevante de date și liber accesibile privind solul, utilizarea terenurilor și clima pentru întregul teritoriu.

## **2. Tehnici de teledetecție la identificarea și cartografierea zonelor predispușe eroziunii**

Utilizarea tehnicilor de teledetecție a avut ca scop identificarea zonelor predispușe eroziunii, utilizând monitorizarea istorică prin satelit a suprafeței Pământului. Au fost abordate două sarcini: implementarea indicilor de diferență normalizați pentru cartografierea celor mai vulnerabile la eroziune zone ale solului și utilizarea imaginilor satelitare în evaluarea tendințelor în timp a eroziunii malurilor râului.

*Indicii de diferență normalizați* cuantifică prezența unei anumite entități materiale într-o imagine de teledetecție pe baza diferențelor în reflectanța acestei entități în diferite intervale spectrale. În acest studiu au fost utilizați doi indici: Indicele de vegetație a diferențelor normalizate (NDVI), care evaluează fracția de acoperire cu vegetație într-un pixel și Indicele de apă a diferențelor normalizate (NDWI), care reflectă conținutul de apă din sol și vegetație. Identificarea punctelor critice de eroziune din bazinul r. Bălțata s-a bazat pe imaginile satelitare și instrumentele de analiză disponibile gratuit, cu contribuția unor informații suplimentare, cum ar fi utilizarea terenurilor și tipurile de sol, rigole și alunecări de teren obținute în urma interpretării manuale a imaginilor din satelit și a cercetărilor pe teren. Imaginile din satelit au fost achiziționate de senzorii Thematic Mapper (TM) și MultiSpectral Instrument (MSI) de pe bordul misiunilor Landsat 5 și Sentinel-2. În general, s-au folosit șase scene, câte trei pentru primăvară și toamnă, acoperind perioada între 1986 și 2020.

Analiza rezultatelor cercetărilor a arătat, că doar 8,37% din suprafața bazinului Bălțata este afectată de eroziune sau expusă acesteia. Formele dominante ale eroziunii sunt alunecările de teren, care acoperă suprafețe de două ori mai mari decât rigolele, ocupând 40% din zona predispusă la eroziune unde se observă o expunere moderată pe 32%, o expunere redusă pe 23% și o expunere sporită cu puțin peste 4% a acestei zone. Analiza a inclus și distribuția eroziunii în funcție de pante, soluri și utilizarea terenului.

Evaluarea tendințelor temporale în eroziunea malurilor a avut ca scop determinarea și cartografierea zonelor potențiale ale acesteia, folosind o serie de imagini satelitare pe termen lung. Studiul efectuat a arătat că imaginile de satelit cu rezoluție medie reprezintă un echilibru optim între scara analizei, durata acesteia și timpul consumat pentru colectarea și prelucrarea datelor. În special, au fost utilizate imagini de satelit achiziționate de senzorii Thematic Mapper (TM) și Operational Land Imager (OLI) de pe bordul misiunilor Landsat 5 și Landsat 8, respectiv. Imaginile



Landsat au permis de a prelungi perioada de studiu din 1985 până în 2022 și a avea compatibilitate relativă a două instrumente: o rezoluție spațială destul de grosieră a scenelor Landsat (30 m) este compensată de eșantionul disponibil pentru 37 de ani. În total au fost utilizate 27 scene TM anuale pentru aa. 1985-2011 și 10 scene OLI anuale pentru aa. 2013-2022 în perioada 15 martie – 15 octombrie. Pentru fiecare scenă a fost calculat Indicele de eroziune a căii ferate cu diferența normalizată (NDReLI), care se încadrează în intervalul  $[-1; +1]$ ; cu cât este mai mare acest indice, cu atât mai mare este erozivitatea. Apoi, a fost rulat un model de regresie liniară NDReLI în funcție de timp. O tendință pozitivă, ca urmare a creșterii NDReLI în timp, sugerează creșterea eroziunii malurilor râului, iar o tendință negativă indică diminuarea acesteia.

Rezultatele modelării au evidențiat o tendință de creștere semnificativă a eroziunii malurilor râului în bazinul Bălțata: aproape 80% dintre pixelii valizi și peste jumătate dintre toții luați în considerație au fost supuși acestui proces. Foarte puține sectoare, reprezentând doar 0,3% din lungimea cursurilor principale, au arătat o reducere a eroziunii malurilor în perioada analizată. Rezultatele arată, de asemenea, că terenurile cultivate ar putea avea cel mai puternic impact asupra eroziunii malurilor râului în timp, pe când zonele relativ mari acoperite cu apă sunt mult mai importante pentru o eroziune în creștere, decât orice alt tip de utilizare a terenului.

### **3. Cartografierea cu drone a punctelor fierbinți de eroziune**

Conform programului proiectului, dronele ar fi trebuit folosite pentru a cartografia eroziunea de suprafață la nivelurile bazinelor de apă. În timp ce zonele mari cu eroziune sporită au fost identificate de indici, dronele au oferit rezultate suplimentare la scară mică prin cartografierea punctelor fierbinți de suprafață și evaluarea eroziunii malurilor râului. Pentru acest studiu a fost folosită o nouă versiune a celei mai inteligente drone Phantom 4 PROSpess a DJI. Această dronă este echipată cu doi senzori duali de imagini din spate și sisteme de detectare în infraroșu care indică obstacolele în 5 direcții și zboară în jurul lor în 4 direcții. Tehnica dronei de cartografiere a eroziunii a implicat capturarea imaginilor ale unei zone-țintă, prelucrarea și analiza acestora, folosind un softwar special. În cadrul studiului imaginile de înaltă rezoluție colectate au fost analizate printr-o varietate de instrumente software, inclusiv GIS, pentru care a fost nevoie să se creeze hărți detaliate necesare pentru a identifica zonele cu risc de eroziune sau poluare și pentru a măsura efectele negative actuale și potențiale viitoare ale acestora.



Acest studiu a inclus evaluarea eroziunilor de suprafață și a malurilor cu ajutorul dronei. Prima evaluare a fost demonstrată pe exemplul celor două parcele ale bazinului hidrografic Bălțata, denumite convențional Bălțata de Mijloc și confluența Bălțata de Jos - gura r. Recea. Ortomozaicul din Bălțata de Mijloc a combinat 25 de imagini ortofoto cu numărul mediu al punctelor-cheie de aproximativ 73,3 mii la o rezoluție de 1,1 cm/pixel. Modelul digital de suprafață (DSM) a arătat că aici parcelele de eroziune de intensitate scăzută ocupă 0,013 ha (1%), intensitate medie - 0,0026 ha (0,21%) și intensitate puternică - mai puțin de 0,005% din întreaga suprafață. Lungimea tronsoanelor de mal supuse eroziunii este de 55% pentru malul drept al r. Bălțata și 31% - pentru malul stâng. Pe parcela a doua, practic, ambele maluri ale rr. Bălțata și Recea sunt supuse unor procese de eroziune, inclusiv mai multe forme microerozive de eroziune liniară. În general, eroziunea malurilor pe aceste două râuri se dezvoltă pe lungimile lor de aproximativ 2800 m și, respectiv, aproximativ 2300 m de la gurile de vărsare pe o fâșie riverană îngustă.

Eroziunea suprafeței a fost estimată de dronă pe două parcele, denumite provizoriu Bălțata de Nord și Sagaidac. Sondajul cu dronă a arătat că în prima parcelă cea mai afectată de procesele de eroziune este partea sa mijlocie (cea mai abruptă), în timp ce manifestările eroziunii de intensitate medie și scăzută apar aproape pe toată zona. Suprafața totală de intensitate scăzută a eroziunii identificată este de aproximativ 1,2 ha, eroziunea de intensitate medie — 0,97 ha și de intensitate mare — 0,91 ha. În parcela de studiu Sagaidac predomină eroziunea de suprafață de intensitate diferită în părțile sale inferioare și medii ale acestui versant. Suprafața totală a zonelor identificate de eroziune de intensitate mică constituie 0,013 ha, cu eroziune de intensitate medie - 0,006 ha și de intensitate puternică - 0,003 ha.

#### **4. Amprentarea**

Pentru identificarea surselor de sedimente în suspensie din râul Bălțata s-a folosit metoda amprentei. Această metodă leagă proprietățile fizice sau geochimice ale sedimentelor de sursele corespunzătoare din cadrul bazinului hidrografic, pe baza celor două ipoteze majore: (a) sursele potențiale de sedimente se disting datorită unor proprietăți de amprentare și (b) contribuțiile relative ale sursei la sedimentul în suspensie poate fi determinat prin compararea proprietăților de amprentare a sedimentului cu probele de material sursă. Abordarea comună, care a fost folosită în acest

studiu de amprentare a sedimentelor, a fost de a selecta multe proprietăți de amprentare și de a aplica proceduri statistice pentru a le optimiza pentru a distribui cel mai bine sedimentul în suspensie la diferite surse potențiale. Evaluarea amprentei a inclus evaluarea contribuțiilor totale de sedimente din trei surse primare: versanții de deal, rigole și malurile râurilor.

Probele din eșantionul de sedimente, necesar pentru amprentarea lor în bazinul hidrografic al râului Baltata, au fost recoltate prin apucarea ieșirilor acestuia și subbazinelor la adâncimea de 5,0 cm în septembrie 2022, după evenimente de precipitații intense aici, pe zona cu utilizare diferită, folosind metodologia standard ISO 10381-1:2002. În total, au fost selectate 26 de probe de sol și 3 de sedimente. Au fost adoptate diferite proceduri statistice pentru a cuantifica contribuția relativă a fiecărei surse potențiale de sedimente, livrate în canalul principal al pârâului Baltata. Valoarea totală a metalelor grele din probele de sol, cu excepția plumbului și zincului, se situează sub concentrațiile maxime admisibile, în primul rând în zonele de așezare. Concentrațiile de metale grele din sedimente sunt apropiate de probele de sol.

*Colectorul de captare a deșeurilor* plutitoare, ca instrument de prevenire a poluării râurilor, a fost instalat pe râul Răut. Instalația permite colectarea deșeurilor din plastic și alți poluanți fizici flotabili de pe suprafața unei porțiuni a râului. Colectorul de captare a fost proiectat, construit și instalat de ONG-ul subcontractant al proiectului „Renașterea Rurală” (Chișinău). Colectorul de captare este compus din două tuburi cu lungimea de 12 metri, fiecare ancorate de blocuri de beton grele amplasate la fundul râului. Tuburile direcționează deșeurile către coșul de gunoi construit din plasă metalică. Colectorul de captare permite deplasarea cu barca sau caiacul de-a lungul râului fără acțiuni speciale și nu prezintă un impediment pentru floră și faună. Colectorul de captare este instalat pe râul Răut, pe teritoriul Parcului Național „Orheiul Vechi”, care și-a asumat responsabilitatea de mentenanță a acestuia și curățenia periodică a coșului de gunoi. Colectorul de captare adună aproximativ o tonă de deșeu pe lună, împiedicând ca acesta să ajungă în râul Nistru, iar apoi în Marea Neagră. Toate deșeurile colectate sunt sortate, iar plasticul este transportat la fabrica de reciclare.





The editors of the material:  
*Ilya Trombitsky and Roman Corobov*

Address: Eco-TIRAS,  
*11a, Teatrala str. MD-2012, Chisinau, Moldova*  
Phone: +373 22 225625  
E-mail: [ecotiras@mail.ru](mailto:ecotiras@mail.ru)  
Website: [www.Eco-Tiras.org](http://www.Eco-Tiras.org)

Joint Operational Programme Black Sea Basin 2014-2020

Editors: Ilya Trombitsky & Roman Corobov

Date: May, 2023

Joint Operational Programme Black Sea Basin 2014-2020 is co-financed by the European Union through the European Neighbourhood Instrument and by the participating countries: Armenia, Georgia, Greece, Republic of Moldova, Romania, Turkey, and Ukraine

This publication was produced with the financial assistance of the European Union. Its contents is the sole responsibility of the Eco-Tiras and can in no way be taken to reflect the views of the European Union and do not necessarily reflect the views of the European Union.